Spatio-temporal evolution of earthquake swarms in the Nordland area of Norway

Kristoffer Igland

Master of Science Thesis
in Geodynamics

Abstract

The double difference earthquake relocation method (DD) is used to improve the seismicity image for regions with high seismic activity. Common location techniques include standard hypocenter location (absolute locations) and the double difference method (relative locations). In this thesis I apply the double difference method of the hypoDD software, on the seismicity in Nordland area Norway. The main aim, is to see if the double difference method, which is known to be more accurate than standard hypocenter location method, provides an improvement on earthquake locations. Which will possible reveal structures with associated orientation. A comparison between absolute locations and relative locations will be conducted using figures, inversion outputs and synthetic test. The double difference method on the seismicity in Nordland was found to be more accurate than standard hypocenter locations. A synthetic test on both real and synthetic data. Shows a reduction in error compared to standard hypocenter location. This indicates that the relocated locations are reliable and robust.

The findings of this study in the reveal that the earthquake activity is divided into two parts. The first part is randomly distributed in time and space, and the second part consists of multiple linear alignments of earthquakes trending in NW-SE direction. Further South from the swarm, more linear alignments are trending NW-SE and W-E direction are found. Earthquakes in some sequences are suggested to migrate in time to the South east and dipping towards Northeast and Northwest. Directions of these structures correspond well with previous studies of the area. This indicates that the structures and corresponding seismicity are related to different stress generating mechanisms like ridge push, post-glacial uplift, sediments along the coast and high topography.

Acknowledgement

Bergen, June 15, 2016

Kristoffer Igland

Contents

1　Introduction

The Nordland area Norway, has since the first registered earthquakes, been exposed to a high level of seismicity. The seismicity is concentrated along the coast of northern Norway. In some areas earthquake swarms are identified. Many causes have been suggested to be the reason for the high level of seismicity. Most suggested are the ridge push force, post glacial rebound and sedimentation and erosion on the margin. Accurate hypocenter locations can be essential to determine the cause of the events. Finding earthquakes occurring in a linear feature could mean they are connected and occur from a similar structure. Mapping the faults and their respective orientation may help determine causes for the earthquakes. Today the area is well covered with high quality seismometers mostly deployed by the NEONOR2 project (between August 2013 and May 2016). These stations are mainly used for gathering my data consisting of 1208 events from August 2013 to March 2016. During the last two decades a new method for relocation of seismic events was developed, which allows for a precise relative locations of seismic events [Waldhauser and Ellsworth, 2000]. This possibly improves the seismicity image for regions of high seismic activity.

1.1　Study Area

The study area of this thesis, Nordland, is located south of Troms and North of Nord-Trøndelag. Geologically, this area is dominated by crystalline, Precambrian metamorphic rocks, fragments broken off the nappes of the Caledonian thrust sheets [Hicks et al., 2000a]. Extensional shear zones, normal extension faults and compressional structures trending NW-SE and W-E are present in the area [Rykkelid and Andresen, 1994b, Hicks et al., 2000a, Dehls et al., 2000, Braathen et al., 2002b, Olesen et al., 2013a]. Topographically, the region is characterized by high mountains, a glacier (Svartisen), fjords and valleys. Multiple summits in the area rise to elevations above 1000 m.a.s.l.

Figure 1: Overview map of my study area, Nordland.

The study will mainly be focused (interpretation) on the seismicity along the coast between North Helgeland and South Helgeland, more specifically between Saltfjellet in the North to Korgfjellet in the South. Further in the thesis, this area will be referred to as the main study area.

1.2 Research Aims and Objectives

The purpose of this study is to provide a better overview of the seismicity in the Nordland, especially around the area where earthquake swarms occur. Three other swarms have been identified close to my study area, Meløy, Steigen and Rana [Bungum et al., 1979, Atakan et al., 1994, Hicks et al., 2000a]. These swarms have not been located using the double difference method before, which means that additional information may be given in terms of structures within or time migration within them. Previous work in this area also identify normal fault extension in NW-SE and W-E directions [Hicks et al., 2000a,b].

The aims of this study are:

- Improve hypocenter locations using the double difference method.

- Give a description of how the double difference method works and reasons for the choice of parameter values.

- Identify structures (linear trends) that may show inside or outside the swarm after the relocation, and if possible give orientations. Possibly suggest fault plane.

- Discuss and propose causes for why the seismicity occurs along the coast of northern Norway.

The study attempts to achieve these aims with the following objectives:

Use the double difference method implemented in the hypoDD software, to relocate 1208 seismic events. Use a synthetic test to determine if the new locations of the earthquakes (relocations) are reliable and robust. Investigate the results from the double difference method and interpret the structures in the study area i.e look for structures, pattern in time of occurrence (migration in time), orientations (dipping direction) and suggest fault planes. Compare the results with previous studies and look for similarities and possible explanation for the observations.

2 Geological Setting

2.1 Tectonic Background

Due to plate tectonics and associated continental drift, Norway's position has varied through time, went from being on the western margin of Baltica, moving to the center of Laurussia and to the northwest of Eurasia where it lies today on the Fennoscandia part of the plate [Torsvik and Cocks, 2005]. During Proterozic time most of the continental fragments were assembled as a supercontinent known as Rodinia. In Late Proterozoic/Early Cambrium, the supercontinent Rodinia began to rift and break apart, which led to the formation of paleocontinents, including Laurentia, Baltica and Gondwana. Contemporarily, the rifting formed the Iapetus ocean between Baltica and Laurentia, resulting in a sea-floor spreading and rotation of the Baltic Shield [Meert and Torsvik, 2003, Torsvik and Cocks, 2005]. This event continued up to Early-Ordovician age, which marked the onset of plate subduction and closure of the Iapetus Ocean. Driven by the subduction, Baltica and Laurentia converged up until Early Devonian, which ultimately resulted in the Caledonian Orogeny and formation of the supercontinent Laurasia. Fig. 2 illustates the palegeographic evolution around the Caledonian event [Roberts, 2003]. By the end of Paleozoic, Gondwana and Laurasia were once again joined, together with smaller terranes, to form the supercontinent Pangea.
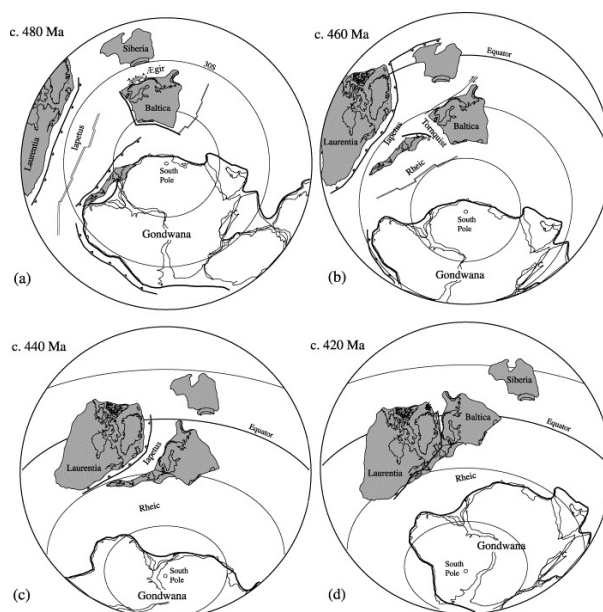
Figure 2: Development of the Baltica and Laurentias continents positioning from 480 Ma to 420 Ma, resulting in a collision and the formation of the Caledonian orogeny in Scandinavia, the orogeny is maintained on both sides of the North Atlantic ocean [Roberts, 2003].

2.1.1   The Caledonian Orogeny

The Scandian Caledonide orogeny (Fig. 3) represents a major continental collision, resulted by the closure of the Iapetus Ocean, and involved the Baltoscandian margin of Baltica and the opposing eastern margin of Laurentia (i.e. Greenland, North America and Canada)

The Scandian Caledonide orogeny started in Late Silurian (410 Ma) and reached its end around early Devonian time (400 Ma) [Torsvik et al., 1996, Roberts and Gee, 1985, Roberts, 2003] with a gradual oblique convergence of plates Baltica and Laurentia that led to a collision involving subduction of the Baltoscandian margin of Baltica (Norway, Sweden and British Isles) under Laurentia (Greenland, North America and Canada) resulting in the closing of the lapetus ocean [Roberts, 2003]. This process happened relatively fast due to active subduction zones on both sides of the lapetus ocean. The first collision started with island arc and oceanic crust transporting in over Laurentia and Baltica producing oceanic and arc terranes derived from the lapetus ocean. Resulting in Greenland colliding with Baltica (Scandian orogeny) (Fig. 3), and leading to major folding, metamorphism and formation of several thrust fronts in Norway, and the formation of the Baltic shield that Norway is a part of. Most of the bedrocks and rocks that is preserved on mainland Norway, are from Precambrian to Devonian time, formed in palaeogeographic settings, and gathered when they thrusted over Baltica as a belt during the Scandian Caledonide orogeny (Fig. 4). [Torsvik et al., 1996, Roberts and Gee, 1985, Roberts, 2003].

Figure 3: Caledonian orogeny in Scandianvia, the orogeny is maintained on both sides of the North Atlantic ocean. Shows how the relationship between Baltica and Laurentia was [Lorenz et al., 2012].

The Caledonian Orogeny can be divided into four main tectonic phases: The Finnmarkian in Late Cambrian time; The Trondheim in Early Ordovician time; The Taconian event

in Mid to Late Ordovician time; and The Scandian in Mid Silurian to Early Devonian time.

The Finnmarkian event around 500 Ma forms the outermost of the Baltoscandian margin and is suggested to the result of a collision with Baltica and an ocean positioned magmatic arc in the Ægir sea [Roberts, 2003]. The Trondheim event is not well understood, it is suggested to have affected the Baltoscandian margin around 480 Ma, characterized by deformation and metamorphism [Eide and Lardeaux, 2002, Roberts, 2003], may represent a seaward subduction of a microcontinent [Brueckner et al., 2004]. At this point, Baltica started to rotate and move towards Laurentia. The Taconian event 470-450 Ma is characterized by subduction and accretion along the continental margin of Laurentia. The Scandian event 420–400 Ma represents the main continental collision between Baltica and Laurentia. During rapid exhumation, multiple thrust sheets were emplaced onto Baltica, to form the Caledonian Allochthons (Fig. 4) in Norway [Gee, 1975].

Based on tectonostratigraphic subdivision, the thrust nappe complexes of the Scandinavia Caledonides can be grouped into six different units: Autochthon, Parautochthon (units in the foreland to the east), and Lower (thin foreland units), Middle, Upper and Uppermost Allochthon [Roberts and Gee, 1985].
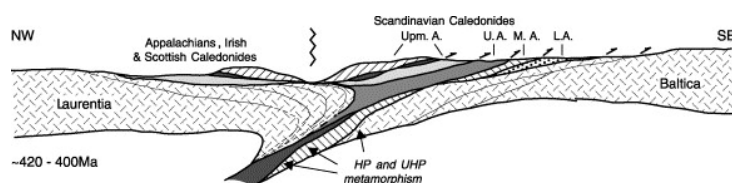
Figure 4: Baltica - Laurentia collision, shows the collisional events from Baltican margin subducted under the Laurentian plate, and the thrust sheets Allochtons, M.A: Middle Allochtons, L.A: Lower Allochtons.

After the Scandian event Baltica, Avalonia and Laurentia became the continent Laurussia. Laurussia further merged with Gondwana to form the supercontinent Pangea approximated around 330 Ma the end of the Palaozoic [Van der Voo and Torsvik, 2001, Torsvik and Van der Voo, 2002, Torsvik and Cocks, 2004, 2005] Pangea would last until Mesozoic when the supercontinent started breaking up in stages. The breakup of Pangea triggered major rifting phases initiated since the separation of Greenland and Norway in Late Palaeozoic, and formation of the Northeast Atlantic Ocean in Early tertiary (54 Ma) [Brekke et al., 2001, Torsvik and Cocks, 2005]. Norway has been relative still, beside uplifting and extensive isostatic adjustment during the last 3 Ma. The main cause of this is deglaciation and regional uplift of the mainland area, and deep erosion of the Barents Sea shelf. Also deposition of sediments along the Norwegian-Greenland Sea [Brekke et al., 2001]. All these processes are suggested to cause seismicity in Norway.

2.1.2   Local Geological setting

The structural framework of Northern Norway encompasses major extensional shear zones and compressional structures. The shear zones vary in orientation, from NE-SW trending

extension (oblique to the orogeny) in northern Central Norway to approximately E-W trend in northern Norway [Rykkelid and Andresen, 1994b, Braathen et al., 2002b]. NW-SE horizontal normal extensions faults have been identified in northern Norway [Hicks et al., 2000a, Dehls et al., 2000, Olesen et al., 2013a]. The offshore parts of northern Norway are mostly strike-slip and reverse faulting, while the focal mechanism solutions onshore are dominated by normal faults. These are suggested to have been formed or reactivated in Devionan time, during the gravitational collapse of the Caledonian mountain belt [Rykkelid and Andresen, 1994a, Braathen et al., 2000, 2002a, Olesen et al., 2002, Nordgulen et al., 2002, Osmundsen et al., 2003, Osmunden et al., 2003].

Neotectonic activity has been identified in Nordland [Olesen et al., 2000, Dehls et al., 2000, Olesen et al., 2004, 2013a]. Studies around the Ranafjorden [Olesen et al., 1995, 2000] have suggested that E-W trending Basmoen Fault most likely experienced post glacial movement. These studies of neotectonics activity have uncovered crustal movement, especially in the northern Fennoscandia, and proven that areas previously considered as stable, are in fact frequently hosting earthquakes swarms at shallow depths [Bungum et al., 1979, Atakan et al., 1994, Olesen et al., 1995, Hicks et al., 2000a, Pascal et al., 2005, Olesen et al., 2013a]. Because of the present stress conditions, structures in this area has the potential to reactivate. Likely to cause movements along preexisting zones of weakness [Gabrielsen et al., 1986].

The stratigraphy of mainland Nordland is mainly composed of the thrust nappes that derived from the Caledonian Orogeny. The Caledonian nappes of high grade metamorphic shales, were thrusted onto Precambrian granitic gneiss basement during the Scandian continent - continent collision [Roberts and Gee, 1985, Olesen et al., 2002]. The Nordland area is dominated by the Uppermost Allochthons. Additionally, the Lower unit (Rødingfjell nappes) occur locally in the area, with visible Precambrian basement [Hicks et al., 2000a].

2.2 Seismicity

Seismicity is defined as the distribution of earthquakes in a region (geographic) or historical. Historical data indicates that earthquakes occur along the coast of Norway and surrounding offshore areas frequently [Olesen et al., 2013b]. Magnitude 5 or larger occurs every 8-9 years, in Nordland more specific Rana area, the largest known historical event in 1819 had a M_S of 5.8 [Wood, 1988, Bungum and Olesen, 2005].

The seismicity in Norway is low to intermediate in intensity and located in the upper 30 km of the crust. The seismicity of mainland Norway is entire intraplate, and is concentrated along the rifted continental margin. Especially in the heavily faulted regions near North Sea shelf edge. The onshore parts of mid-Norway is split when it comes to seismicity. The southern part is almost aseismic, while the northern part is experiencing a high level of shallow seismic activity. Which may be because the southern part has a low elevation, while the northern part has a large region with high elevation (topography effects). The understanding of seismicity in Norway has improved over the years with the advances in instrument quality and coverage, especially around the coastal areas and northern parts [Havskov et al., 1992].

2.2.1 Earthquake Swarms

Earthquake swarms are defined as earthquake sequences of seismic events that are spatially concentrated and occur over longer periods of time [Mogi, 1963, Bungum et al., 2010]. They can occur on both interplate and intraplate settings, and all types of tectonic regimes. In the northern part of Norway, events occur at shallow depths (0-10 km) with low magnitudes, and hence characterized as low to intermediate [Bungum et al., 1991].

Earthquake sequence can be distinguished between foreshocks, mainshocks and aftershock distribution and earthquake swarms. earthquakes commonly involve initial foreshocks (smaller earthquakes preceding the mainshock), followed by a mainshock, with subsequent aftershocks (smaller earthquakes following the largest shock of an earthquake sequence). This mainshock type will have a sudden increase in stress rate that will release seismic activity. An earthquake swarm will be a series of many earthquakes with no large quake followed by smaller ones i.e. no distinct main shock, but mostly events about the same size [Sykes, 1970]. The seismic activity will increase proportional to the increasing stress rate.

2.3 Seismicity in the study area

The seismicity in Nordland show a clear coastal trend with a constant level of seismic activity, with occurrence of specific clusters in time and space and frequently associated with the neotectonic faults in northern Fennoscandia. The occurrence of earthquake swarms can be explained by the different forces that act on the Nordland coast area. More detailed studies have shown that swarms in Nordland region have a power law distribution similar to other earthquakes, which is not that different from ordinary earthquakes. Regions where earthquake swarms occur have commonly been affected by a large numbers of glaciations cycles over time and extensive glacial erosion. Examples of this include the North Atlantic, Svalbard, western coast of Greenland, Canada, as well as northern Norway. Bungum et al. [2010] question if the shallow normal faulting earthquakes that occur in the coastal zone of northern Norway are related to the continuous post glacial uplift, or to erosion or sedimentation. However, their study suggest that post glacial rebound is still a source of stress for seismicity in the northern Norway [Hicks et al., 2000a, Bungum et al., 2010].

2.3.1 Earthquake Distribution

Byrkjeland Bungum and Eldholm [2000] showed that the seismic activity is irregular distributed, and that it follows the tectonic features like the margin, sedimentary depocenters, failed continental rifts and the coast line. Most of the earthquakes in Norway occur close to the Viking Graben lineament in the North Sea, along shelf edges from the northern Norway to Svalbard and along the coast of western and northern Norway [Bungum et al., 1991]. Fig. 5 shows events recorded for Nordland between August 2013 and March 2016, distributed along the coast at depth within 20 km. Seismic studies in

the Steigen, Meløy and Rana area suggest the seismicity to be swarm related [Bungum et al., 1979, Atakan et al., 1994, Hicks et al., 2000a]. Over 10 000 events was recorded at stations during 10 weeks at Meløy. In Steigen 207 events were recorded within a year. The observed mechanisms implied that they were generated by the same stress directions [Bungum et al., 1979, Atakan et al., 1994]. Similarities between these two sequences are of interest, including their time of occurrence are only 13 years, geographical locations differ with 100 km, shallow focal depths (5-8 Steigen, 3-9 Meløy), and similar NE-SW fault plane solutions. However, their duration times differ, as Meløy lasted for 4 months and Steigen for one year. Also their dip directions are opposite, Meløy Oblique fault plane has a prominent SE dip, whereas the Steigen fault shows prodominent NW dip [Atakan et al., 1994].
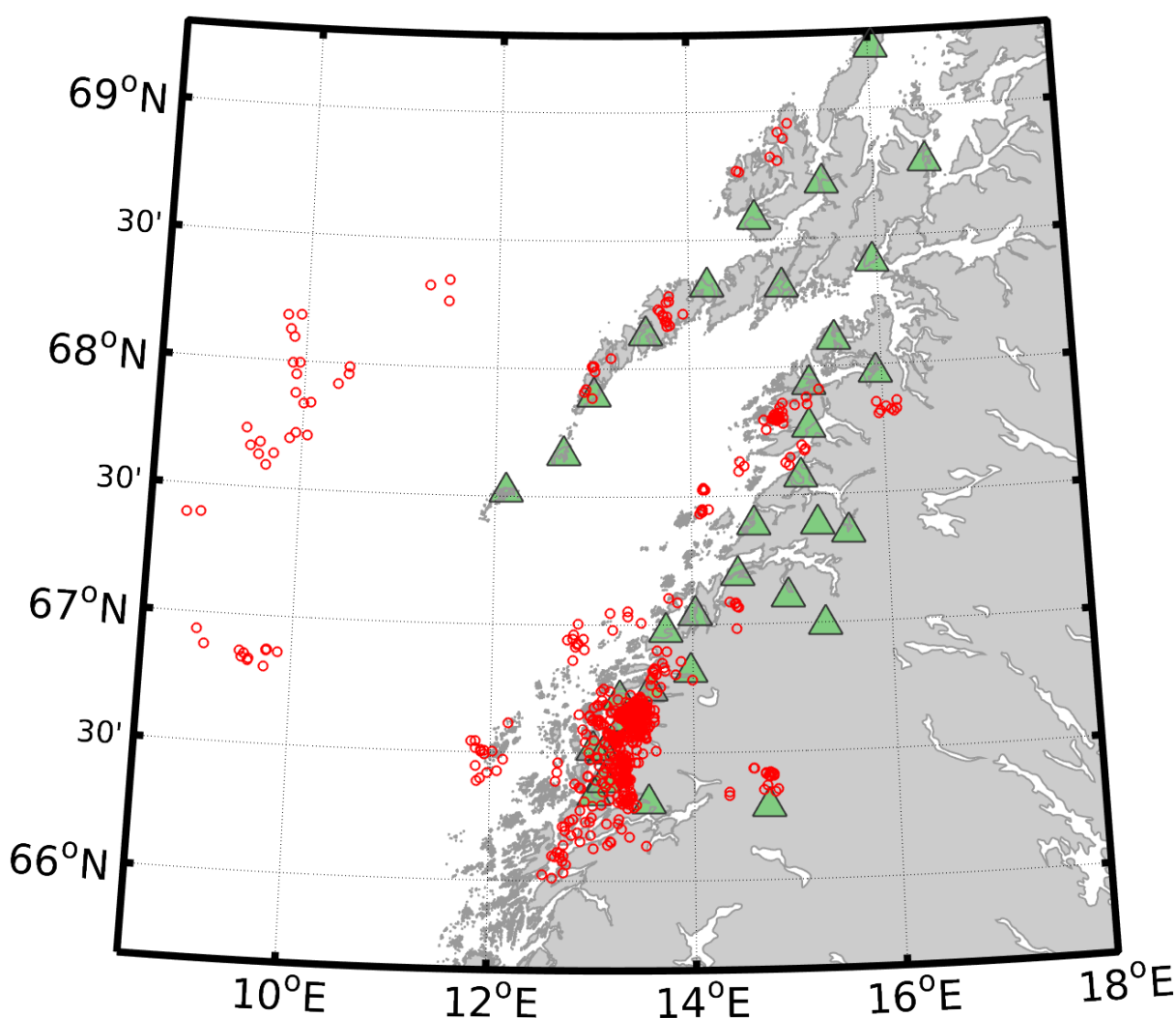

Figure 5: Map of the seismicity in the Nordland area between August 2013 to March 2016 gathered by the Norwegian National Seismic Network (NNSN). The green triangles indicate the different seismic stations in the area, while the red dots shows the locations of the events (absolute location). Seismicity on the map shows that there is a clear coastal trend.

2.3.2   Cause of Earthquakes

To explain the seismicity in Northern Norway region, one has to account for several forces and geological processes, both regional and local factors has shown to influence the seismicity. The seismicity depends on the stress regime. In the Fennoscandian, the suggested main sources of stress are ridge push from the mid-ocean ridge in the Atlantic (plate-related), post glacial rebound, lateral variation in lithospheric structures (density difference) and topography (mountains) and flexural stress (loading and unloading) shown in table 1.[Hicks et al., 2000a, Fjeldskaar et al., 2000]. The dominant stress mechanism in northern Norway is suggested by [Bungum et al., 2010] to be plate-related stress from the ridge push, which is capable of exerting stresses in the order of 20-30 MPa. However, this is not enough to explain all the seismicity along the area.

Earthquake focal mechanismes solution and overcoring measurements reveal a predominance of normal faulting, with the tensional stress axis perpendicular to the coastline [Hicks et al., 2000a]. Fig. 6 shows directions of horizontal stress [Hicks et al., 2000a], formed with the different stress induced processes mentioned above. Direction of the normal extension, cannot be explained only with the ridge push force. Where we might expect more reverse faulting and different orientations. Indicate that other sources of stress must play a part, to form normal faults with extensional stress in NW-SW and W-E direction.
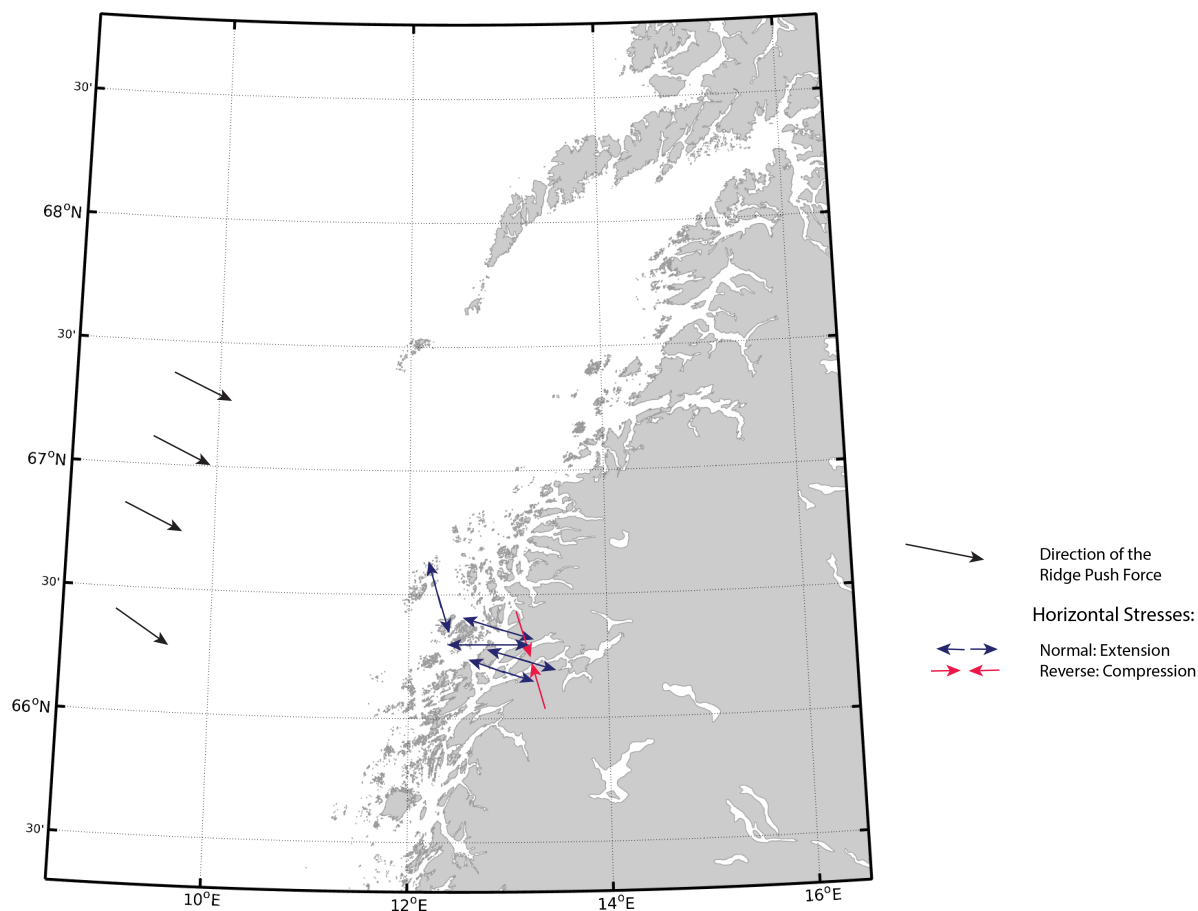
Figure 6: Map of the Nordland area with showing horizontal stress from focal mechanisms solutions and overcoring measurements gathered from Hicks (2000) and ridge push force from the North Atlantic ridge. Normal faulting is plotted with blue arrows in a direction of horizontal tension, Reverse faults are plotted with red arrows in a direction of horizontal compression. The sources of stress sediment loading create vertical stress around the coast, the same effect counts for high mountains(topography) at the coastal area. Post glacial rebound also act like a vertical stress, only the opposite direction that sediment loading and topography.

Another controlling stress source appears to be the post glacial isostatic rebound [Hicks et al., 2000a, Bungum et al., 2010]. Studies have shown that since the end of the last ice age (approximately 10 000 years ago), seismicity has increased in the northern Fennoscandia. This is due to a combination of high pressure, crustal deweighting and tectonic compression changes [Wood, 1989, Hicks et al., 2000a, Bungum et al., 2010]. The rate of uplift is calculated with data from tide gauges, accurate levelling and GPS, and gravity measurements. Fjeldskaar et al. [2000] found the rate of uplift is close to zero along the Norwegian coast. Increasing to 8 mm/yr in central parts of Baltic Sea, and in northern part up to 19 mm/yr. The estimated uplift gradient field has a maximum in Nordland [Keiding et al., 2015]. It is yet to find out how much regional uplift effects the local tectonic response.

Sedimentation and erosion is another cause suggest to a role in the present day seismicity [Fejerskov and Lindholm, 2000]. During the Tertiary time period, almost simultaneous with the opening of the North Atlantic ocean, there was an increase in sedimentary accumulation and subsidence in the continental margin. This was resulted by regional uplift along the Norwegian mainland, exposed for erosion, and sourced a sedimentary cover, unconformable above Precambrian crystalline rocks [Bungum et al., 1991, Torsvik and Cocks, 2005]. Sediment loading is a stress generating mechanism that may induce large exural stresses. An example is the Lofoten basin influenced by a rapidly accumulation of deposits [Olesen et al., 2013b]. In the Nordland area the seismicity increases around the shelf edges, suggesting that rapid sediment loading from the Pliocene-Pleistocene glacial wedge has reactivated the faults of Late Jurassic-Early Cretaceous. Additionally, pre-existing faults zones may represent weak zones in the crust, and therefore tend to localize earthquakes and reactivate during preferential oriented stress conditions, like crustal fluids or movement of the crust.

The NEONOR project from 1997-2000 was the first project aimed to assess the neotectonic activity in Norway, using earthquake records and GPS measurements that would measure faults, stress, monitoring of seismicity together with borehole data, and observations of stress release features. All indicated that there is neotectonic activity around the Nordland area [Olesen et al., 1995, Dehls et al., 2000, Hicks et al., 2000a, Olesen et al., 2004]. The NEONOR2 project is a continuation to try determine the causes of the movements.

Stress field	Lateral endurance	stress generating mechanism
First order (continental)	1000 km	Plate tectonic force Ridge push
		Ridge push
First order (continental)	100-1000 km	Large-scale density
		inhomogeneities
		flexural stress
		Deglaciation
		Sediment loading
		Major topographic loads
Third order	100 km	Topography
		Fjords
		Mountain ranges
		Geological feature
		Faults

Table 1: Table from Fjeldskaar et al. [2000], show the different stress forming mechanisms.

3 Data and Methods

This chapter gives an overview of the data, relocation process and the applied methods used, to gain better understanding of the seismic activity in northern Norway. Analysis of the Nordland Norway seismicity requires the use of different software's, including Matlab 2015b, SEISAN [Ottemöller and Havskov, 2014] and HypoDD [Waldhauser, 2001].

3.1 Waveform Data and Processing

The full data set for my study consists of 1208 local earthquakes located in Nordland. The earthquakes are recorded by seismometers from the Norwegian National Seismic Network (NNSN) (Fig. 7) and the NEONOR2 project (Fig. 8), in a time period between August 2013 to March 2016. The seismometers are operated by the University of Bergen (UIB) department of Earth Science. The majority of the stations used in this study were deployed under the NEONOR2 project. The NNSN consist of 33 single seismic stations that monitor both onshore and offshore seismic activity in Norway and the artic islands Jan Mayen, Bjørnøya and Svalbard. The stations are distributed around Norway, but for my study the stations located near the northern Norway area are of highest importance. The waveform data are stored in miniSEED format and processed in SEISAN after the data is gathered. MiniSEED recording data is the standard, and is usually kept in one format for simplicity. Before using miniSEED data it is necessary to convert them into S-files for use in SEISAN and hypoDD.
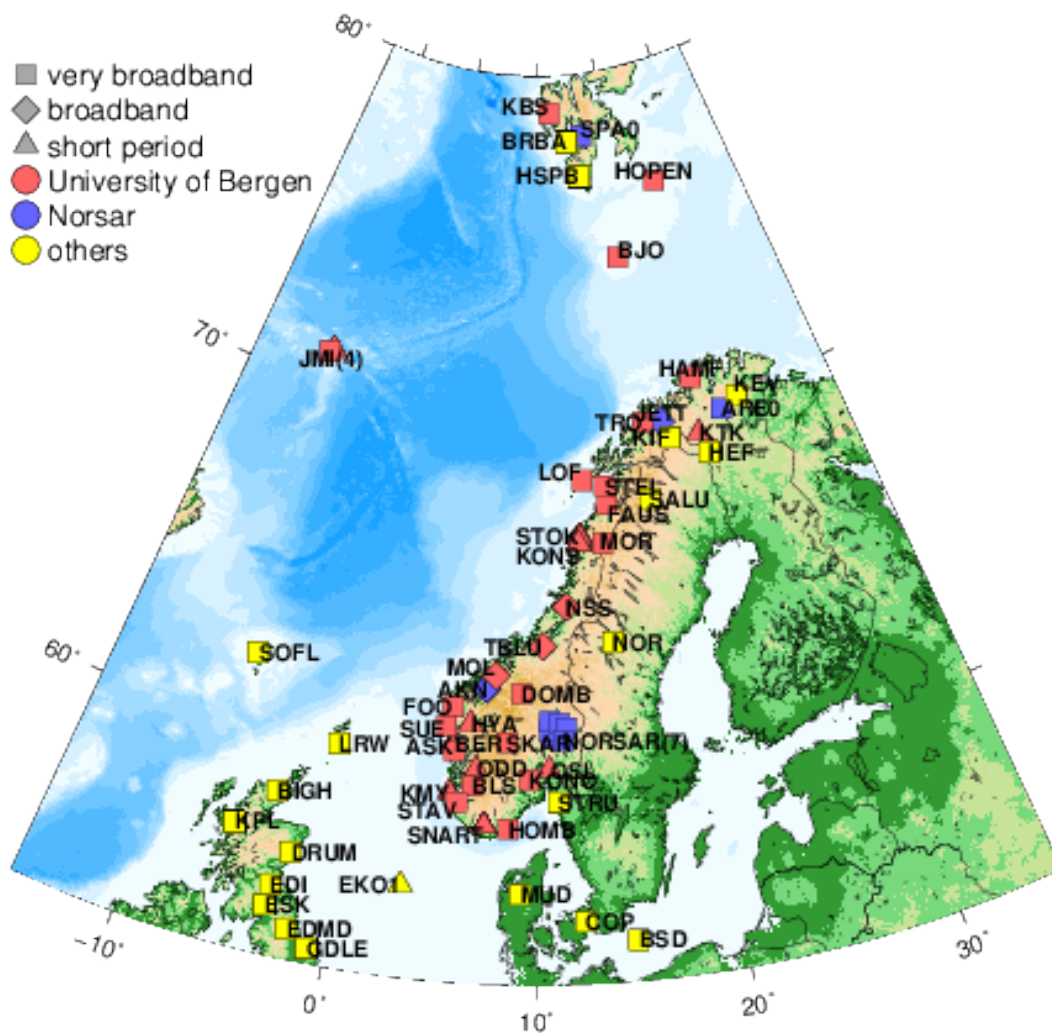
Figure 7: Map of the different seismic stations distributed in Norway, operated by NNSN, NORSAR and others. Where the department of Earth Science, University of Bergen has the main responsibility to operate the 33 stations. For my study the seismometers in the northern Norway area are of highest importance, gathering the most precise data used in hypocenter location and cross correlations.
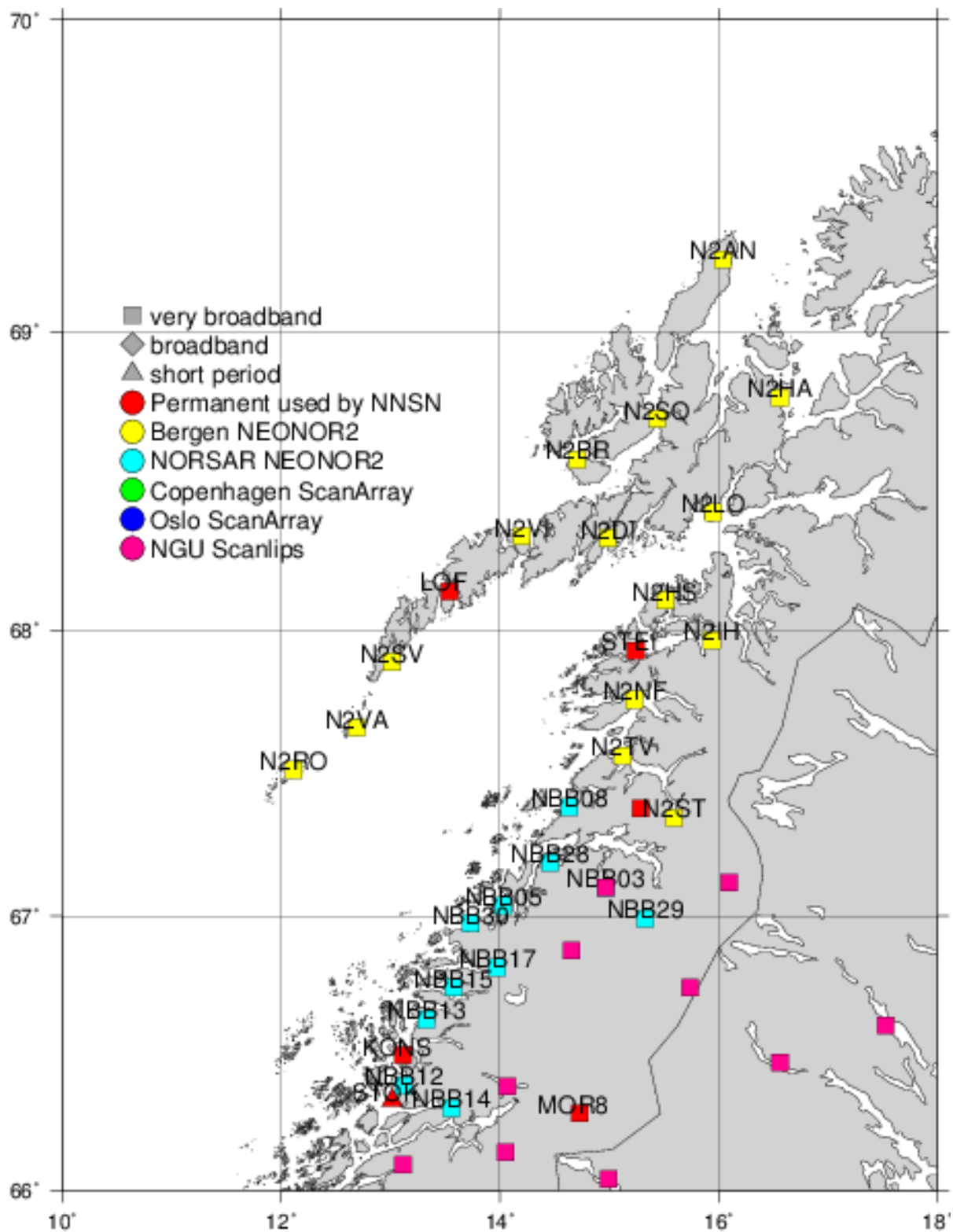
Figure 8: Map of stations in northern Norway, includes the stations deployed for the NEONOR2 project and the permanent local stations.
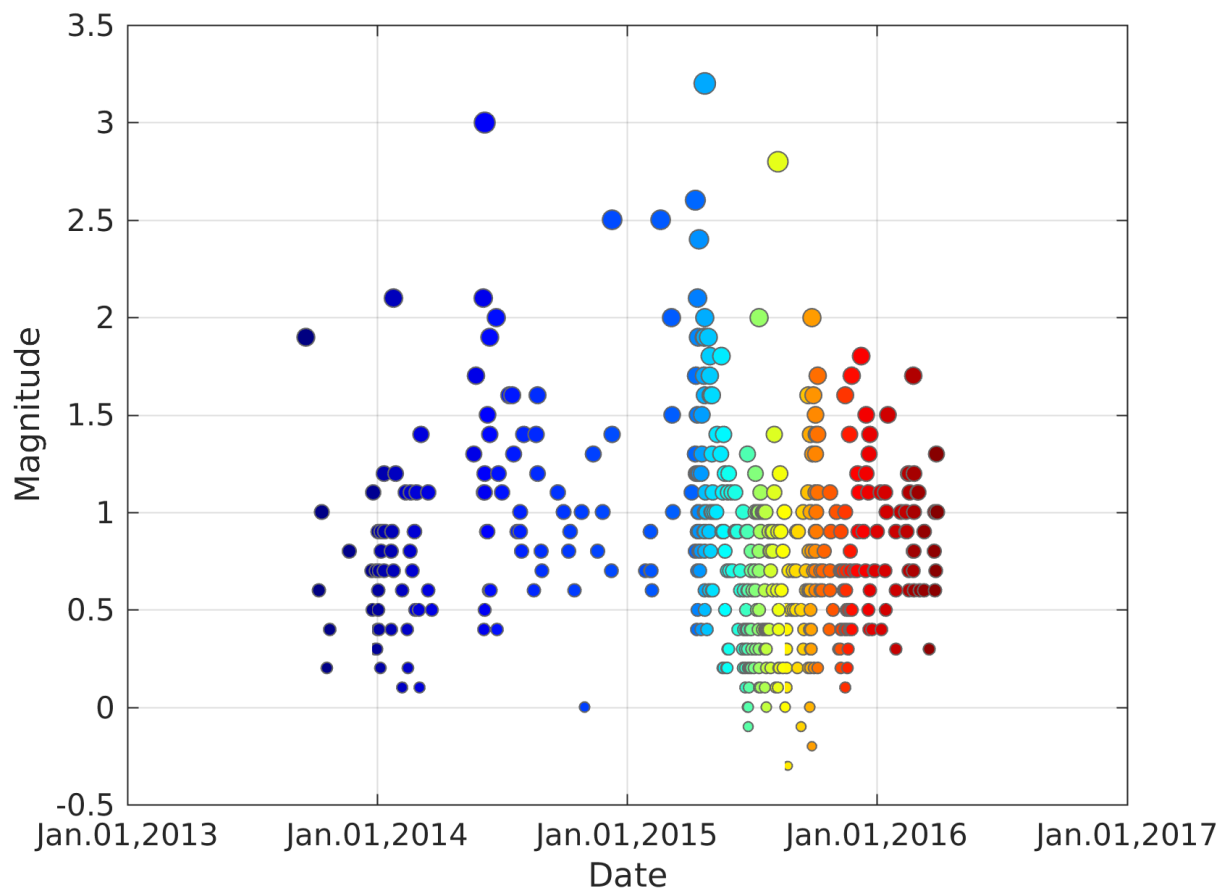
Figure 9: Magnitude range in M_L through time for the relocated events.

3.1.1 SEISAN - Earthquake Analysis Software

SEISAN v10.3 is a data processing software developed by Havskov and Ottemöller, used for analysis of earthquake data and observation. It can be used to process earthquakes and obtain number of parameters. P and S-waves values for number of chosen earthquakes, picking phases, travel times, focal mechanism, spectral parameters and finding hypocenter location for local and global earthquakes. The software offers an efficient way to gain information about the events. The P and S-wave arrival times are picked manually for datasets. The miniSEED files is later converted into SEISAN format (S-files) for further processing in the SEISAN software. The system uses a filesystem that is organised into multiple subdirectories shown with Fig. 11. The files contain information about the event like arrival times, amplitude, period, azimut and apparent velocity. Used for my study to locate hypocenters and form catalogue data.

The processing of seismograms in SEISAN shown with Fig. 10. Starts with choosing a correct filter (frequency range), usually to enhance the signal to noise ratio (SNR). Must be handled with care due to the filtering may change the shape of the wavelet and lead to phase shift of the signal. If possible, the phase does not contain a lot of noise, the phase should be picked without applying a filter. Relative high frequency filters or band pass filters are applied, when processing local earthquakes and the magnitude is small. The

next step after the filtering is to pick phases and polarity (if focal mechanisms is needed). Picking the proper phases (P and S) and as many as possible from all stations would contributes in decreasing the location error to get a more accurate estimate of the location of the earthquake and origin time. For my study area the most normal phases picked are P, S, Pn (Moho refracted P phase), Sn, Pg (Direct crustal P phase), Sg. The P-phase is picked on the vertical component because it usual records the highest amplitude for compression, the same counts for the S-phase on the horizontal component. The amplitude is also measured on the Z-channel, selecting a window on the trace picking where the maximum amplitude is strongest, it is important to assure that the maximum amplitude is picked (may also be picked on the horizontal) when defining the local magnitude, to get the local magnitude M_L for the events using the Wood-Anderson seismograph.
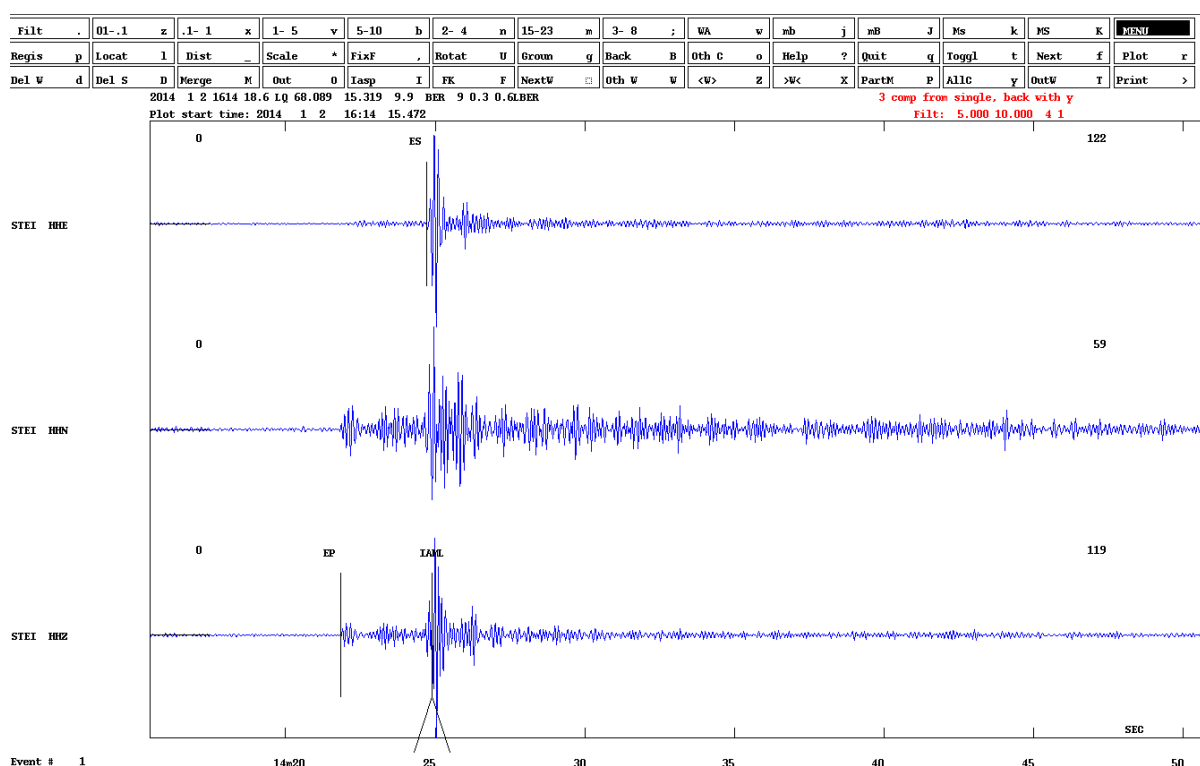
Figure 10: example of picking phases in SEISAN on a three-component seismometer. P-phase is picked on the vertical component together with the amplitude and the S phase is picked on the horizontal component. The seismograms are filtered with a 5 to 10 Hz band pass filter.

After picking as many phases as possible the next step is to use these phase readings to locate the events with SEISAN using an inversion program called HYPOCENTER [Lienert and Havskov, 1995, Ottemöller and Havskov, 2014], the hypocenter location process is further described in the next section.
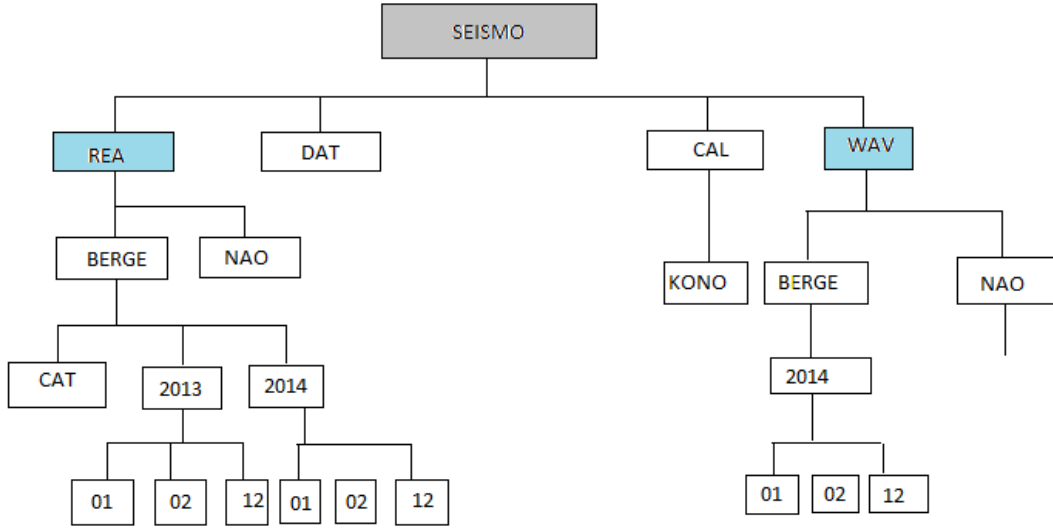
Figure 11: Structure of SEISAN filesystem. Illustration of the Database with two directories and its subdirectories. The database has two directories REA and WAV. REA is subdivided into multiple directories, that are created by the user to store all event data that are going to be looked at and analyzed. The SEISAN system is located under a main directory called seismo, with several subdirectories that contain files and information that is used to run the programs. WAV directory can also be subdivided into multiple directories in case of large numbers of waveform data. To store data in the WAV database the waveform names must be yymm(1303) or yyyymmdd (20130303).

3.2   Standard hypocenter Location

Locating an earthquake is an inversion problem which can be expressed as follows:

$$d = A(m) \tag{3.1}$$

where d=given data, A=function relating measured data to the model parameters and m=model parameters. Solving the inverse problem involves finding the model, m, given the data d. Basically shows how the data can be calculated from assuming a model. For the earthquake location problem, the data are the travel time of the waves picked as wave arrivals at stations. Model parameters are the earthquakes location (source location and origin time, $m = (x, y, z, t0)$).

The location of the earthquake or the hypocenter location labeled with x_0, y_0, z_0 is the physical location of an earthquake (Fig. 12). The basic method for determine hypocenters locations with several stations available, is the iterative method, based on linearizing the inversion problem. First step, is to start by guessing a start model (hypocenter) and origin time x_0, y_0, z_0 t_0, by closing in on the real hypocenter through iteration (Fig. 13). First, t_0, the origin time, is set to as the first arrival time using a location near the station.
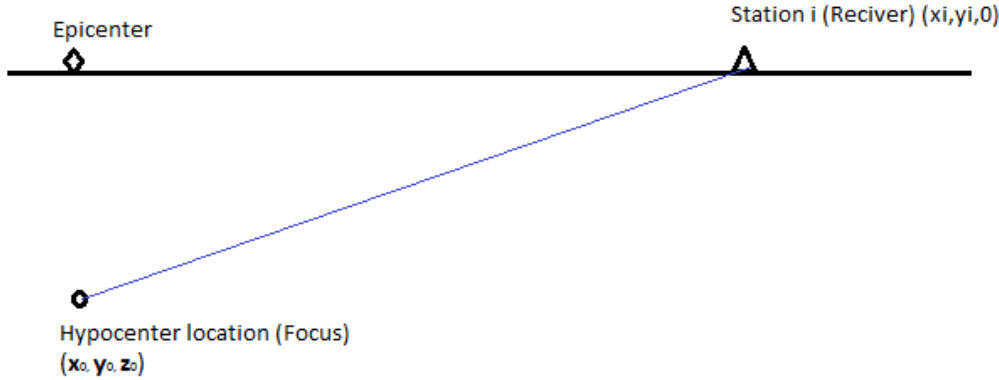
Figure 12: Simple illustration of Earthquake location (hypocenter) shown with x_0, y_0, z_0, the station reciving the seismic signal from the earthquake indicated with x_i,y_i,0 and the epicenter right above the hypocenter location. Modified from Stein and Wysession [2003].

We assume that the true hypocenter is near the guessed value in order to linearize the problem. The corrections required to move the trial hypocenter to the true hypocenter are a linear function of the travel time residuals. We then use the calculated arrival times at a certain station, from the trial location. The residuals we get is due to errors in hypocentral parameters. Arrival times contains errors because of uncertainties like the geology in the subsurface is not perfectly known, mistakes in the processing or effects like noise. Best way to solve these error is to seek the origin time and source locations that solve the overdetermined. Ideally we want to minimize the residuals by iterations, to get as close to zero as possible (for each iteration a smallest misfit to the data). Higher residuals mean that more correction needs be applied to the solution. To correct for the residuals we use Taylor series, which we use to calculate the corresponding correction that has to be made in travel times equation (3.2).

$$\Delta di^o = di' - di^o \approx \sum \frac{\partial di'}{\partial mj}\bigg| m^o \Delta mj \tag{3.2}$$

Equation (3.2) want to solve it for Δmj This expression represent the change that is applied to the starting (guessed) start model (m^o) for each iterations [Stein and Wysession, 2003]. Δdi^o is the difference between the observed and calculated travel times. di' is the observed travel time. di^o is the calculated travel time. $\frac{\partial di'}{\partial mj}$ is the partial derivative matrix. Consider di' as having the errors.

The solution is obtained with the least square method which gives Δm. The original trial solution is then corrected and improved with the results of the inversion $d = Gm$.

The new solution is used as the trial solution for the next iteration. This procedure is repeated till we have the smallest misfit between our data (smallest residual), and achieved

the maximum improvement to the location illustrated with (Fig. 13. The iteration method
is used in the SEISAN software to locate hypocenters. Furthermore, inversion for station
corrections can reduce errors introduced by a simple velocity model and lead to improved
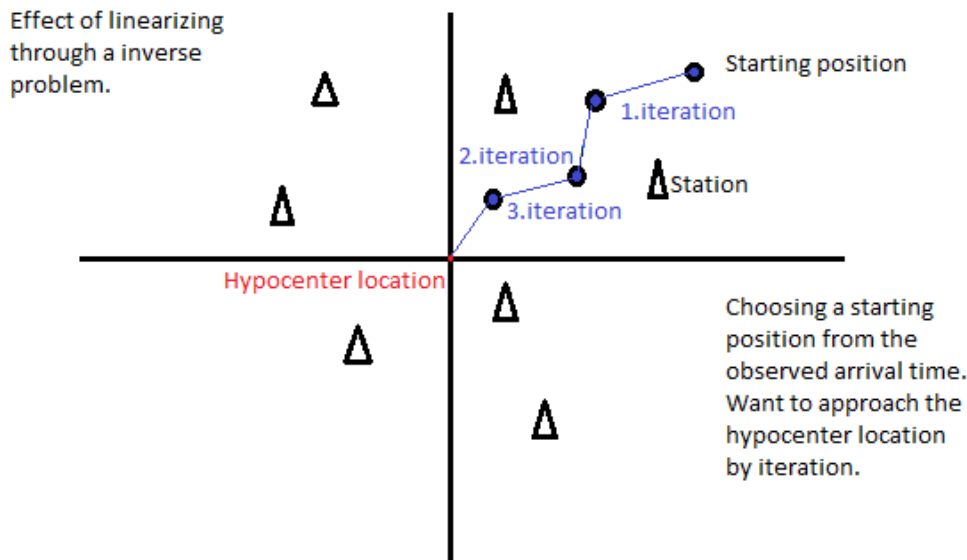locations.

Figure 13: Illustration of finding the earthquake location by iteration and the effect
of linearizing. By finding a new model with values from the predicted models and the
observed data from the starting position, then moving closer to the hypocenter location
by each iteration, till finally the error are minimized as much as possible (residual are as
close to zero as possible).

3.3   Double Difference Earthquake Location Algorithm

Double difference earthquake location algorithm of Waldhauser and Ellsworth (2000) is
used to relocate seismic events. The method is used to determine high resolution hypocen-
ter locations over large distances, without the use of station corrections [Waldhauser and
Ellsworth, 2000]. The aim of the double difference algorithm is to improve relative loca-
tion accuracy by calculating travel time differences between pairs of events, adjusting the
location of the pairs relative to one another that will result in a minimization of the travel
time residuals (reducing errors) of earthquake pairs. Improvements in relative locations
are clearly shown in the results in Waldhauser and Ellsworth [2002].

The difference between standard hypocenter location and double difference location is
that it allows us to use precise travel time differences obtained through cross correlations
P and S wave differential travel times. These differential travel times will determine the
relative locations of the waveforms, which can be used to calculate accurate P and S-wave
differential travel times. Together with any combination of manual phase readings from
earthquake catalogs, that determine the absolute locations. The cross correlation times
calculated for similar events can achieve a reduction in relative location errors. Relative

errors are reduced by a factor of ~ 2 using catalog arrival times and further reduced by a factor of $\sim 5 - 10$ using catalog arrival times together with cross correlation data, shown with a synthetic test [Waldhauser and Ellsworth, 2000, Hauksson and Shearer, 2005b, Balfour et al., 2012]. No source or station corrections are required, because one of the basic assumptions in double dfference relocation is that events are so closely located to each other that the effect of velocity inhomogeneities can be disregarded.

With this assumption, the double difference equation is linearize the location problem, by minimizing the residual between observed travel times and theoretical travel-time difference for pairs of earthquakes at each stations. Using a velocity structure that is suitable for the seismicity area, the algorithm will minimize errors, without the use of station correction. If two earthquakes with a hypocentral separation which is small compared to the source receiver distance, the velocities along the ray paths for these earthquakes are very similar. Most of the influence of velocity heterogeneities will be gone, and the only requirement will be the velocities in the source region. The vector differences between hypocentral pairs is changed by iteration, by finding the least-squares solution. This method is useful and works better in regions with earthquake swarms, or a dense distribution of clustered events, where the event distances are only a few kilometers or less from each other. Linking thousands of events together, it is possible to get high resolution hypocenter location over large distances. To estimate the accuracy and location errors, a statistical resampling method is applied. The uncertainties in the equation are improved by an order of magnitude or more compared to catalogue locations.

3.3.1   Double Difference Algorithm

The double difference method uses differential travel time data from accurate cross-correlation measurements, or travel times picks (catalogue data), or a combination of both. The precise travel time differences are used to determine relative locations while catalog data are used to determine absolute locations [Waldhauser and Ellsworth, 2000].

Given a ray path expressed with k, Where T is the arrival time for an earthquake at i the Seismic station, τ is the origin time of the event i and u is the slowness field. The relationship between the travel time and the event location is nonlinear [Geiger, 1910]. A linearization has to be performed, because the data do not depend linearly on the model parameters, which can be achieved by expanding the location problem in a Taylor series for m [Stein and Wysession, 2003].

$r_k^i = (t^{obs} - t^{cal})$ gives the travel time residual r_k^i, t^{obs} is the observed t^{cal} is the theoretical travel time, for an event i recorded at a station k (Fig. 14).

$$\frac{\partial t_k^i}{\partial m}\Delta m^i = r_k^i \tag{3.3}$$

A linear equation, where perturbation Δm_i is related to travel time residuals vector r of model parameter vector m, hypocentral parameters for the earthquakes location is the model parameters. Equation (3.3) i used for measured arrival times.

$$dr_k^{ij} = (t_k^i - t_k^j)^{obs} - (t_k^i - t_k^j)^{cal}. \tag{3.4}$$

Eguation (3.4) is the double difference. dr_k^{ij} is the residual between observed and calculated differential travel time between two events. Using either phases with measured arrival times, where t is the observed absolute travel times, or cross correlation relative travel-time differences.

$$\frac{\partial t_k^i}{\partial m} \Delta m^i - \frac{\partial t_k^i}{\partial m} \Delta m^j = dr_k^{ij} \tag{3.5}$$

Followed the linearization for earthquake location, using the double difference equations [Waldhauser and Ellsworth, 2000]. Events i and j, recorded at station k. From equation (3.3) we find the change in hypocentral distance between two events i and j, using travel time difference residuals ("double difference") $r_k^i = (t^{obs} - t^{cal})$ and using slowness vector and origin term for the events.
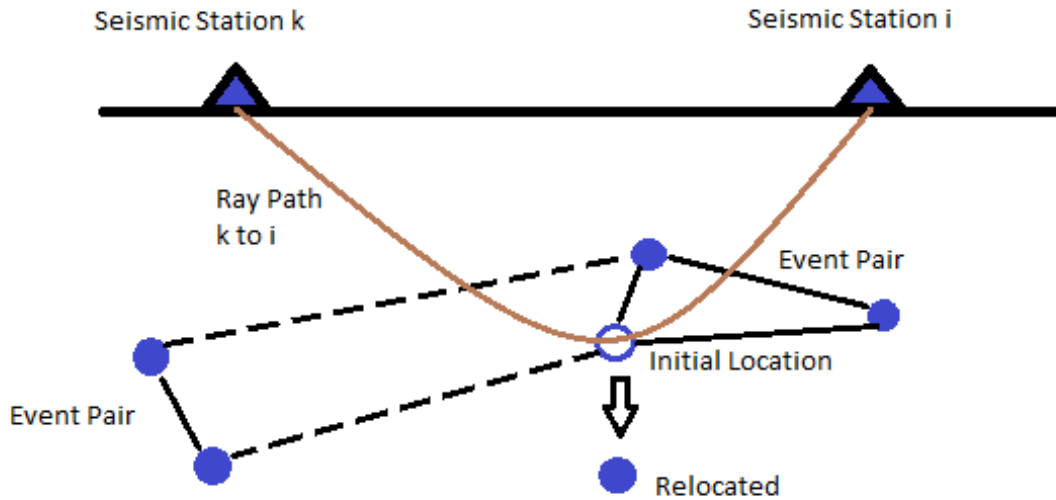
Figure 14: An illustration of the relocation process. The dots are showing the trial hypocenters that are connected to the nearby events by cross correlation(solid lines) or catalog data(dotted lines), also referred to as neighbor events. The open dot indicates the initial location for the event. The arrow is pointing from the initial location of the event to the relocated event, obtained from equation (4). Ray paths are shown with the brown line between station A and B (travel time differences, slowness vectors).

For the current hypocenters and location, it is necessary to calculate the partial derivatives of the travel times t for the events i and j, with respect for their location (x,y,z) and origin time (τ). To make the model fit the data better, we must add changes from Δx, Δy, Δz and $\Delta \tau$ in hypocenter parameters. We have to minimize the double difference

residuals for pairs of event at each station, to solve the hypocentral parameters for each event. New and updated locations and partial derivatives are obtained after the iteration process. Where the same steps are repeated until the residuals are small enough. Before that a system of equations is formed.

$$WG\Delta m = W\Delta d, \qquad (3.6)$$

Equation (3.5) is a system of all hypocentral pairs for a station, and all stations (equation 3.5 written out full) to form a system of linear equations (3.6). W contains the quality weights in a diagonal matrix. G is a partial derivative matrix ($SizeM * 4N$) of the theoretical travel time difference to the model parameters [Waldhauser and Ellsworth, 2000]. Δd is the data vector of the double difference travel times for all event pairs, that contains the changes in hypocentral parameters. Δm is a vector of length 4N that contains the change in the hypocentral parameters that we want to find.

Since this is an inverse problem, we solve it to change the model Δm. That gives the change in Δd when multiplied with the partial derivative matrix G [Stein and Wysession, 2003].

The matrix G of partial derivatives cannot be inverted before it is changed to a square matrix $G^T W$. Equation $\Delta m = (G^T W^{-1} G)^{-1} G^T W^{-1} d$ gives Δm the least square solution. Generalized inverse of G gives the best solution in a least square sense and results in the smallest misfit [Stein and Wysession, 2003].

$$W \begin{pmatrix} G \\ \lambda I \end{pmatrix} m = W \begin{pmatrix} d \\ 0 \end{pmatrix} \qquad (3.7)$$

Iteration process:

Solving equation (3.6), we find the change that needs to be applied to improve the starting model, using the start model and a priori weights. The process will repeat itself using the new improved model with updated locations, residuals and the partial derivatives in G. The double-difference residuals for pairs of events at each station are minimized for each repeat. This process will continue till we have reached its maximum number of iterations (chosen in the hypoDD.inp) or when the change in solution vector is below a chosen threshold [Waldhauser and Ellsworth, 2000].

To iterate we use a prior weight to get the best possible stable solution (5 using LSQR), continuing to iterate by reweighting the data. Data that is reweighted is iterated with distance and misfit weighting applied. Observe from the output table 6. from hypoDD, where the forth (CT) and fifth (CC) column give the percentage of catalog data and cross correlation data, used in each iteration. The values tell us how much data is removed by reweighting. If the columns show 100 percent no reweighting has been done, but if there is for example 91 percent, there has been applied some misfit and weighting to the data.

For a small well-conditioned system with event from < 100, $WG\Delta m = W\Delta d$ equation can be solved by the method of singular value decomposition(SVD). Advantage from using SVD is a estimation of proper least square error.

For a larger system SVD is inefficient (with event > 100), solution to the equation $\Delta m = (G^T W^{-1} G)^{-1} G^T W^{-1} d$ is found by using the conjugate gradient algorithm LSQR [Paige and Saunders, 1982].

$$\left\| W \begin{pmatrix} G \\ \lambda I \end{pmatrix} m - W \begin{pmatrix} d \\ 0 \end{pmatrix} \right\|_2 = 0 \tag{3.8}$$

LSQR finds m by solving the damped least-squares problem. This is a very efficient method and requires minimum storage and is therefore a good choice when solving large problems that consist of thousands of events and million equations [Waldhauser and Ellsworth, 2000]. If the condition system and initial locations are precise, iterations from 5 to 10 are necessary to solve large problems.

The double difference equations are used to combine each event to neighboring events, and achieve a connection with all events so that the adjustments that has to be done for each hypocenter can be resolved for all at the same time.

3.3.2   Cross Correlation

Correlation is calculated between to time series, and give indications of how strong the relationship between the time series are. Correlation over many different time shifts is called cross correlation.

$$w(t) = u(t) \star v(t) = \int_{-\infty}^{\infty} u^*(\tau) v(\tau + t) dt \tag{3.9}$$

u and v are continuous functions, representing two time series. w(t) is called the "lag" (delay of u versus v). $\tau =$ is the time shift

$$w(t) = u(t) \star v(t) = \int u^*(\tau - t) v(\tau) dt \tag{3.10}$$

at the time lag where $u(\tau - t)$, is most similar to(best matches) $v(\tau)$

Cross correlation is a measure of similarity of two waveforms as a function of the lag of one relative to the other (sliding dot product). It is useful for determining the time delay between two signals. The result from calculating the cross correlation between two signals, gives the point in time where the signals are best aligned that will be the maximum of the cross correlation function (that is one for my example). In seismology it is used to measure the similarities of waveforms between seismic events, if the similarities are large enough it can determine relative arrival times for seismic waves between two events. Waveform similarities are caused when hypocenter locations are close for two events, indicates form from the same structure. Two waveforms recorded at the same station are considered similar when half of the squared coherency value, in a specified frequency range and time window is exceeding the chosen correlation coefficient [Waldhauser and Ellsworth, 2002]. (Fig. 15) Show four traces, two similar and two not similar. The two similar events shows a high correlation coefficient (almost 1). Suggest that these two signals occur from the same fault.

Using the cross correlation method on similar seismograms to obtain accurate phase arrivals, could reduce the location uncertainty that will lead to more efficient detection of waveforms that are more similar to already known events [Ottemöller and Thomas, 2007]. We obtain differential times of each event pair at a common station using cross correlation.
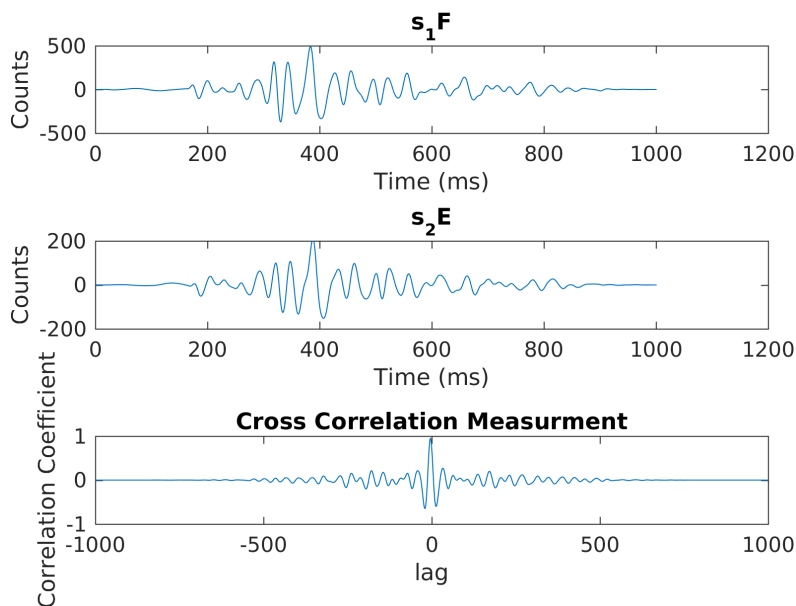
(a) Example of cross correlation between two similar signals (z comp).
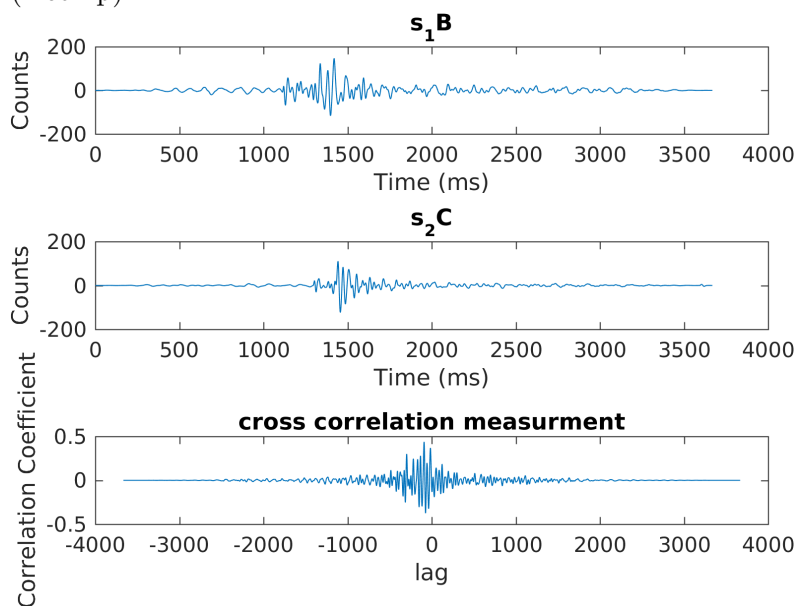
(b) Example of cross correlation between two different signals (z comp).

Figure 15: Cross correlation between two similar signals E and F and two not similar signals B and C, recorded on the same station(N2VG). The two similar events may suggest two events occurring on the same fault. Both filtered in the frequency band with cutoff frequencies at minimum frequency 2 Hz and maximum frequency 9 Hz. By using a Butterworth filter (band pass filter). The vertical component is used for correlating P waves arrivals, seismograms. The time scale and amplitude is similar for all traces.

3.3.3   Cross Correlation Calculation Program CORR

Cross correlation is computed with the program CORR in SEISAN, and can be used to measure relative arrival times. The cross correlation data is used as a input to the HypoDD program (dt.cc). It is using the accurate differential arrival times weighted according to the cross correlation coefficient.

The CORR program gives out the maximum correlation of similar waveforms, that can be used to identify event clusters. Procedure starts with picking phases that is chosen from the list of events. Can select to cross correlate the hole trace or set a phase window. Phase arrival time (absolute time) is given by the maximum of the cross correlation function. The signals are filtered since events have different sizes, and will also give phase shifts to the signals. The CORR program can also be used to determine correlation of a master event, where phases of other events in the list of events created can be determine through cross correlation of the trace window with the master event.

Procedure: File list (filenr.lis) of all events (S-files) using dirf as an input to the CORR program. In my case 881 events. Then select what phases I want to use in the cross correlation either P or S or both. The CORR program needs a list of station that are used in the calculation, one for the P phases and one for the S phases, where also selected the frequency window.

Corr.inp Parameters that have to be modified: S-FILE MASTER: Master event converted to S-file name. An event chosen to be representative for the group of events. Commented it out, because i am running the program to determine cross correlations for all events and identify groups of similar events. S-FILE EVENT: events (S-file name) to be cross correlated with all on listed her, or compared to master event. SFILE INDEXFILE: The filenr.lis created with dirf command of all events is put her, used to give a list of S-file names instead of listing them with the S-FILE EVENT.

Parameters:

Output files: corr.out: Contains all the phase readings, but the content will be different if run in different modes, for example in continuous mode the file contains more than one phase reading per channel and in group identification mode the file will have the event list. corr.trace: contains information about the program for example information about the cause of error. dt.cc: Contains relative phase times and correlation, used as input file to the hypoDD program for relocating hypocenter location. cc_pairs.out: Contains a list of the pairs that are found, S-file of the first event and second event, number of stations and average correlation of all stations.

When the CORR program is finish calculating correlations, it give out an output file dt.cc that is used in the double difference location program HYPODD.

3.4   HypoDD Software relocation of Earthquake

The double-difference earthquake location algorithm is used in a computer program package called HypoDD, for relocating earthquakes [Waldhauser, 2001]. I use the latest version

hypoDD 1.3.

The HypoDD software calculates travel times in a layered velocity model (where velocity depends only on depth), for the current hypocenters at the station where the phase was recorded. The goal is to relocated earthquakes by using all relevant data, often combining them. The hypoDD is carried out by two steps. First step involves an analysis of catalog phase data and/or waveform data to calculate travel time differences for pairs of earthquakes [Waldhauser, 2001]. Step two, is to use the differential travel time data that we obtain from step one, to determine double-difference hypocenter locations.

HypoDD can process any combination of catalog and cross-correlation. Both P- and S-wave data singly and together. While the aim is to relocate earthquakes by combining all the available data, relocating events using each data type independently is useful to assess the consistency of and the relative quality between the data types in order to determine the proper weights necessary for using a combined data set. Cross correlation waveforms are used to minimize the error to make hypoDD more efficient, by reduce the uncertainty in travel time differences between event pair.

3.4.1 Input data

Relocation of earthquakes with hypoDD, includes three steps that are basically used. First, form event pairs and linking them to neighboring events. Event pairs are two hypocenters recorded at common stations, in an area that is predefined (see illustration). Second, create clusters of earthquakes that will improve the image of seismogenic features in situations where adequate data are available [Waldhauser and Ellsworth, 2000]. Third, the double difference relocation using a program in the software called ph2dt. Ph2dt turns catalog P- and S- phases data into input files for hypoDD. Five files are created after running ph2dt. 1) dt.ct 2) dt.cc 3) event.sel 4) event.dat 5) ph2dt.log

To calculate the differential travel times for event pairs the program ph2dt is used to find event pairs. The ph2dt program is establishing links between neighboring event pairs i.e. between event pair that within a certain distance of another event pair. We can set a maximum number of how many neighbors, each pair can link up with, within a chosen distance (area). The area is linked with common stations and phase arrival times. When linking event pairs together and forming clusters, ph2dt also removes delay times that are larger than the maximum expected delay time for event pair, also called outliers. The ph2dt program searches in the catalog P- and S-phase data for event pairs, using travel time data at picked stations to increase the quality of the phase pairs and the connection between them. This will under the next step of the relocation determine the clustering. A cluster is defined as a group of linked events, that is not linked with other groups of events (clusters). The aim by making connection between event pairs, is to develop a network of many links between events, or a chain of connected event pairs. With the smallest possible distance between them.

We must set parameters values to run the ph2dt program. These values are controlling the forming of event pairs, and the input to the hypoDD program. Parameters and some standard values are shown in table 2. The first parameter is the MINWGHT, minimum

pick weight. Any phase used with a picked weights smaller than this number, is being ignored if it is larger than zero. Next is the maximum hypocentral separation distance between event pairs or MAXSEP. This parameter controls the connectivity between events and the amount of events that is connected. If MAXSEP is small, then fewer events are connected. Events that are located (distance) over the set parameter value of MAXSEP from each other's, will not be connected. For example if MAXSEP is choose to be 10 km and the distance between two events are 12 km, these two events will not be connected and formed as a event pair shown in Fig. 16. The nearest neighbors are connected within the radius that is chosen or set with the MAXSEP.

MAXNGH value is the maximum neighboring that each event can have, ph2dt builds links with each event till it reaches the set MAXNGH, within the radius given by MAXSEP. MINLNK is the minimum number of links required to define a neighbor. Consider as weak neighbor if the set MINLNK is not exceed. MINLNK is typically set to at least eight. MINOBS is minimum number of links per pair saved and MAXOBS is maximum number of links per pair saved. Is used to restrict numbers of links for each event pair, by set a minimum(MINOBS) and maximum (MAXOBS) number of observations for each event pair.

By changing the parameters you control the links between events and generate a differential data set (dt.ct), by allowing for more neighbors for each event like increasing MAXNGH or MINLNK, or include more distant events by increasing MAXSEP.

ph2dt.inp:

MINWGHT	MAXDIST	MAXSEP	MAXNGH	MINLNK	MINOBS	MAXOBS
0	200	10	15	8	8	100

Table 2: Example of ph2dt.inp. MINWGHT: Minimum picked weight. MAXDIST: Maximum distance between event pair and station. MAXSEP: Maximum separation distance. MAXNGH: Maximum neighbors each event can have. MINLNK: Minimum number of required to define a neighbor. MINOBS: Minimum number of links per pair. MAXOBS: Maximum number of links per pair.
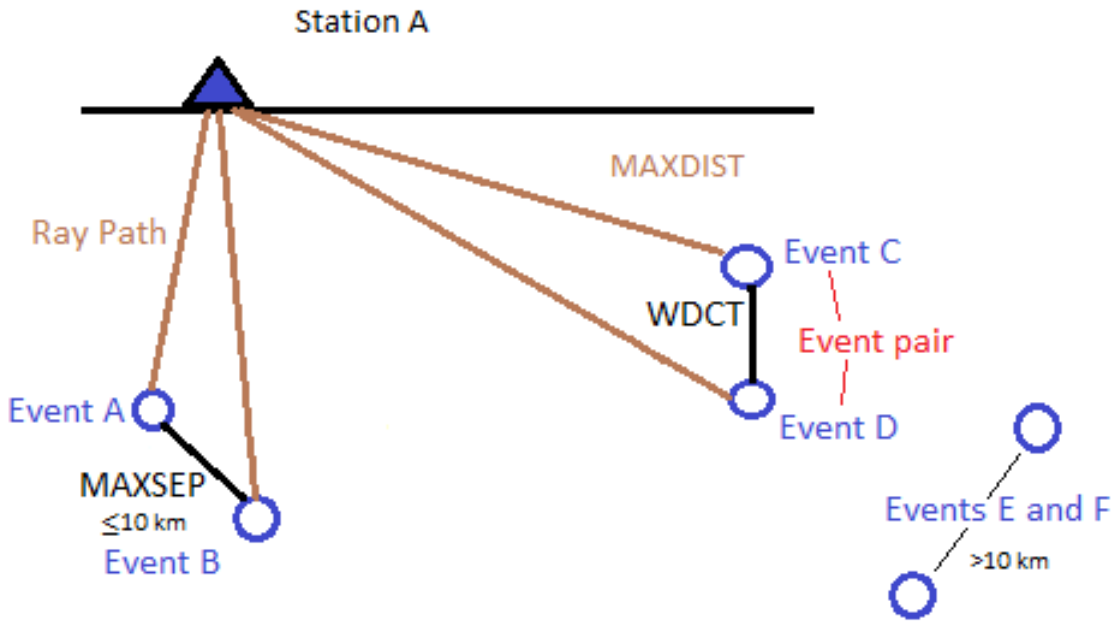
Figure 16: Illustration of the Parameter MAXSEP (maximum separation distance), WDCT (the maximum distance between two hypocenters to form event-pairs) and MAXDIST (maximum distance between event pair and station). Shows event pair A-B and C-D linking up within the set MAXSEP, WDCT and MAXDIST. Events like E and F, with more than 10 km separating them, are not connected. From the illustration MAXSEP and WDCT are quite similar, which also is the case. Waldhauser [2001] advice to choose a small value for the WDCT (parameter in hypoDD.inp) than the MAXSEP (parameter in ph2dt.inp), to still connect all events.

After running the ph2dt program and turned catalog P- and S- phases data into input files for hypoDD.inp, the hypoDD input file must be defined with parameter values before run with a program called hypoDD. The file contains input parameters and files such as station, DD time and output files.

Clustering is defined by the numbers of observations which is chosen by assigning values to OBSCC and OBSCT, these two values defines the minimum numbers of cross correlation and catalog links, to form continuous chain needed to make a cluster (identify). By using more links between events through these two parameters it is possible to improve the stability of the inversion and better constrain the solution. The strength of the links between event pair are determine with these parameters together with the weighting scheme. OBSCC value tells us what the minimum number of links between event pair for cross correlations differential time (CC) is. OBSCT value tells us what the minimum number of links between event pair for catalog differential time (CT).

For a large dataset with thousand events, relocation has to be done in the LSQR mode (solves the damped least square problem) to assess the best possible reliability of the locations, compared to a dataset with a small number of events using the SVD. LSQR

(conjugated gradient method) is a method used to minimize the DD vector by weighting least squares. Solutions are then gained through iterations adjusting vector differences between hypocentral pairs [Waldhauser, 2001]. When using the LSQR mode, it is important to do error estimations for the relocation of the hypocenters and test the robustness of the relocation result. Testing the error can be done with a synthetic test or investigated by relocating a smaller amount of events by using SVD to get a proper least square error estimation.

A large number of events produces large condition numbers, if the condition numbers are being driven up by a poorly constrained event, the damping must be adjusted. DAMP is the damping factor that damps the hypocentral adjustment, this parameter can be the reason for mislocations if chosen wrong in hypoDD.inp. A condition number between 40-90 is usually gained from setting the damping between 1 and 100, it all depends on the condition of the system, if the condition number that is expressed with the CND is high and it need to be lowered, we need to set the damping higher, if the CND is low and it need to be increase then, and if the condition number is very low then a lower damping has to be applied. This happens because of weak links between events, data outliers, large spread in weights etc. Picking the wrong damping value, events may be located to close to each other or too far and give a wrong image of the seismicity in the area. The damping affects the number of iteration we want to apply, by controlling how fast a solution converges.

By weighting and reweighting you control the amount of different data types (catalog and cross correlation) you use in your relocation, it is important to do with precision. When picked wrong, the seismicity image can deviate from the expected image. By weighting, you decide which data that is most used in the inversion (iteration). Want the catalog data to restore the large scale picture till the locations are controlled. When the locations are controlled by the catalog data, they are downweighted in the next iterations relative to the cross correlation data, and further on till only the cross correlation data is used to resolve the structure at the scale of individual earthquakes [Waldhauser, 2001].

Under the general choices of prior weights and the re-weighting functions are described. Cross correlation data is a priori weighted by the square coherency. For most times we down-weight the Catalog data by a factor of 100 because the time measurements from Cross correlation are about one magnitude more accurate than first motion picks, when we are using both data's as input for the hypoDD program.

HypoDD.inp:

IDAT: Numbers between 1-3 decides what datatype to use in the program. 1=only cross correlation, 2=only catalog data(absolute) and 3=catalog and cross correlation data. IPHA: Numbers between 1-3 decides what phases to pick for the program to run for, 1=P-wave, 2=S-wave and 3=P and S wave. DIST: Chose a distance for max distance between centroid of event cluster and stations. OBSCC and OBSCT described above, is minimum number of cross correlation and catalog links per event pair to form a connected cluster. ISTART Initial locations: 1 = start from cluster centroid; 2 = start from catalog locations ISOLV Least squares solution: 1 = singular value decomposition (SVD); 2 = conjugate gradients (LSQR). NSET Number of sets of iteration specifications following.

The NITER that is the number of iterations, the first few iterations contributes most to the shift in hypocentral location. The iterations could possibly be stopped if the shift in hypocenter adjustment or the RMS residual goes below the noise level of the data.

WDCT and WDCC is the maximum event separation, in kilometers, for the catalog and cross correlation data. WDCT is the maximum distance between two hypocenters to form event pairs. WTCCP, WTCCS, WTCTP and WTCTS are the weights for the four data types. WRCC, WRCT, WDCC and WDCT is the reweighting and controls the cutoff of outlier data. During the first iterations its normal to put higher weight to catalog data than correlated data or down weight the cross correlation data, and further iteration more weight to cross correlated ones. Want the catalog data to restore the large scale picture till the locations are controlled. When the locations are controlled by the catalog data, they are downweighted in the next iterations relative to the cross correlation data, and further on till only the cross correlation data is used to resolve the structure at the scale of individual earthquakes [Waldhauser, 2001].

Parameters WDCT and WDCC are controlling the maximum distance between two hypocenters to form event-pairs, in other words they are controlling the separation distances in hypoDD and therefore controlling the connectivity between events, shown in figure (13). These parameters can be chosen from the density of the hypocenters distribution of the average distance between strongly linked events All event pair data that are above the value (separation distance) picked for WDCT and WDCC are removed when running hypoDD. After hypoDD has finished running it gives out the amount of clusters and its content of events. The Parameter CID can be used to relocated and look closer into one of the clusters that is found. It is also possible to specify a subset of events, take out events that belongs to specific cluster from the event file by modify the parameter ID. The model specifications for the 1D velocity model is found at the bottom of the hypoDD.inp file shown with table 4. Where modifications can be done to the model for example how many layers (NLAY), Vp/Vs ratio (RATIO), depths of top layers in kilometers (TOP) and layer velocities (km/s).

The number of events before and after relocation changes, where events gets deleted if the lose linkage, so you could start out with 1000 events and after relocation you have 750 events. This is controlled with the reweighting.

NITER	WTCCP	WTCCS	WRCC	WDCC	WTCTP	WTCTS	WRCT	WDCT	DAMP
5	0.01	0.01	-9	-9	1.0	0.5	-9	-9	65
5	0.01	0.01	-9	-9	1.0	0.5	4	4	65
5	1.0	0.5	-9	2	0.01	0.005	4	2	60
5	1.0	0.5	6	2	0.01	0.005	2	2	50
5	1.0	0.5	6	0.5	0.01	0.005	2	2	45

Table 3: Shows parameters for Weighting and Reweighting in the hypoDD.inp program. The values assigned is standard, also used for some of my results.

NLAY	RATIO							
9	1.73							
TOP								
0.0	2.0	4.0	6.0	12.0	23.0	31.0	50.0	80.0
VEL								
6.2	6.27	6.34	6.4	6.6	7.1	8.05	8.25	8.5

Table 4: 1D velocity Model specifications

3.4.2   hypoDD output

Output from the hypoDD.inp reflects the performance from each iteration by numbers, to get a view of the parameters are good enough or they if they need to be modified more. Table 5. shows the parameter output from the relocation (inversion) events using hypoDD with the LSQR. The first two columns with IT above, indicates the iterations numbers. Initial are the numbers of each iteration that goes from one to the numbers of iterations that we want to do, while the second is the numbers of successive iterations done, means that there might be some gaps from each successful iterations. For example if AQ (air quakes) are not zero, this column will be not numbered which mean that the iteration has to be repeated. EV column are telling us how many events in percentage are used in each iteration. Event pair will be removed if they lose linkage with other events pair, because of outliers are removed i.e that are large delayed times, distant cutoff. Events are also removed if they are located above the surface as air quake. CT and CC columns are the percentage for Catalog data and Cross correlation data used in each iteration. The values that is written out of table 5. are telling us how much of the data that taken away by the reweighting. Sixth and seven the RMSCT and RMSCC columns indicate percentage change from the previous iteration for both catalog and cross correlation data's and the RMS residual(ms). Can use these values for every run of the program hypoDD, these values should decrease with each iteration if the locations are improved. If not, that could give an indication that the numbers of iterations must be changed. The eight column RMSST is the largest RMS residual observed at a station.

DX, DY, DZ and DT columns nine to twelve are giving the average change in hypocentral location and origin time during each iteration. After the first iteration these values changes should be in the range of the initial location from the catalog, and decreasing till they are within the noise level of the data.

Column thirteen OS is the absolute shift in cluster origin, means the shift between the cluster centroid to the initial location and till the cluster centroid to the relocation, more information found in hypoDD.log.

AQ column tells how many airquakes detected, iterations with airquakes need to be reiterated to take them away. Airquakes may indicate that the damping value is to small or the velocity model needs to be modified for the right area. Last column CND tells us if the system is overdamped or underdamped, where a low value may indicate overdamping and a high value underdamping of the solution. CND is the condition numbers for the system of double difference equation, means the ratio between the largest and the smallest

eigenvalue.

IT	EV	CT	CC	RMSCT	RMSCC	RMSST	DX	DY	DZ	DT	OS	AQ	CND

Table 5: hypoDD Output

Six output files from the hypoDD program: 1) hypoDD.loc - contains events individual locations before the relocation of them. 2) hypoDD.reloc 3) hypoDD.sta 4) hypoDD.res 5) hypoDD.src 6) hypoDD.log - resume of the data and parameters used in hypoDD.

hypoDD.log contains extra information, a resume of the parameters and data that are used.

3.5   Example of hypoDD from Calaveras Fault

An example of the double difference method applied to the earthquakes on the Calaveras fault, under a period from 1984 to 1999, by Waldhauser and Ellsworth (2001). To illustrate, what similar improvements are expected to be for my results. The Calaveras fault (Fig. 17) is a member of a series of linked strike slip faults parallels the San Andreas fault, where earthquakes are repeating themselves due to creeping [Nadeau et al., 1995]. The data set including catalog data P- and S-wave data and cross correlation data, consisting of 308 events. One major cluster is formed and relocated for these parameters, containing 304 events [Waldhauser, 2001].

ph2dt.inp parameter values used in the example: A maximum distance of 500 km (MAXDIST) were used between station and clusters, the maximum separation (MAXSEP) applied were 15 km and maximum number of neighbors (MAXNGH) were 15. Minimun linkage (MINLNK) and minimum observation (MINOBS) uses both a value of 8.

HypoDD relocations were performed using only catalog data (Fig. 18a) and both catalog (dt.ct) and cross correlation data (dt.cc) (Fig. 18b). When performed on only the catalog data, it shows a linear and more dense form, the seismicity follows the fault aligned with the map fault. Using both catalog and cross correlation data in the relocation the structures comes more into detail and follows the fault linear features even more denser. The depth plots are also getting denser and more defined. The use of both catalog and cross correlation data shows an improvement of the locations of the hypocenters. This example of Waldhauser and Ellsworth reveals linear features in a higher resolution illustrated in a 3D plot Fig. 19 and determine a more precise location and depth of the faults with the use of both catalog and cross correlation data. The same procedures will be performed for the Nordland area, achieving improved locations and visible features that may indicate structures in a similar way as for the Calaveras fault.
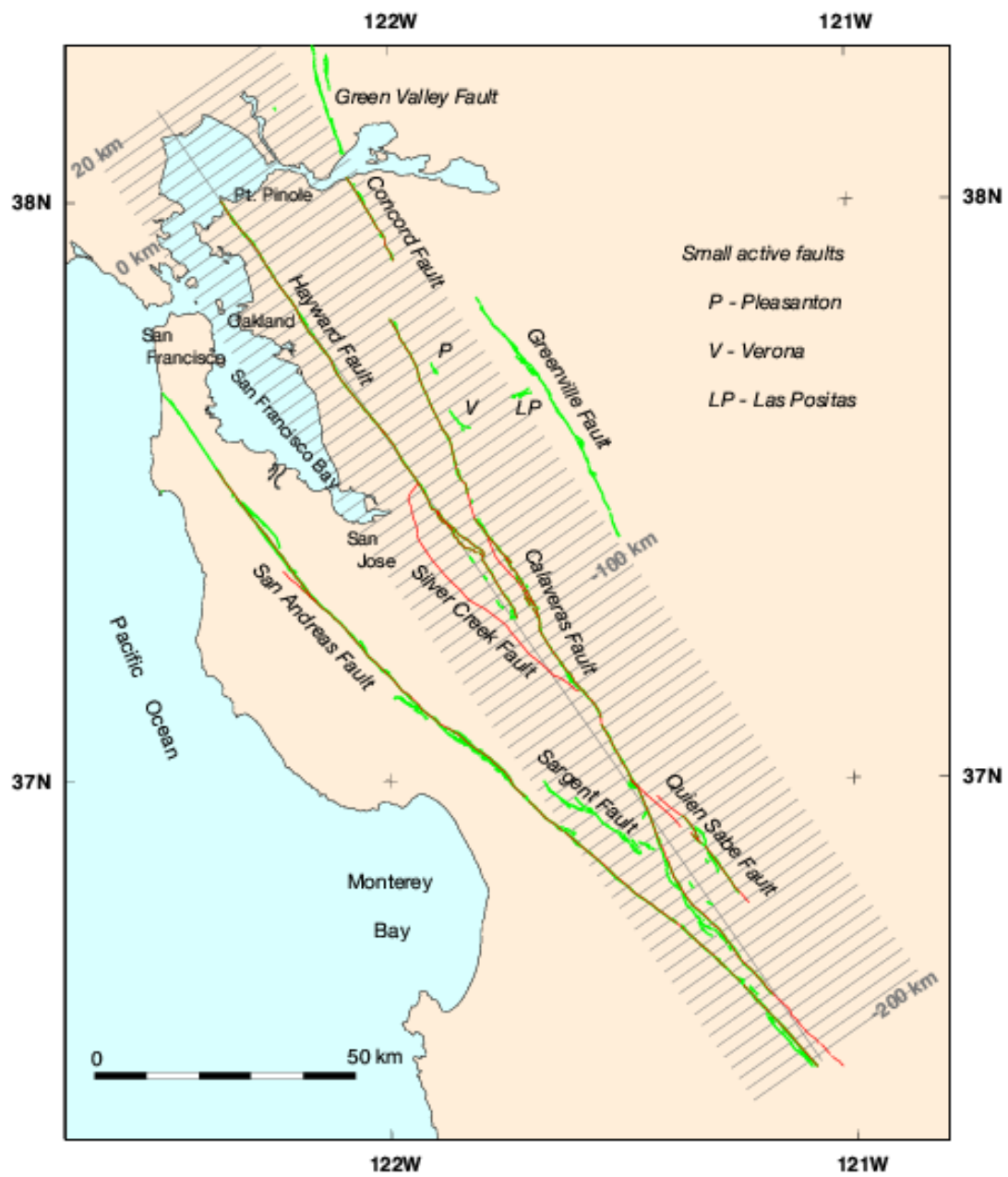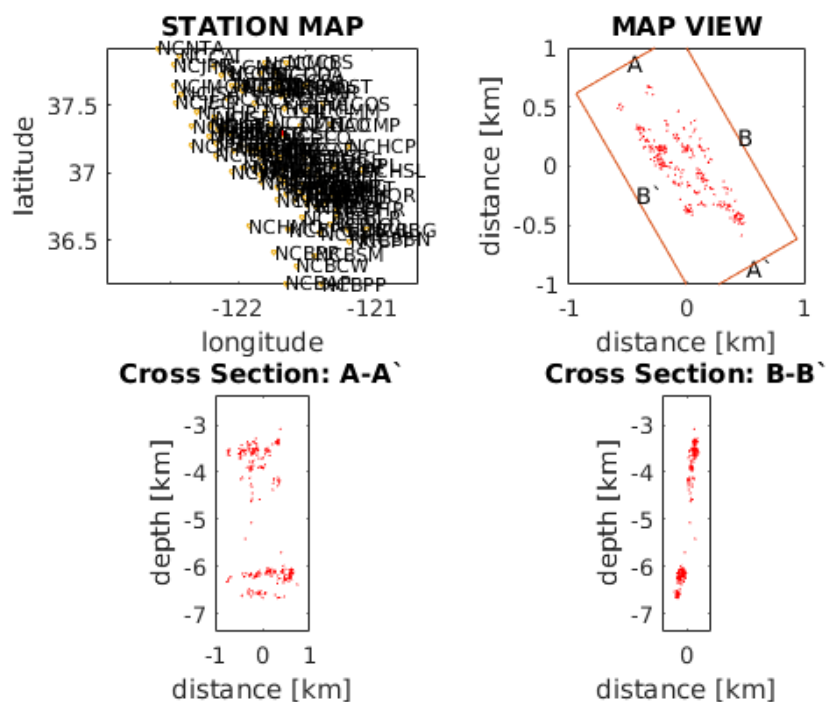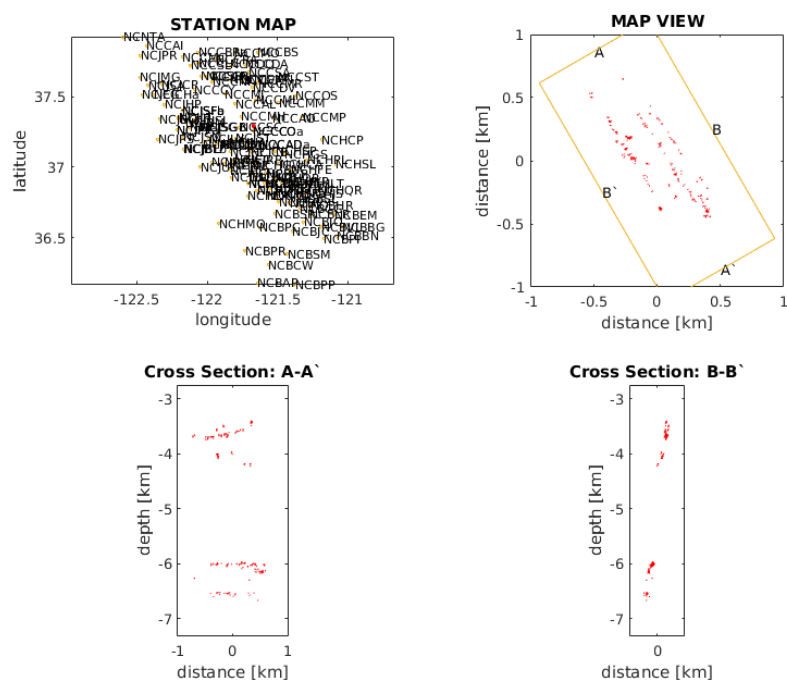
.

Figure 17: Location map showing, cross section profiles of the San Francisco area on the west coast of USA [Simpson et al., 2004]

(a) Relocation of events in on the Calaveras Fault, using catalog data.

(b) Relocation of events in on the Calaveras Fault, using both catalog and cross correlation data. Shows the improvement the cross correlation gives on the relocations of the hypocenters locations , smaller linear features and an overall improvement of the major structure of the fault both horizontally and in the subsurface.
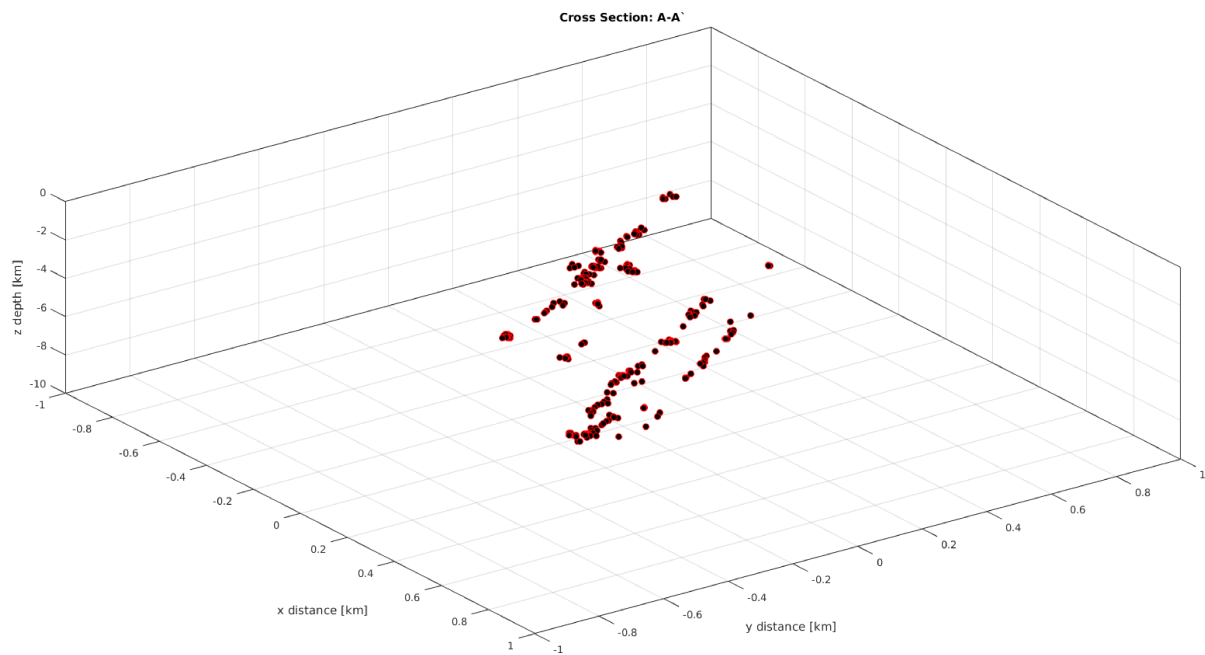
Figure 19: Relocation of events in on the Calaveras Fault in 3D, using both catalog and cross correlation data.

4 Results

The result part is mainly focused on events gathered between North Helgeland and South Helgeland along the coast, more specific between Saltfjellet in the North to Korgfjellet in the South.

In this chapter, a synthetic test is introduced to assess if the behavior of hypoDD is working with my data and calculations of the error reduction, by the hypoDD. Then the results obtained using the hypoDD software on the phase data is presented. Furthermore, the hypoDD runs with different maximum separation (MAXSEP) values from 5, 10 ,15 and 20 km, and last in this section a more careful study of the different features acquired from running the hypoDD with the best selection of parameters is presented.

Figure 20: Main study area, between North Helgeland and South Helgeland along the coast, more specific between Saltfjellet in the North to Korgfjellet in the South.

4.1 Synthetic Data Set

Relocations of events with hypoDD reduces errors between events, that could lead to events being located on the same structure revealing a fault, that will improve the seismic image of the area. Using synthetic data and real data studies will show how much the error is reduced by relocating real events in hypoDD. Results from previous studies using synthetic data and real data, have shown that using catalog arrival times reduces the

relative errors by a factor of ~ 2, using cross correlation data reduces the factor further by $\sim 5 - 10$ [Waldhauser and Ellsworth, 2000, Hauksson and Shearer, 2005a, Balfour et al., 2012]. A couple of tests with synthetic data were developed to measure the error of the system with catalog arrival times. One synthetic file contains coordinates of real events and synthetic phases, another contains the correct synthetic locations and same phase data. Synthetic data set created for testing hypoDD consisting of 1000 hypocenters. Contained in a seismic network of 29 stations, in a square of 5 km, with focal depths at 5 and 10 km, calculated from event locations. Using a Vp/Vs ratio of 1.73 (standard). The synthetic events locations are arranged in a square configuration with two pillars going vertical from corner to corner shown in Fig. 21. We use both horizontal and vertical lines because we want to adopt similar geometry of a focal zone. To show and calculate the improvements made in depth and along linear features.

Using a cluster as a starting location for all events arranged in a square, with calculated travel times for stations. Then relocate the events with new calculated travel times in the square, to see if they would improve the shape of the square, into more defined straighter lines.

By finding optimal parameters values in hypoDD for the damping and weighting that would improve the synthetic test results, would also improve the real data for my study area.

Purpose of this test is to see if hypoDD works on the real data, measure and identify systematic travel time errors of the system and also test the reliability and estimate uncertainties of my results, and give an indication of how the data will behave in reality. The synthetic test using real event locations and synthetic phases (Fig. 21), is performed by first relocate the true locations/starting locations using HYPOCENTER before running it through hypoDD (Fig. 22). With this test I mainly want to show that the relocation process works on real data and improves the locations. Ideally we want to locate events denser on both the horizontal and vertical lines. Observations after the relocation (relative locations) show a clear improvement in shaping the square from the original locations (absolute locations). The mean difference after relocating the events in the synthetic test using real event locations, indicate an absolute mean difference of horizontal X=713 meters and Y=866 meters, and veritcal Z=889 meters.

The other synthetic test using synthetic locations (start locations), is performed to calculate the errors and uncertainties in the relocation. The starting location is not located by HYPOCENTER before running it through hypoDD. Comparing the initial locations (Fig. 25) from the files hypoDD.loc and the relocated from hypoDD.reloc (Fig. 26), an estimation of the average (absolute mean) difference between x, y and z between the original and the relocated locations. 1) Average difference in X (horizontal) = 51 meters. 2) Average difference in Y (horizontal) = 55 meters. 3) Average difference in Z (vertical) = 75 meters. These results conducted on the perfect synthetic data, indicates the highest resolution expected from using the double difference location, i.e the smallest error possible.

Station map: Shows the stations indicated with the names of the stations. Episenters shown with empty circles. MAP View, epicenters and locations of profiles A-A' and B-B'.

The map view shows a linear north-south trend and a west-east trend of seismicity. Want this to be perfectly aligned, but form the figure it possible to see that it is not. Two bottom figures, examine the sub surface using two cross sections. Cross section A-A' (north-south profil): hypocenters at depth 5 and 10 km Cross section B-B'(east-west profile): Linear trend on the cross section profile, is distorted. Grand changes with the focal depths, cross section, with different parameters. Can see that they are not on line and not symmetrical. Want it to be a perfect linear trend. Want to demonstrate that the double difference algorithm can recover absolute hypocenter location.
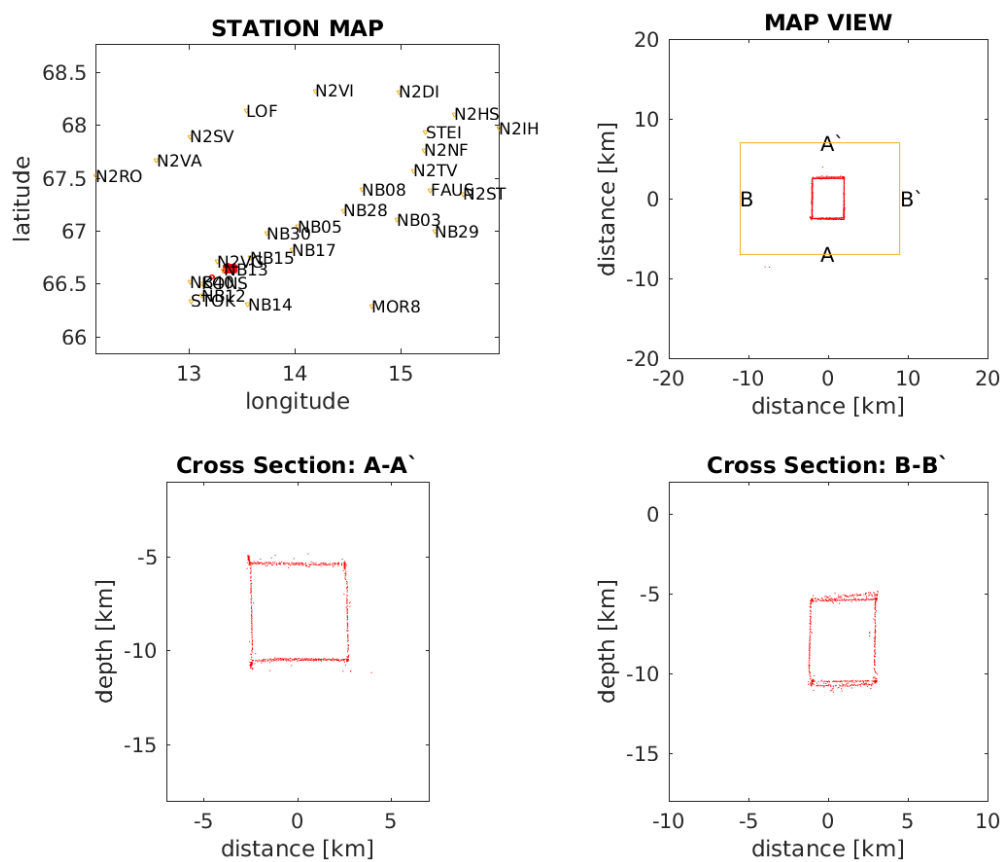
Figure 21: Synthetic test of real events and synthetic phases in a map view, location obtain with DD based on measured times from the catalog data (dt.ct)
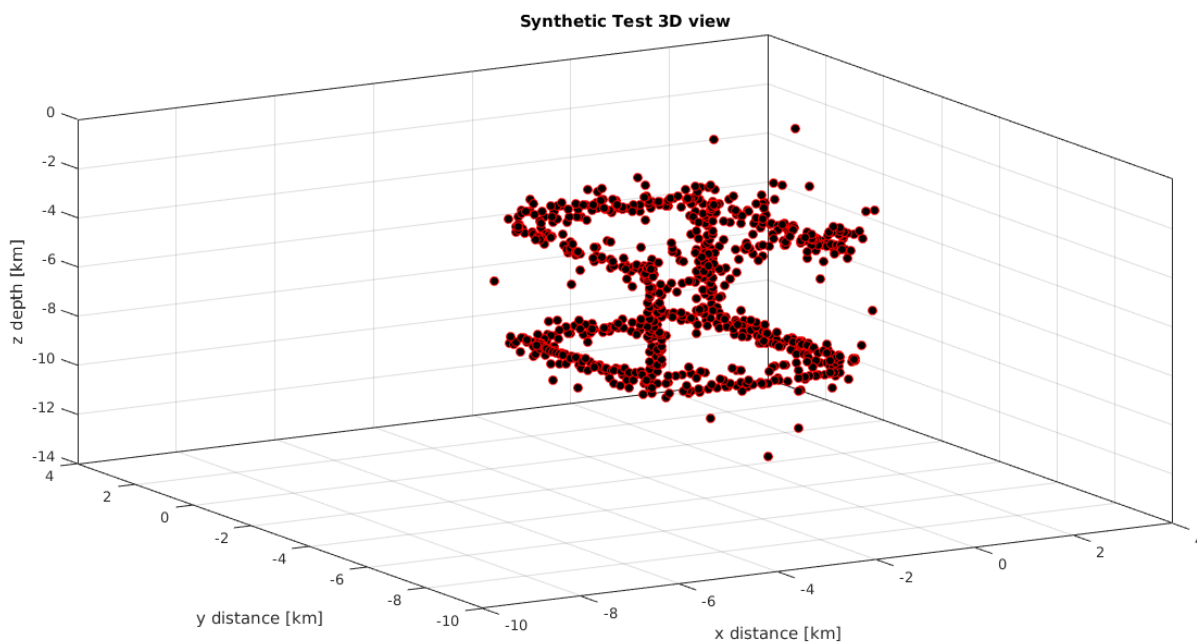
Figure 22: Synthetic test using real event locations run through HYPOCENTER, and synthetic phases shown in a 3D plot. Red dots indicates the hypocenters.
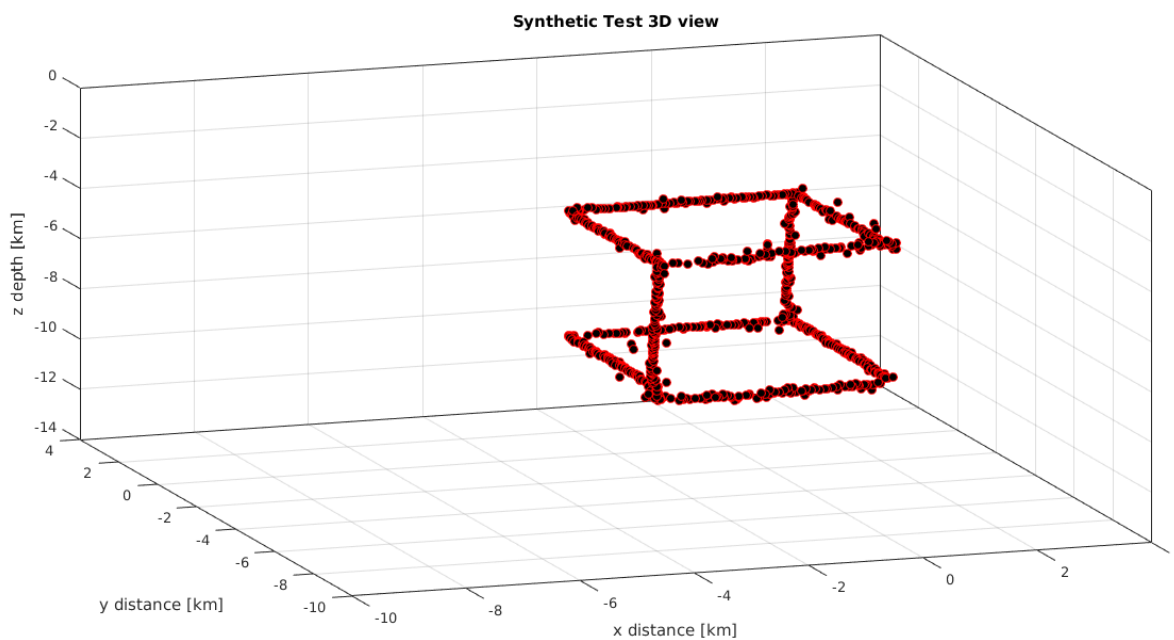

Figure 23: Synthetic test, 3D plot of real events and synthetic phases. Shows the square after relocation with hypoDD, based on measured times from the catalog data (dt.ct). Observing clear improved locations after relocation of the starting locations.
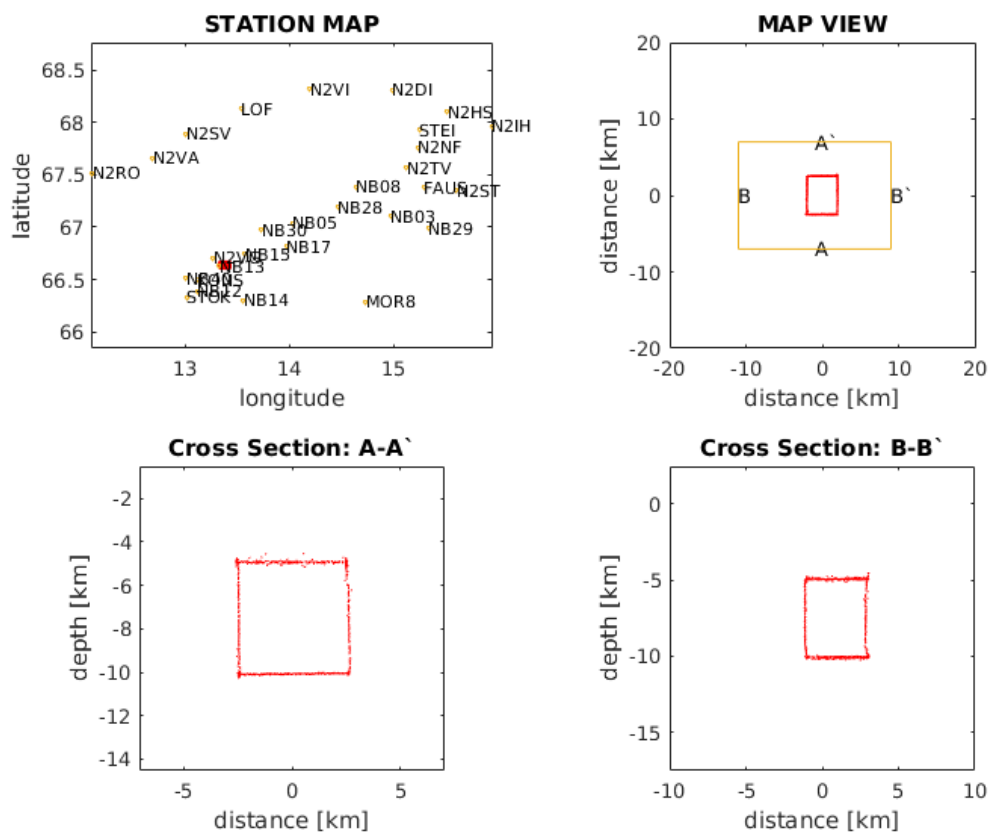
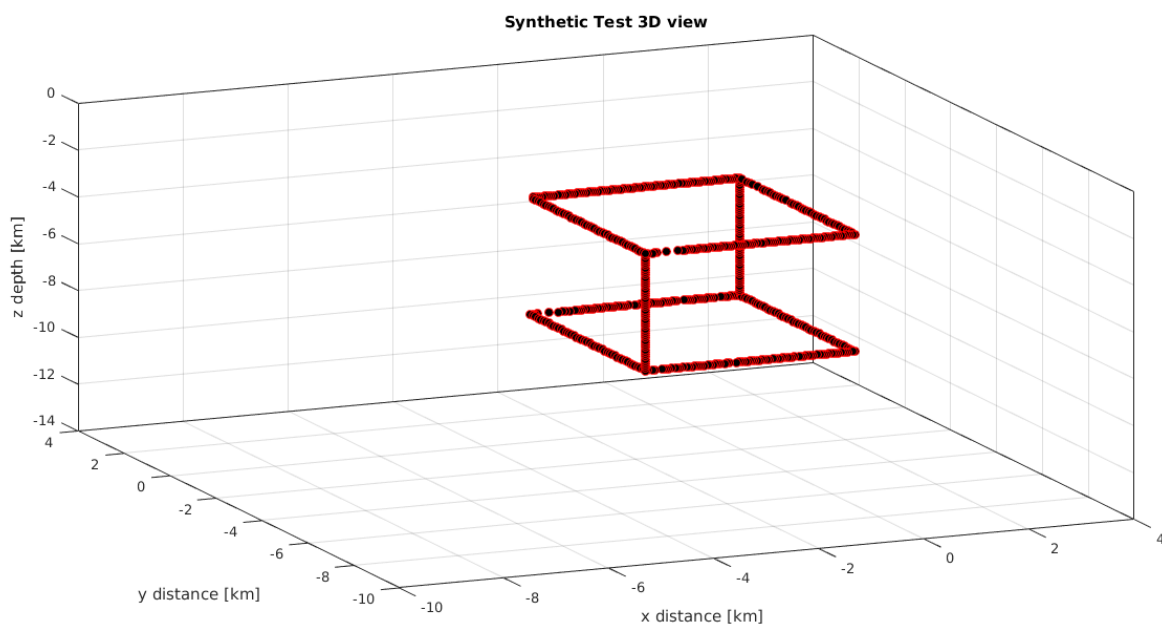**Figure 24:** Synthetic test, relocated events with the correct synthetic locations and same phase data

Figure 25: Synthetic test with perfect synthetic locations and same phase data, shown in a 3D plot.
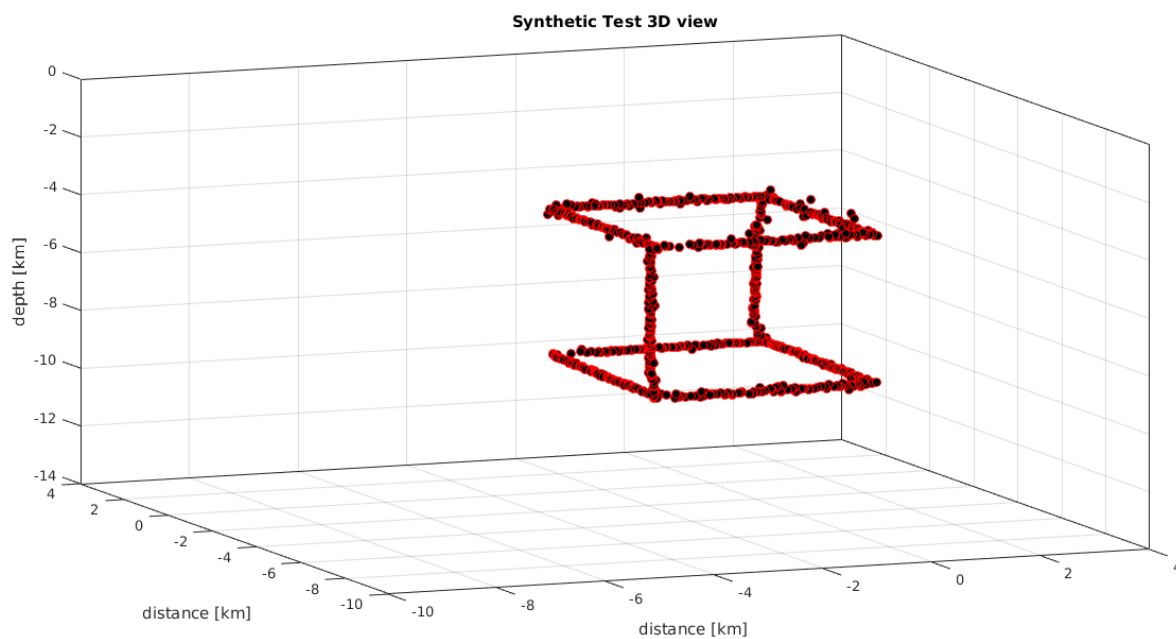

Figure 26: Synthetic test in a 3D plot, relocated events with the correct synthetic locations and same phase data, illustrates the effect the relocation has on the starting locations. Observe small changes on the horizontal and vertical lines compared to the original locations.
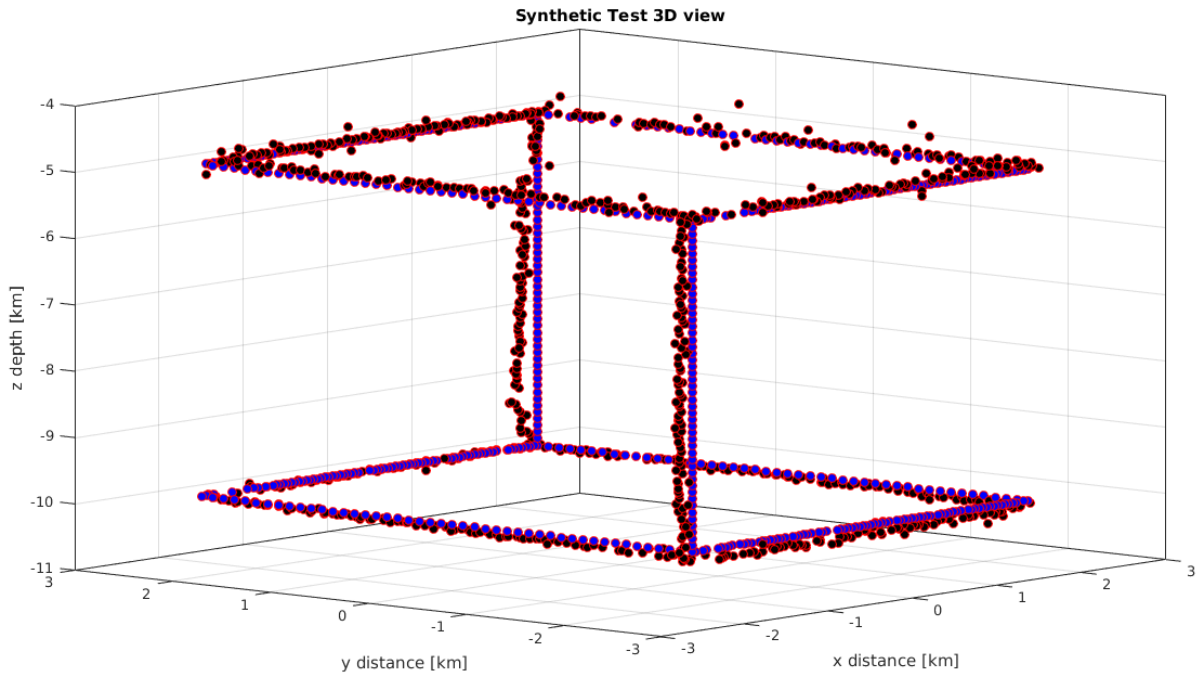
Figure 27: Synthetic test with correct synthetic locations, the plot show a comparison between the initial location coloured in blue and the relocated coloured in red. Mean difference for the horizontal (x and y) are 51 and 53 meters, while for the vertical (z) 75 meters.

4.2   HypoDD applied to my Main Study area

Before earthquakes were relocated with double difference method using the hypoDD software, initial location of the earthquakes in the study area were gathered from the NNSN database and located using SEISAN [Ottemöller and Havskov, 2014] (Fig. 28). The intention was to make a consistent dataset using the same algorithm and velocity model for all locations. For the earthquake locations, ordinary phase picks of P and S waves is used and accurate differential travel times from P and S waves correlation. Relocation have been done with both catalog data and cross correlations data combined, for simultaneous relocation for all events, but also with only catalog data. By doing this it is possible to compare how well the relative locations is with catalog data and cross correlations data, and see the effect they make on the relocation together and separately. For this study I have used the standard NNSN velocity model for Norway, that contains nine layers used to calculate the velocity contrast between layers (using the same depth but adding more layers to the model, and decreasing the thickness of each layer, results in a decreasing in velocity contrast), using a assumed Vp/Vs ratio of 1.73 for the model (table 3 shows the values for the different parameters used). The velocity model was original developed for the southern part of Norway, and is used here as no specified model for the Nordland area has yet been developed. Double difference method applied on the seismicity in the study area will not be much effected by the velocity model, due to the DD method is minimizing the effect of velocity model errors [Waldhauser and Ellsworth, 2000]. So the velocity model used in this study is considered to be valid enough for the

northern Norway area.

In this study I have played around with different values for the ph2dt program and hypoDD inputs, attempt to obtain the best possible results. The results are from a set-up where i have used a maximum event-to-station distance of 200 km. The parameter that causes the largest change to the event-pairs, neighbors and clusters forming is the maximum separation distance (MAXSEP). Therefore a series of runs were done with different values for MAXSEP, where MAXSEP is selected from how large the event station distance is, hypoDD works best if the distance between event pairs is much smaller than the event station distance. Four different values for MAXSEP were used 5, 10, 15 and 20 km for multiple runs, to achieve different views on how it effects the relocations of seismic events and finally pick the one value out of the four that gives the best result. Other parameters were chosen as minimum number of eight links per event, observations per event (OBSCT). MAXNGH is set 15, MINOBS and MAXOBS are set equal to 8 because we want to consider only strongly connected events pairs for all our events (Shown in table 1), and is selected to be the same as OBSCT. The only parameters that were selected to vary except of the MAXSEP, were the damping values. This is because they are crucial in stabilizing the inversion. The reason for not vary the other parameters are to see how the hypocenter locations of the area are changing with the different maximum separation values and forming linkage and clusters between events.

Every relocation was performed with 5 sets of 5 iterations making it a total of 25 iterations. For the weighting only the damping values are changed for each different MAXSEP value to try keeping the iteration process stable (LSQR method). Initial weighting parameters used for all iterations are the same as in the table 2 in the section Methods under hypoDD.inp.
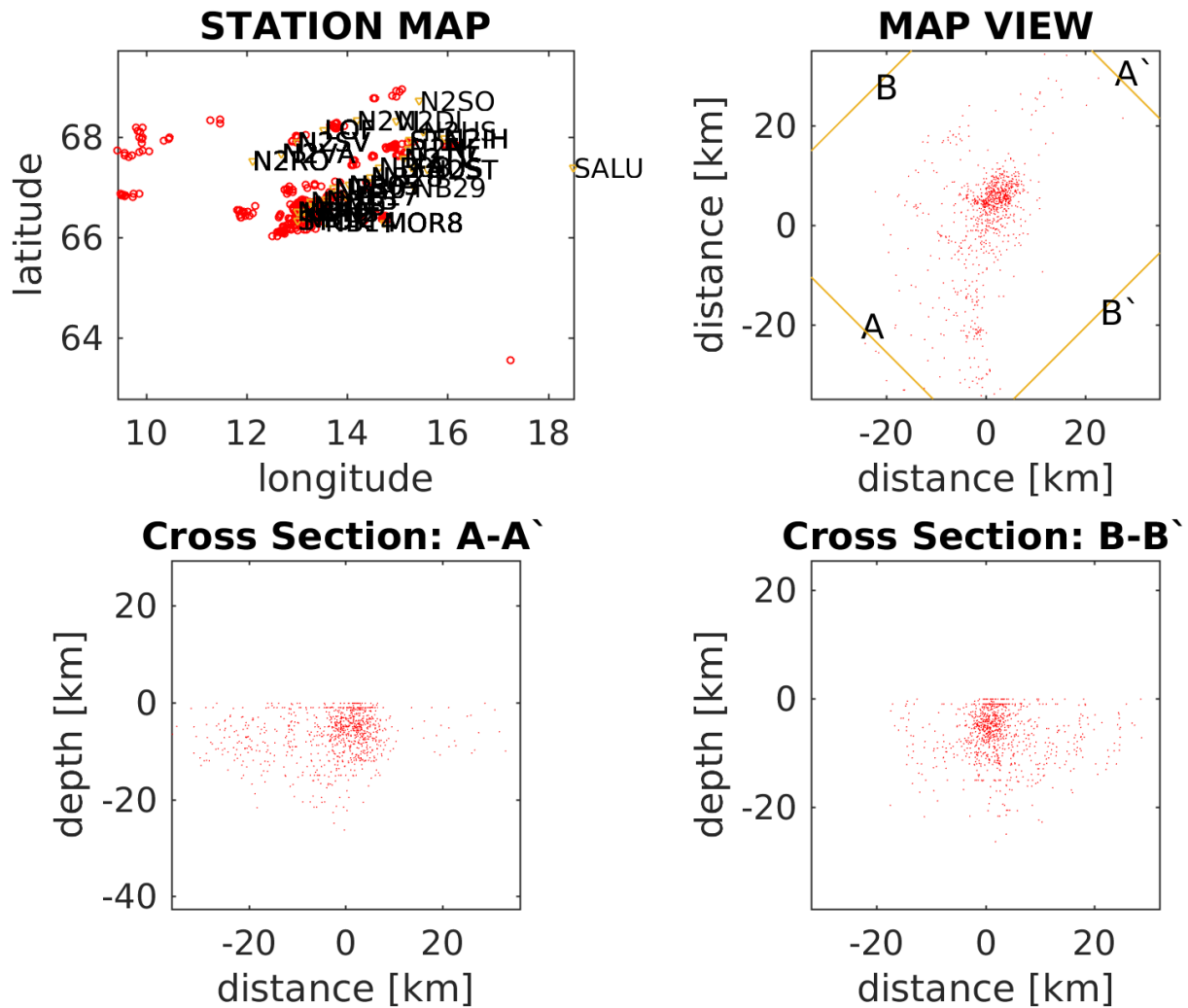
STATION MAP

MAP VIEW

Cross Section: A-A`

Cross Section: B-B`

Figure 28: Original locations(absolute location) for the 1208 events in the Rana area using absolute arrival times.

4.2.1 Catalog data

Between August 2013 and March 2016 a total of 1208 earthquakes were obtained with standard location procedure, manually picking arrival times for first P and S phases using the SEISAN program, forming the catalogue data that is used for the relocation with HypoDD. Running the catalog data through hypoDD with MAXSEP values 5, 10, 15 and 20 km, creates a range between 824 to 1026 clustered events out of the 1208 events. Fig. 29 shows the results of using only catalog data with a MAXSEP value of 10 km. The relocation process reduces the numbers of events, this is because event pairs that has delay times larger than expected, called outliers is removed when running the ph2dt program. Outliers are removed because some events are not being strongly enough related to any other events and therefore deleted during the relocation.

The catalog data is the base that forms the large scale picture for the seismic image, it is therefore important to form high quality and accurate catalog data for input to

the ph2dt program. Fig. 30 shows the difference in depth between (1) initial location found with normal hypocenter determination method and (2) the relocated events found with hypoDD software, clearly see that fewer events are located, and not as many events located near the surface.
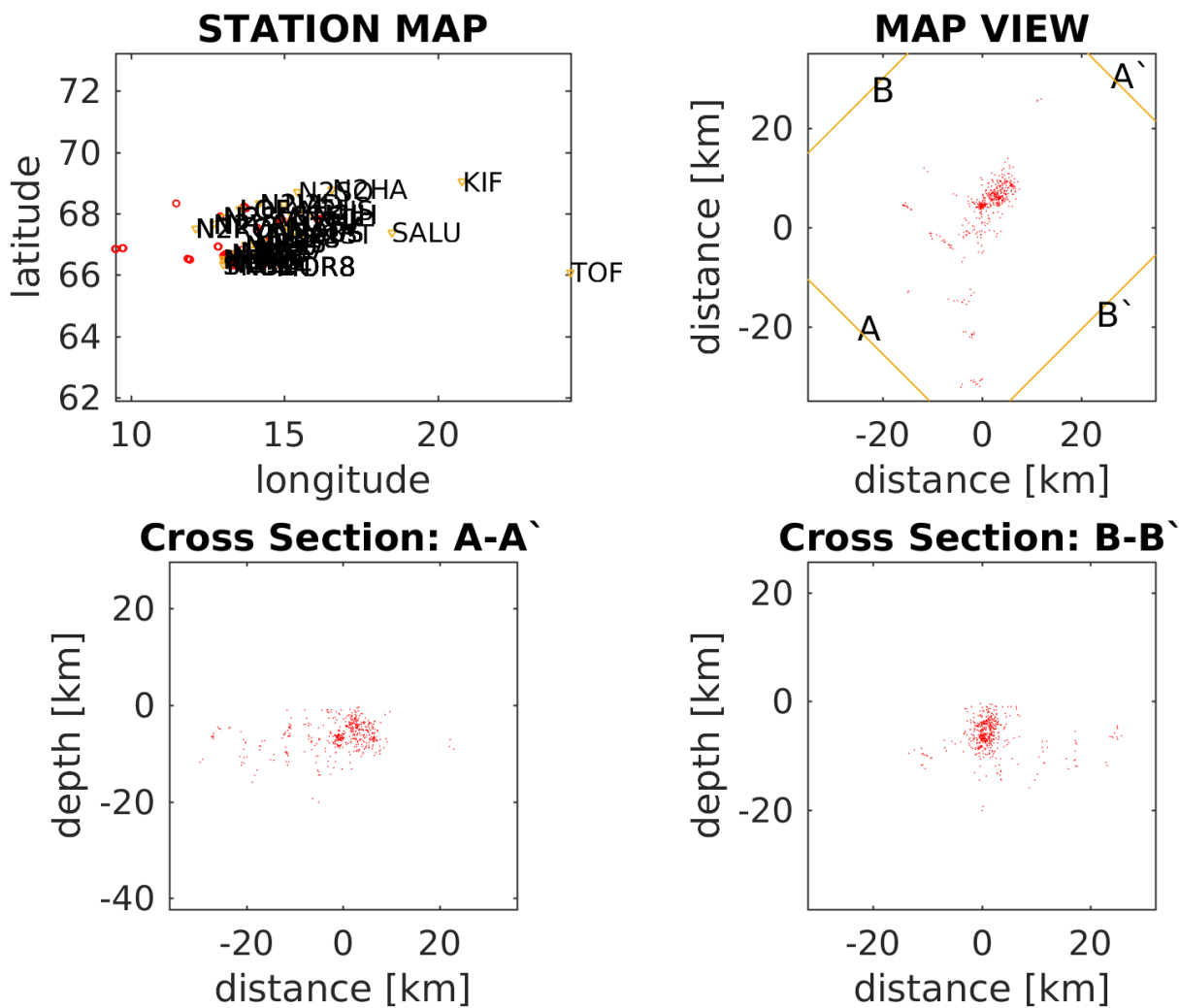

Figure 29: Relocated events with hypoDD in the Rana area, using relative (differential) arrival times from earthquake pairs using catalog data.
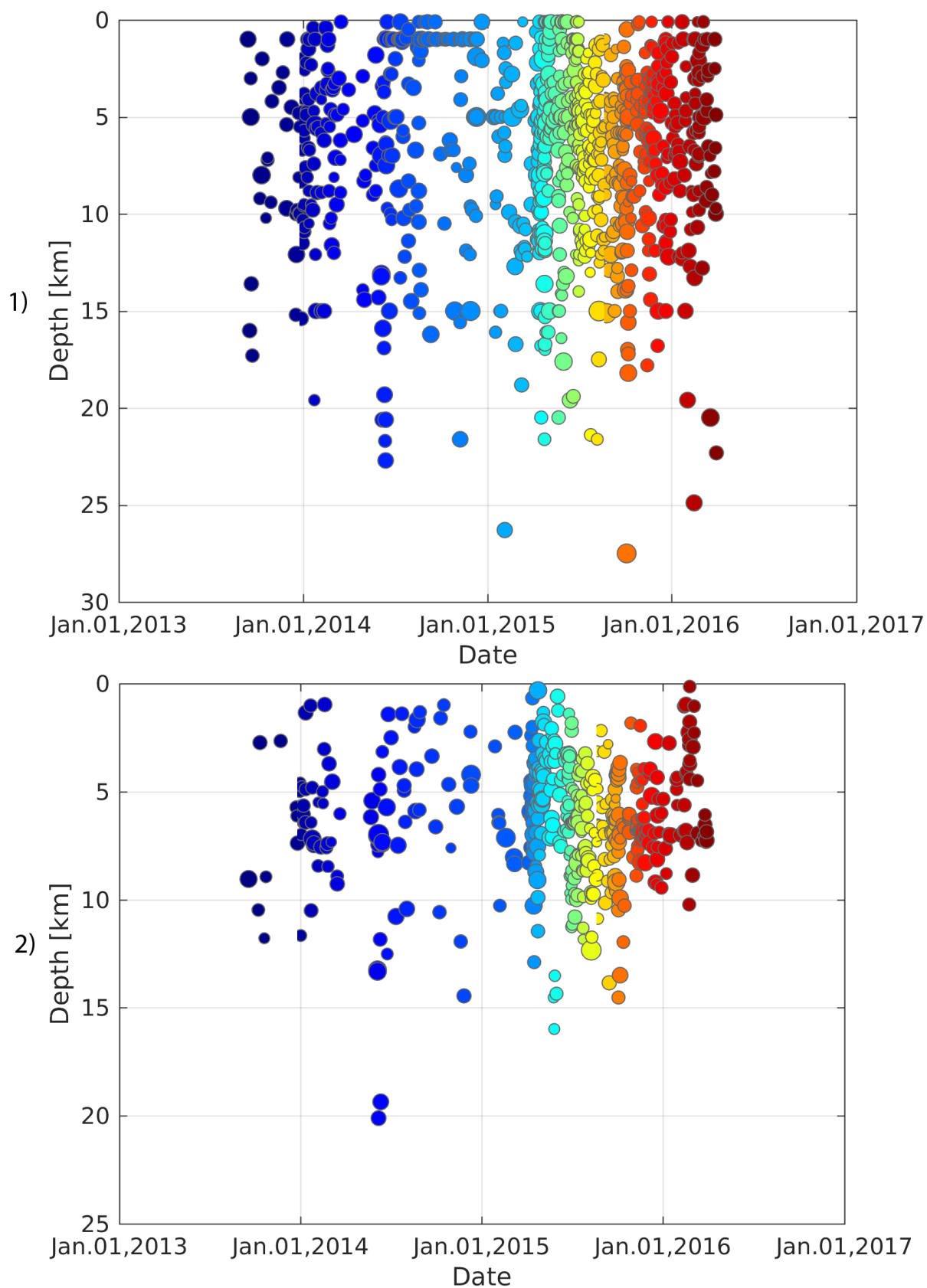
Figure 30: Comparison between 1) initial location depths with 2) relocated event depths, Relative locations with their corresponding depths, a visible clustering of the depths between 2-10 km, excluding events near the surface and deeper seismic events compared to the initial locations.

4.2.2 Cross Correlation data

Waveforms are recorded on a three component seismometers gathered by the NNSN from August 2013 to March 2016, as mention earlier in section 2.3.3, the majority of the stations that is used, were deployed under the NEONOR2 project. For the cross correlation a pass-band of 3-8 hz was used, for filtering local earthquakes, necessary when dealing with events of different sizes. Cross correlation technique(as mention in section 3.3.2) is used to calculate the similarity of waveforms, using measured travel time differential for each event pair with waveforms that correlates at a common station. Finding waveforms that are similar could mean that they come from the same mechanisms i.e the same structure/fault and are repeating through time.

For my data the correlation coefficient is set to a minimum 0.8, meaning that pairs of events that has a cross correlation similarity less than 80 percent is removed from the dataset, to get as much correlations that are similar enough to improve relative location and possible influence the seismic image to show more clearer fault lines.

Running all 1208 events for both P and S phases through the CORR program to calculate all correlated events, results in 2087 measured P-waves dtimes and 2439 S-waves dtimes meets the acceptance criteria. P- and S-phases for cross correlation were both calculated singly (i.e finding correlated events for only P phases or S phases) and together in the CORR program. Calculating them singly cross correlation differential travel times were around 500 for both P and S. When using them together the amount quadrupled from 500 to over 2000 differential travel times. Fig. 31 shows ten similar events in the main cluster, gathered from the same station (N2VG) between a time period from April-May 2015.
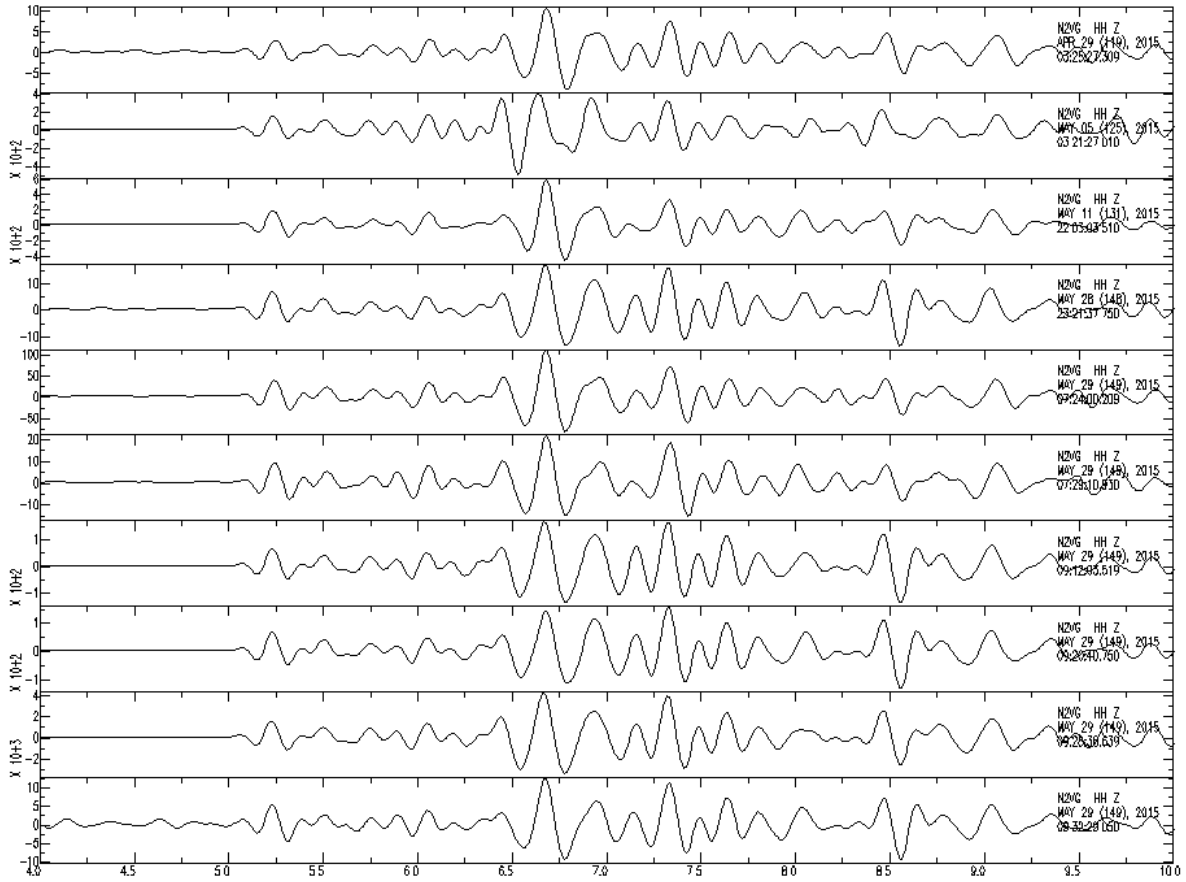
Figure 31: Ten similar traces between April-May 2015, from the same station N2VG measured on the vertical component. Similar traces like these, could indicate that they occur from the same structure/fault.

4.2.3   Catalog and Cross Correlation data

A set with both the catalog data of 1208 events and cross correlation data, a combination of travel time differences obtained through cross correlation of the waveform data together with the phase readings is used for the relocation. Most of the results in the next sections are using both data's and different values for MAXSEP.

The intention of using both data's, is first to get better relative locations with the catalog data using double difference location and complement with the cross -correlation data to attempt to refine the relative locations, i.e a combination of both will give more information than using them singly.

Five sets of five iterations is performed on the data. First two sets is weighted to make the catalog data stronger or more strongly weighted, using 1.0 for catalog P waves (WTCTP), 0.5 for catalog S-waves (WTCTS) and 0.01 for the cross correlation phases (WTCCP, WTCCS). The next three sets are weighted to make cross correlation information stronger. 1.0 for cross correlation P-waves (WTCCP), 0.5 for cross correlation S-waves (WTCCS), 0.01 for catalog P-waves and 0.005 for catalog S-waves.

4.2.4 Relocation using MAXSEP 5km

Relocation of 1208 events where 1071 were selected, forming 824 clustered events presented in Fig. 32. The size of the clusters have a range of 575 event to 2 event over 44 clusters, where three clusters contains 19-72 hypocenters. Nine clusters contains 5-9 hypocenters, and the rest contains 2-4 hypocenters. These small clusters with only a few hypocenters located, are considered to be unsuccessful. Not all 1208 events were relocated because some events are rejected as outliers due to connection loss between event pairs (explained in section 3.4.2), that is controlled over the weighting scheme that specifies each iterations. The relocation process uses 27373 P-wave differential travel times and 32451 S-wave differential travel times from the catalog data. For the cross correlation data 2087 P-wave differential travel times and 2439 S-wave differential travel times were used. The largest cluster contains 575 hypocenters uses 25132 P-wave differential travel times and 30010 S-wave differential travel times from the catalog data, together with 1857 P-wave differential travel times and 2170 S-wave differential travel times from the cross correlation data.

Output from hypoDD (parameters shown in table 4): The iteration process produces condition numbers ranging from 65 to 30, using a damping factor off 65 to 45 to the solution. Waldhauser and Ellsworth [2000] suggest a recommended damping values between 0 and 80 and condition numbers between 40 and 80. By achieving condition numbers from 50 to 40 with as small as possible damping values the solution is considered to be stabilized. In this case a small MAXSEP of 5km keeps the condition numbers relative low although the damping value is high. The total amount of data, catalog and cross correlation data used in each iteration, is going from 96% to 25% for total (EV), 93% to 65% for catalog and 95% to 6% for cross correlation. RMSCT and RMSCC values that tells us the percentage change from previous iteration for catalog data and cross correlation data, are decreasing with each iteration. Indicates that locations are improving for each iterations. Values for the DX, DY, DZ and DT that gives the average change in hypocentral location, are decreasing for each iterations, from starting at maximum 1000 meters and going down to 10 meters. The shifting in cluster centroid location from initial location to relocated given with the parameters OS, is decreasing 100 meters from initial value from the first iteration. Airquakes are also present but is removed with reiterations.
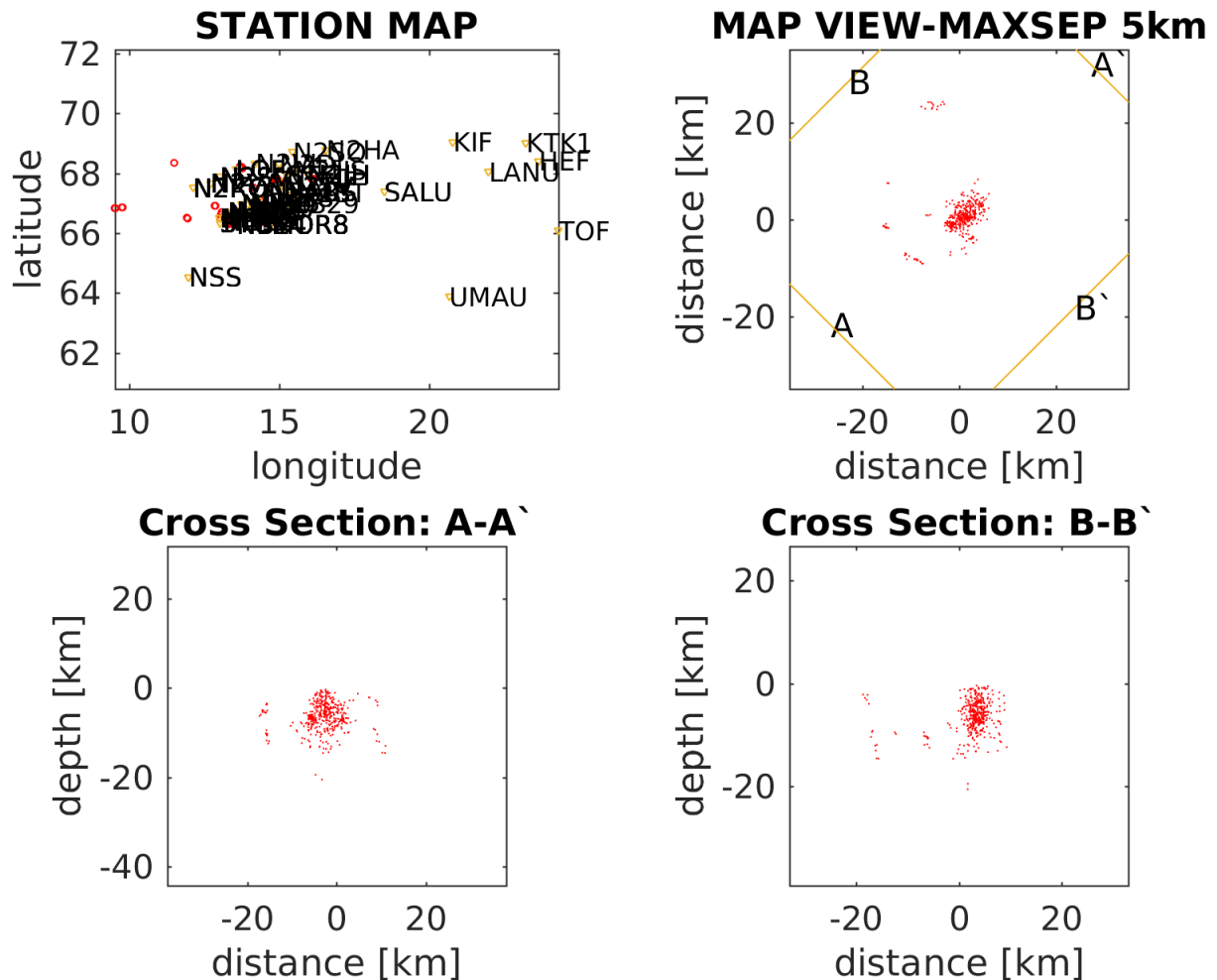
Relocated events in the study area shown in a map view and cross sections from angles A-A' and B-B', using a MAXSEP of 5 km, hypocenter location are indicated with red dots.

Figure 32:]

4.2.5 Relocation using MAXSEP 10km

Out of 1208, 1071 were selected and 943 located as clustered events divided over 29 clusters presented in Fig. 33, where the largest cluster contained 761 events to the smallest containing 2 events. Seven clusters contains 25 to 10 events, ten cluster has 8 to 4 events and the rest has 3 to 2 events in them. The relocation process uses 35379 P-wave differential travel times and 41618 S-wave differential travel times from the catalog data. For the cross correlation data 2087 P-wave differential travel times and 2439 S-wave differential travel times were used.

Output from hypoDD: The iteration produces condition numbers ranging from 77 to 30, using a damping off 70 to 45. Using a MAXSEP of 10 km produces higher condition numbers compared to MAXSEP of 5 km using same damping values, therefore a higher value of damping must be applied to the system. The system is behaving in a same way for the parameters values for the iteration using a MAXSEP of 5 km. The RMSCT

and RMSCC values starts with a higher value than the output for MAXSE 5 km, but eventually decrease down to the same values, the same happens for the DX, DY, DZ and DT values, starting with a higher value but eventually decreases down to the same amount as for the MAXSEP of 5 km. Same applies for the parameter OS, starting at a higher value but decrease down to the same amount.

Main difference between using a larger MAXSEP of 10 km compared to 5 km is that it includes more events. The MAXSEP of 5 km are forming more clusters, but since the distance is only using 5 km, the MAXSEP of 10 km are covering more area and therefore more events are included. Visible from comparing the two figures. The relocation shows three more clusters where two forms lineations south for the largest cluster. The cluster that is closest to the main cluster looks to have the same lineation direction as the others from MAXSEP 5 km. The next one have a different direction more pointing against northeast southwest direction. While the last cluster at the bottom (furthest south) has no distinct direction for the lineation. The double difference method works best on the cluster with the largest concentration of seismicity, comparing the changes from initial locations to the relocated, visible trend lines are shown on the map view, that could possible represent fault lines. The depth distribution looks the same as for the system represent using a MAXSEP of 5 km, finding the events on depths from 2-10 km, only with more events further south. Difference between mean shift in horizontal and vertical direction during relocation for using a MAXSEP of 10 km, compared to average horizontal and vertical initial locations are for horizontal vector X and Y 1073 meters and 777 meters, and for vertical vector Z 2139 meters.
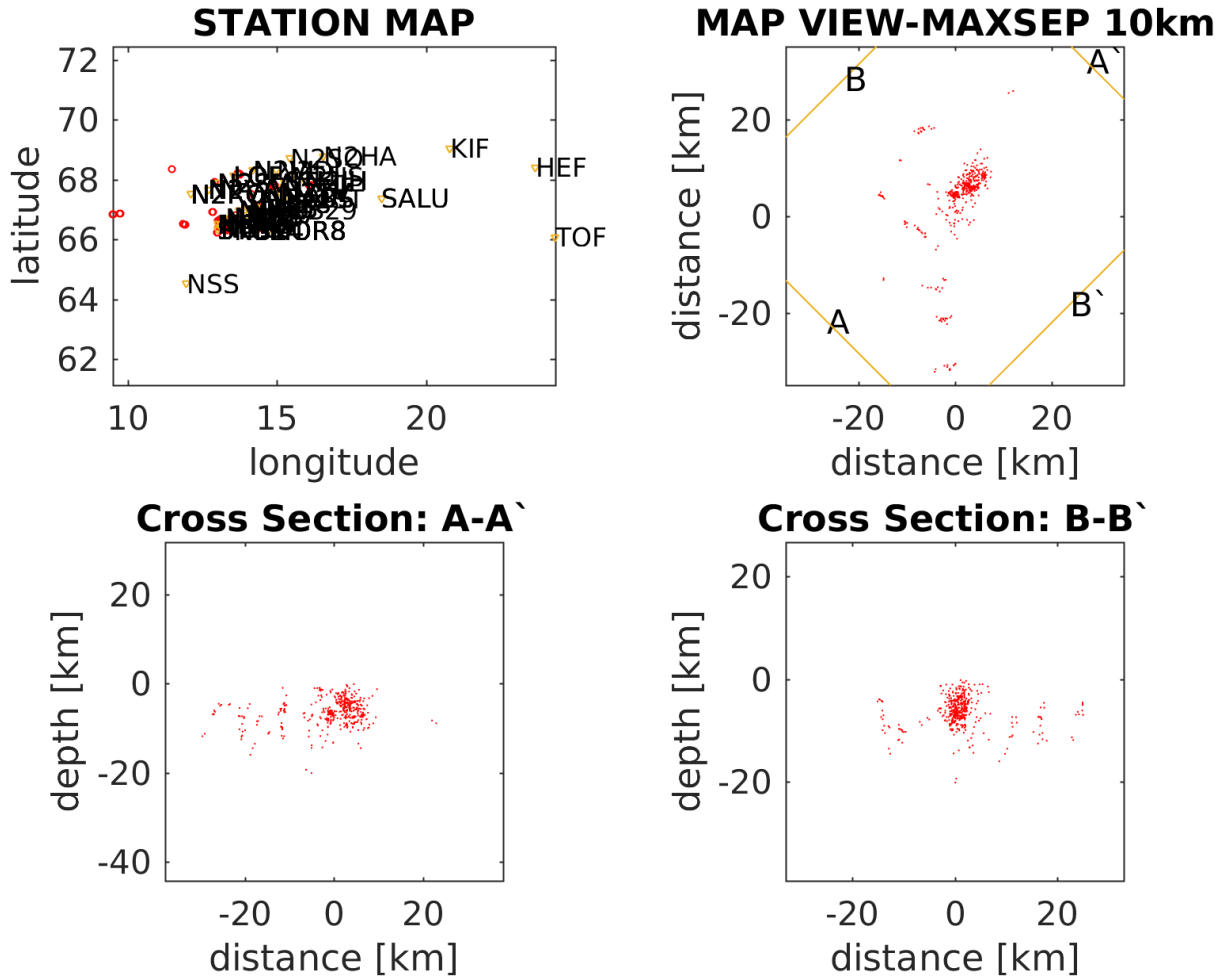
Figure 33: Relocated events from my study area shown in a map view and cross sections, using a MAXSEP value of 10 km. Using relative (differential) arrival times from pairs of earthquake observed at a common station with both catalog and cross correlation data. Hypocenter location are indicated with red dots.

4.2.6   Relocation using MAXSEP 15km

Relocate events using the same set up as the previous relocation with a maximum separation (MAXSEP) of 15 km. Selecting 1071 of 1208 with 1007 clustered events over 25 clusters presented in Fig. 34, where the largest cluster contains 792 events and the smallest containing 2 events. Nine clusters contains 34 to 12 events, four clusters has 8 to 6 events and the rest has three to two events in them. The relocation process for a MAXSEP of 15 km is forming 71026 P-phase pairs total and 85193 S-phases pairs total, from these, 41158 P-wave differential travel times are selected and 47857 S-wave differential travel times from the catalog data. For the cross correlation data 2087 P-wave differential travel times and 2439 S-wave differential travel times were used.

Output from hypoDD: The iteration produces gives out condition numbers ranging from 79 to 30, using damping values of 70 to 45. The condition numbers are slightly higher than the hypoDD output for a MAXSEP of 10 km, using the same damping values. RMSCT

and RMSCC values are going from 347 and 288 and down to 9 and 6, behaving in a normal matter. The DX, DY, DZ and DT values behaves the same way as the difference between MAXSEP 5 km and MAXSEP 10 km, but for MAXSEP 15 km it starts at an even higher value and decreases down to the same amount.

A MAXSEP of 15 km forms more clustered events (64 more events) than the previous MAXSEP values. Main differences are the clusters closest south of the main cluster, where for the MAXSEP of 10 km it seems to be more scattered, but for the MAXSEP of 15 km the events seems to be more aligned, with 2-3 clusters looking to be in the same alignment as some of the others clusters, in a northwest-southeast direction. Except from this most of the seismic image seems to be much like the figure using MAXSEP of 10 km, main cluster is not showing any significant changes both in the density of the events and directions of the linear features, same counts for the linear features around the main cluster. The depth distribution looks to be in the same range approximately 2-10 km for most of the events.
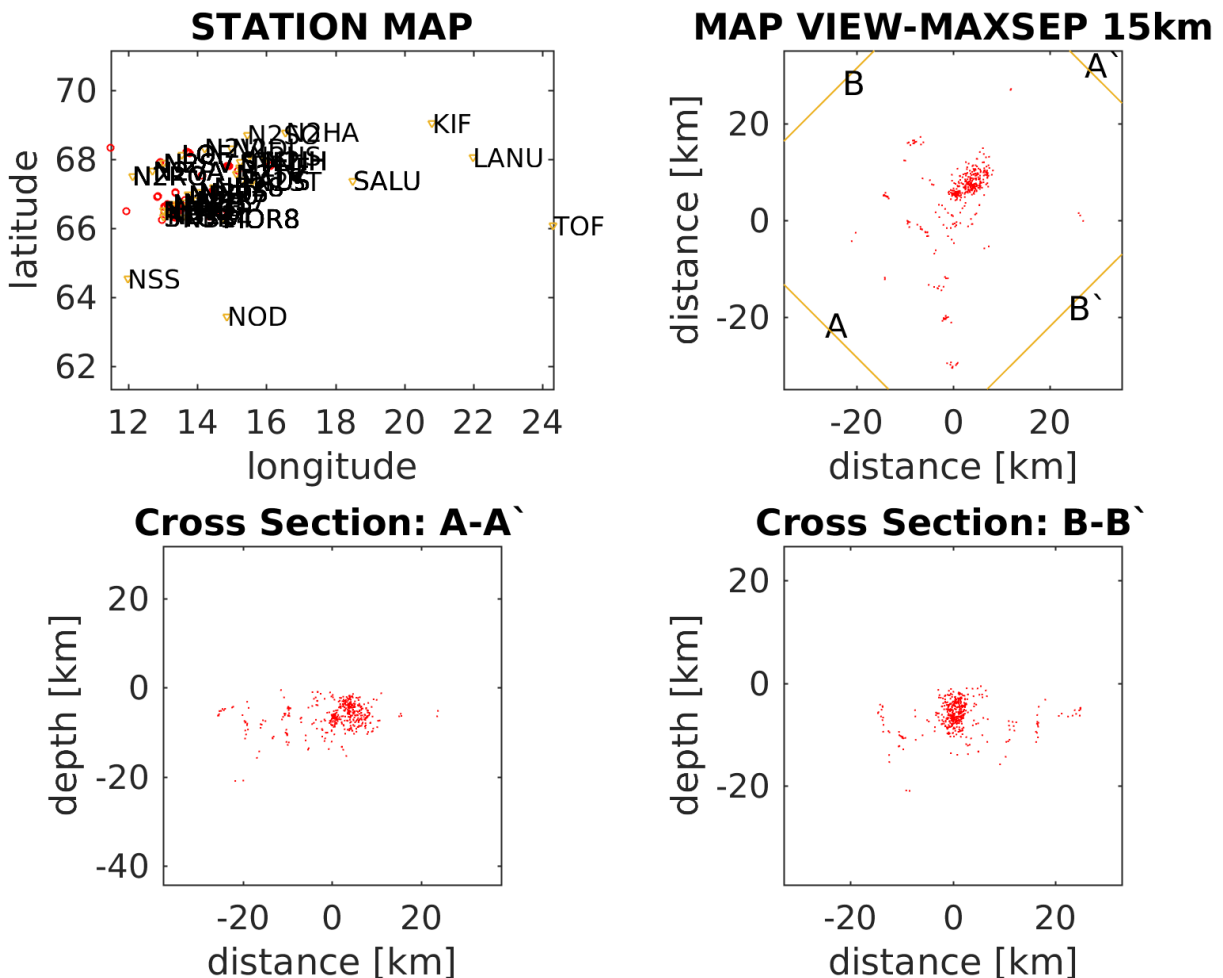

Figure 34: Relocated events from my study area shown in a map view and cross sections, using a MAXSEP value of 15 km. Using relative (differential) arrival times from pairs of earthquake observed at a common station with both catalog and cross correlation data. Hypocenter location are indicated with red dots.

4.2.7 Relocation using MAXSEP 20km

Relocation using the same set-up as the previous relocation with a maximum separation (MAXSEP) of 20 km. Of the 1071 event selected 1026 clustered events were relocated over 12 clusters presented in Fig. 35, where the largest cluster contained 894 events to the smallest containing 2 events. Five clusters contains 29 to 15 events, three cluster have nine to four events and the rest has three and two events in them. The relocation process for a MAXSEP of 20 km is forming out 77126 P-phase pairs total and 92170 S-phases pairs total, from these 44609 P-wave differential travel times are selected and 51520 S-wave differential travel times selected from the catalog data. For the cross correlation data 2087 P-wave differential travel times and 2439 S-wave differential travel times were used.

Output from hypoDD: The iteration process creates condition numbers ranging from 80 to 32, using damping values off 80 to 40. Solution might be unstable, because of the high value of the condition number ideally a smaller condition number would be better for damping value that high. The higher choice in value of MAXSEP formed higher values for the condition numbers, and therefore a higher number of damping values needed to be applied to the inversion. The parameters RMSCT, RMSCC and DX, DY, DZ and DT are after the inversion giving the same outputs as for the MAXSEP 15 km. Where they all starts at a higher value and decreases down to a value around 6-9. Average offset between linked events and strongly linked events are increasing with increased maximum separation (MAXSEP), with approximately 1 km for all MAXSEP values from 5 to 20 km. Starting at 2.24 km for MAXSEP value 5 km and going up to 5.38 km for MAXSEP 20 km.

The relocated events created with MAXSEP value of 20 km, seems to be more denser than any of the other images. The relocation using 20 km MAXSEP is creating the lowest amount of clusters but includes the most events. Compared to the other three MAXSEP values, this one is forming almost no scattered events compared to the other values of MAXSEP. Which indicates that most events are connected in a cluster. The linear features south and west for the main cluster is still present and still pointing in the same directions, but no new features are observed. The depth distribution looks to be in the same range approximately 2-10 km for most of the events.
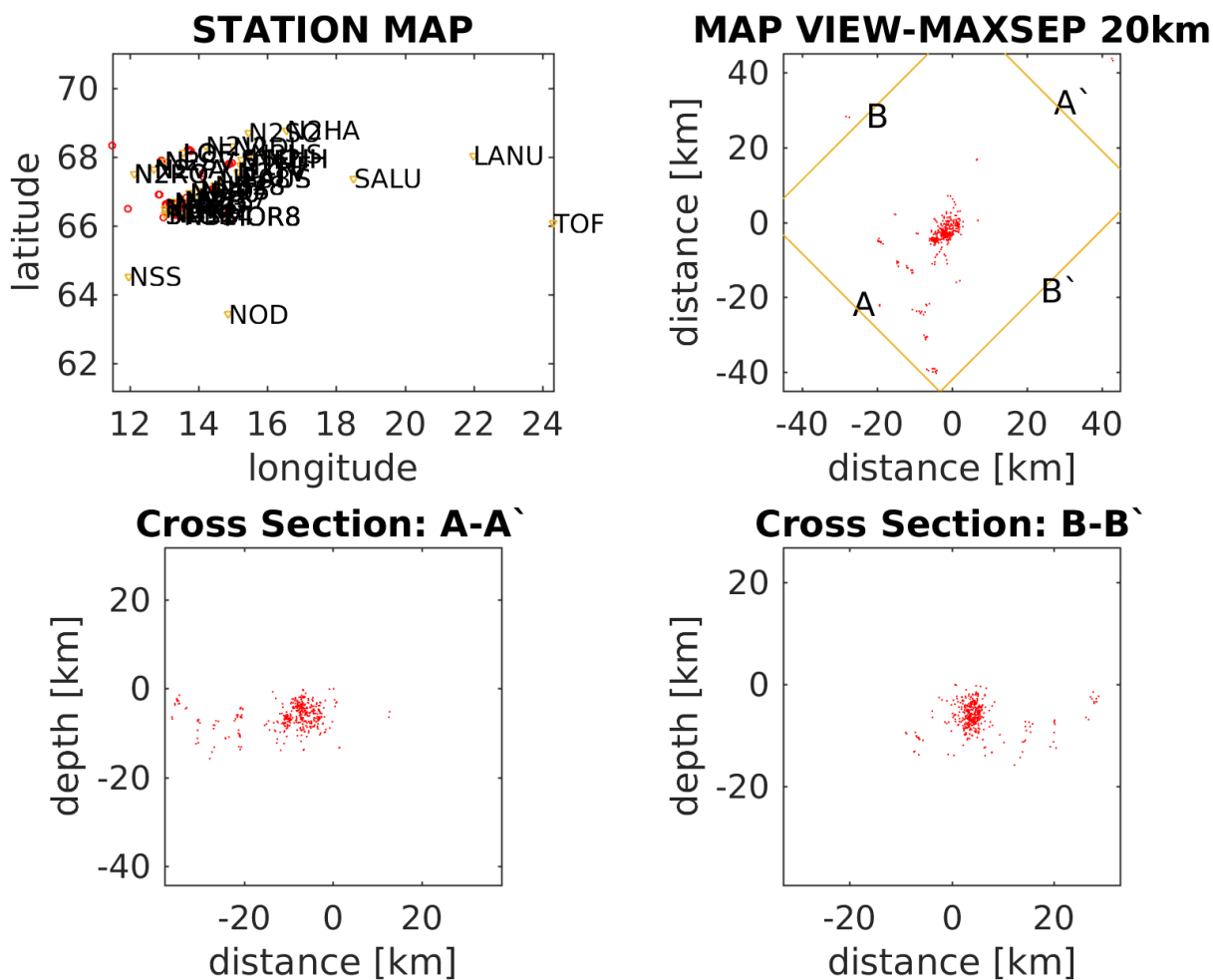
Figure 35: Relocated events from my study area shown in a map view and cross sections, using a MAXSEP value of 20 km. Using relative (differential) arrival times from pairs of earthquake observed at a common station with both catalog and cross correlation data. Hypocenter location are indicated with red dots

4.3 Closer study of the Clusters found using a MAXSEP of 10 km

The relocated events using a MAXSEP value of 10 km have been chosen to be the most promising pick of parameter value and will therefore be used for closer study if the clusters. This is mostly because 5 km is considered to be a to low value i.e it is covering a to small area and important features is not shown. A MAXSEP of 20 km is on the other hand a to large value, considered the small size of the study area and the possibility that it connects events from a to large distance, that does not belong together.

Fig. 36 shows the results in a map view from the hypoDD relocation using a MAXSEP of 10 km. 3D plots will be used to conduct a closer study of the structures. Starting with observing three parts referred to as the main (largest) clusters which we regard as earthquake swarms (Fig. 37), the limitation in magnitude $M_L < 0.4$ to $M_L < 3.2$

(Fig. 9) means that these are swarm like clusters. Further moving West and South to the five clusters, appears to be small linear trends adjacent to the main clusters (Fig. 36). Features that were hidden in the uncertainty of the initial locations (Fig. 28) are now more visible with the use of double difference method. The different clusters and their associated events are plotted with different color which indicated time of occurrence. The main focus using these figures is to see if any of the clusters occur in any pattern, or if they migrate through time and space in any direction, or occurs randomly. Furthermore, explore how the the depths of the hypocenters are arranges, if they are vertical or they dip to one direction or the possibility to observe fault planes.
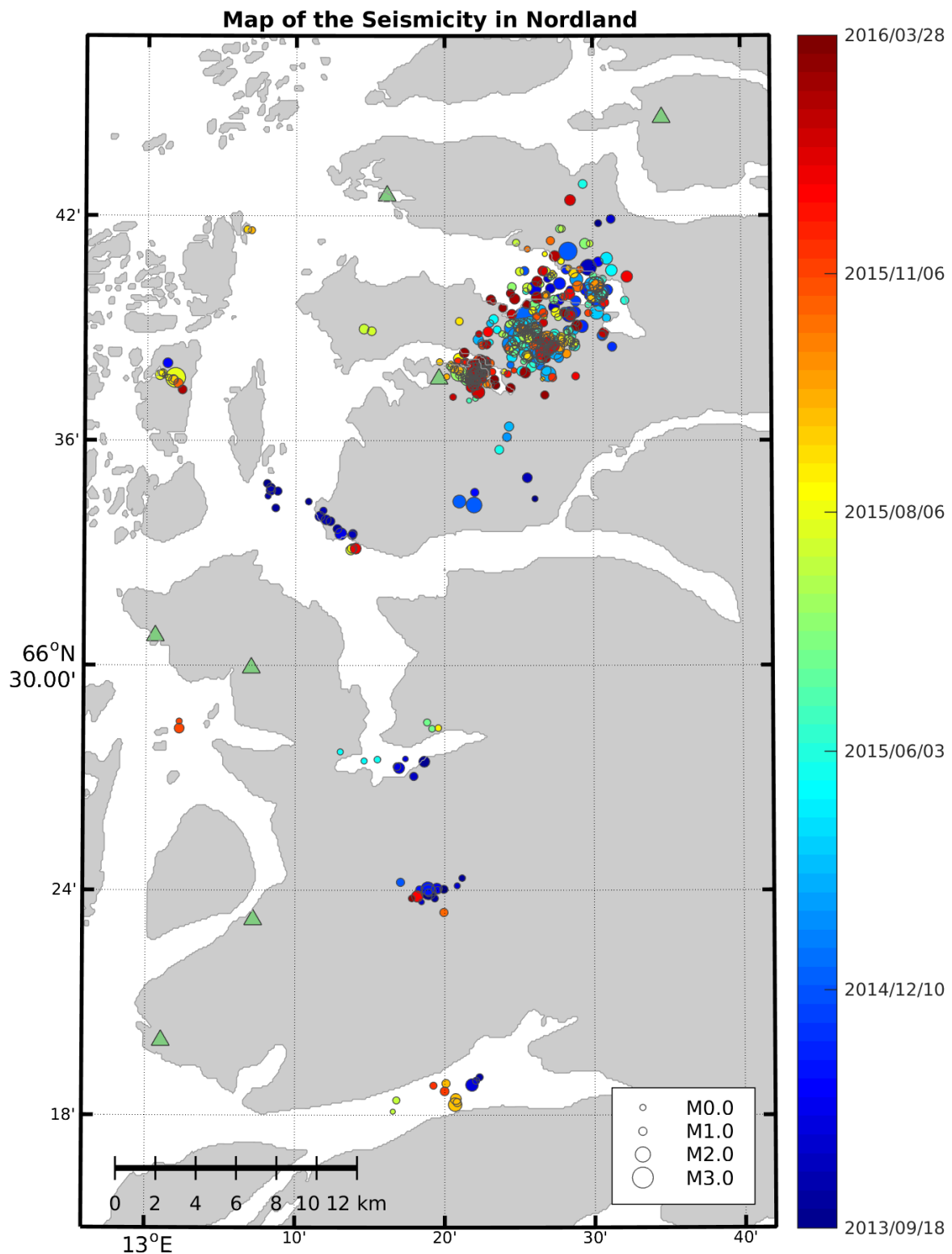
Figure 36: Map of the main study area after relocation of the 1208 events using a maximum separation distance of 10 km. The map shows the different clusters of events from the relocation using double difference location method. Seismic stations are shown with green triangles. The circles shows the relocated events from hypoDD, where the size of the dots gives the magnitude of the events and the different colours indicate the time of occurrence. Seismicity on the map shows that there is a clear coastal trend, most of the events are located between 66 and 67°N.
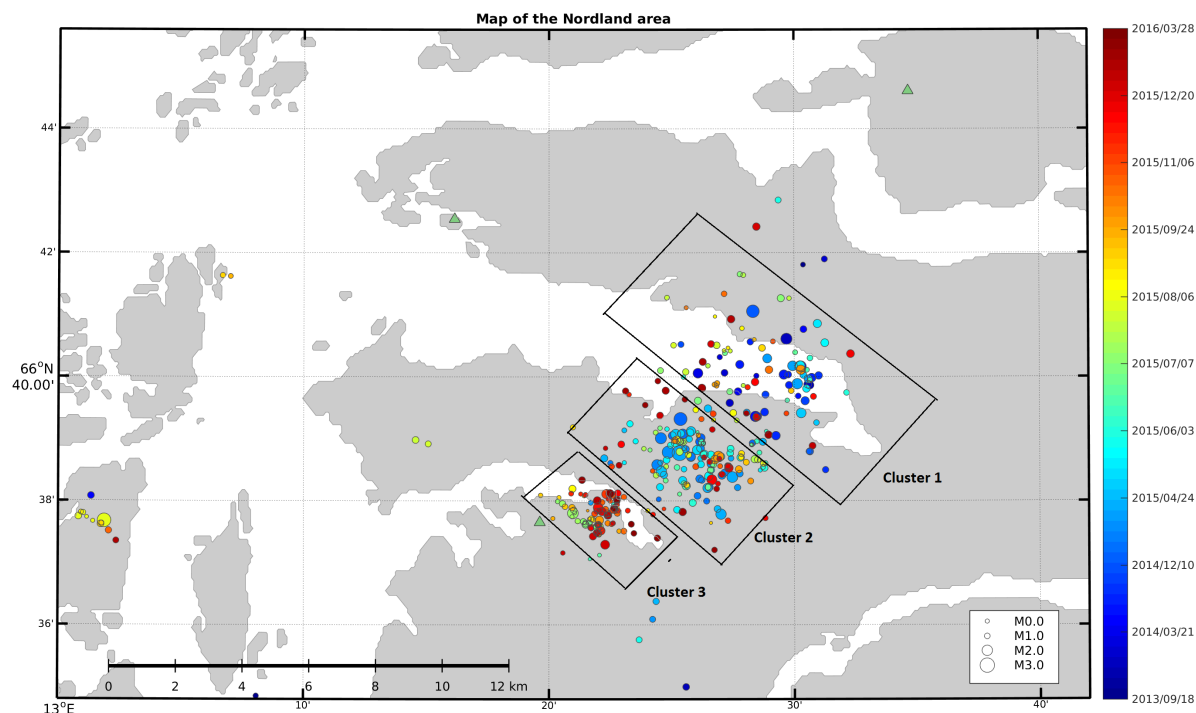
Figure 37: Zoomed in on the three main clusters indicated with black squares, relocated in my main study area from the hypoDD software. Stations locations are represented by green triangles. Earthquakes are plotted with different sizes of circles which indicate sizes of the magnitude, and plotted in colours which point out the date (year/month/day) of occurrence as shown on the bar next to the figure. From the observations the clusters can be divided into three parts, with the latest events in the south, the ones in the middle mostly occurring in the middle of the time scale, and the ones in the north which are a bit random but also have the oldest events.

4.3.1 Main Cluster 1

Fig. 37 shows the seismic zone for the biggest clusters what is considered to be an earthquake swarm with events recorded for a time period over three and a half years, seems to be divided into three different clusters of events and is sub-parallel to the coast in a NE-SW direction. The yellow square seen in Fig. 38a points out the cluster (located furthest North of all main clusters) of the relocated seismicity in this area, approximately covering an area of 4x4 km, containing 95 events with a magnitude M_L between 0.1 - 2.5, and is located between 66.39 - 66.41 °N close to the Svartisen glacier and Reppa power station. A-A' and B-B' indicated which side of the square, which is used for especially figures in 3D to coordinate which side we are looking on.

Fig. 38b show the same cluster in a map view with colors that indicate time of occurrence for the earthquake. From the map view, the relocated events seems to have no obvious major linear trends or structures observed, suggest a volume deformation. Comparison with the other clusters, main cluster 1 has the largest gap between them compared to main cluster 2 and 3 shown in Fig. 37. One observation is that these swarms seems to be starting in the North and moving towards the South. The colors reveals that this cluster

contains the oldest events. While moving further South the majority of events in the clusters are younger.
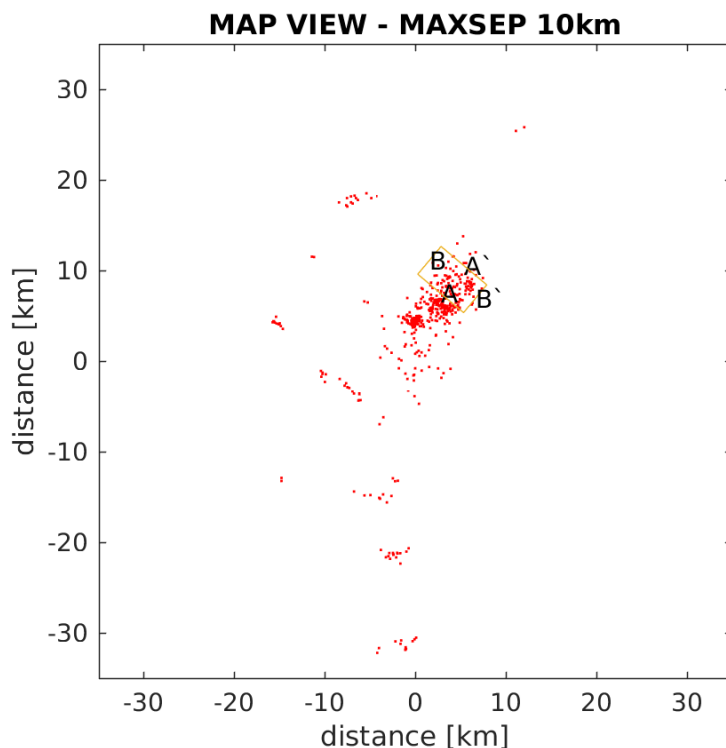
(a) Map view of the entire study area, with the 95 relocated events of main cluster 1 located within the yellow square, with A-A' and B-B' indicating the different sides of the cluster (used explanation for later figures in 3D).
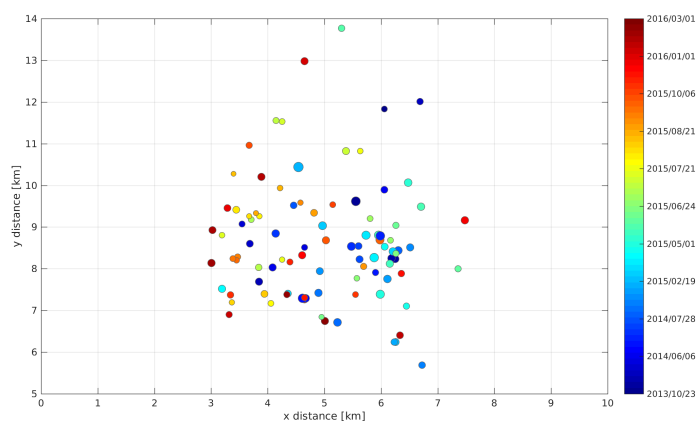
(b) Shows the earthquakes between the red square from Fig. 38a seen from a map view. The hypocenters are shown with coloured dots, where the color indicates their time of occurrence marked on the colorbar at the right.

Figure 38: •

Fig. 39 shows (Angle in A-A' direction) the relocated hypocenters in the seismic zone with

different color indicating time of occurrence in a three dimensional figure, observation of the colors of the hypocenter and their positions gives no clear structures or migration. Observations indicates that the events are randomly distributed. Fig. 40 is viewed from angle B-B' and shows that most events are within a depth range of 2 to 10 km.
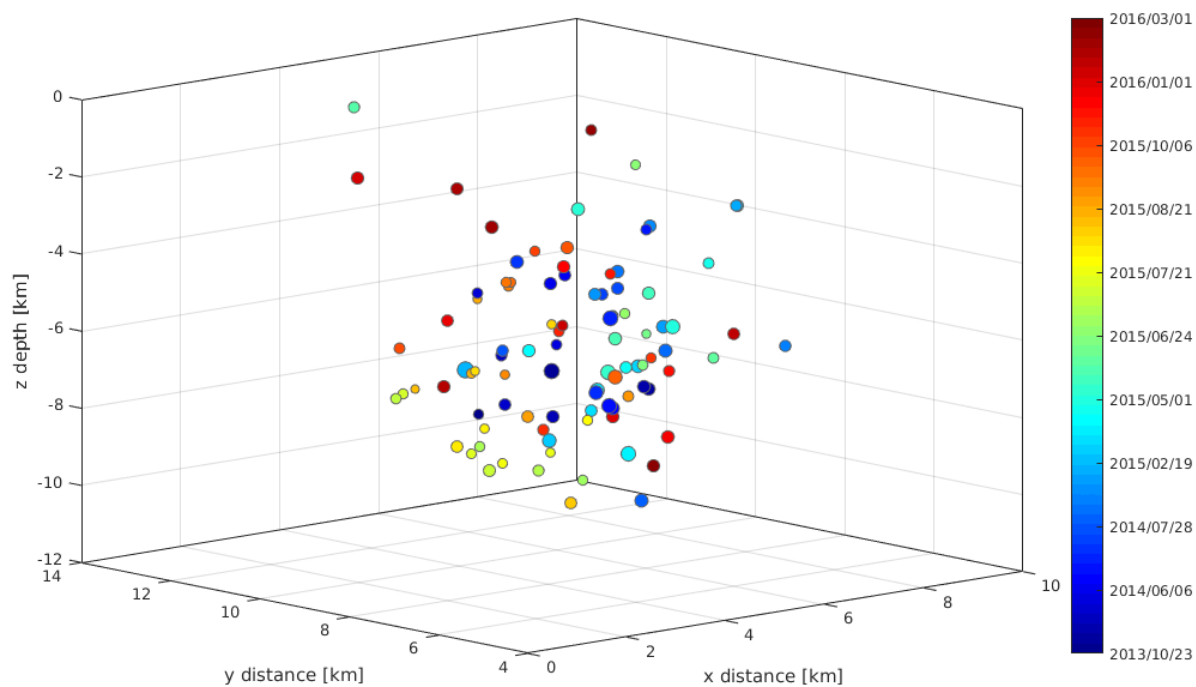

Figure 39: Section A-A' of the main cluster 1, Shows events between 23/10/2013 to 27/03/2016 indicated with different colors and their focal depths. No clear distribution of earthquakes.
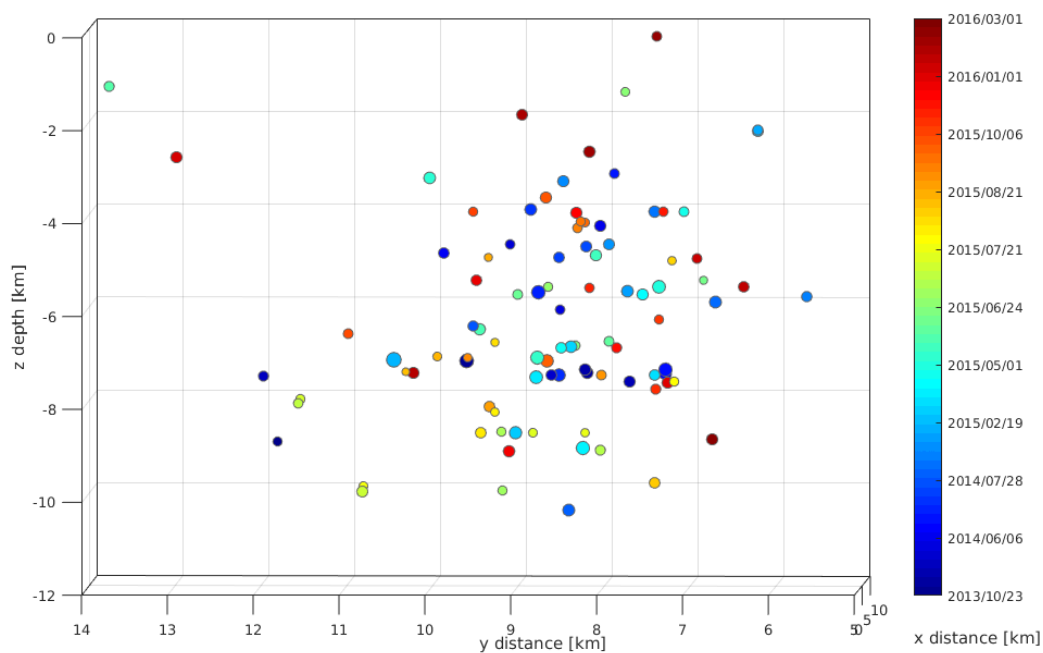
Figure 40: 3D figure of the main cluster 1. Seen from a cross section view B-B', No vertical patterns seen. Most of the earthquakes occurs between 2 and 10 km depths.

4.3.2   Main Cluster 2

The second part of the main cluster contains 156 events with magnitude M_L between 0.1 - 3.2 and is relocated slightly further Southwest (4-5 km) Fig. 37 between 66.37 - 66.39 °N close to the Blokktind mountain (1032 moh). In a map view Fig. 41a the relocated events compared to the previous cluster appear more tightly clustered with event being centred in the middle displayed in Fig. 44b. Compared the time of occurrence with main cluster 1, the majority of the events are occurring in the middle of the time scale or younger.

MAP VIEW - MAXSEP 10km
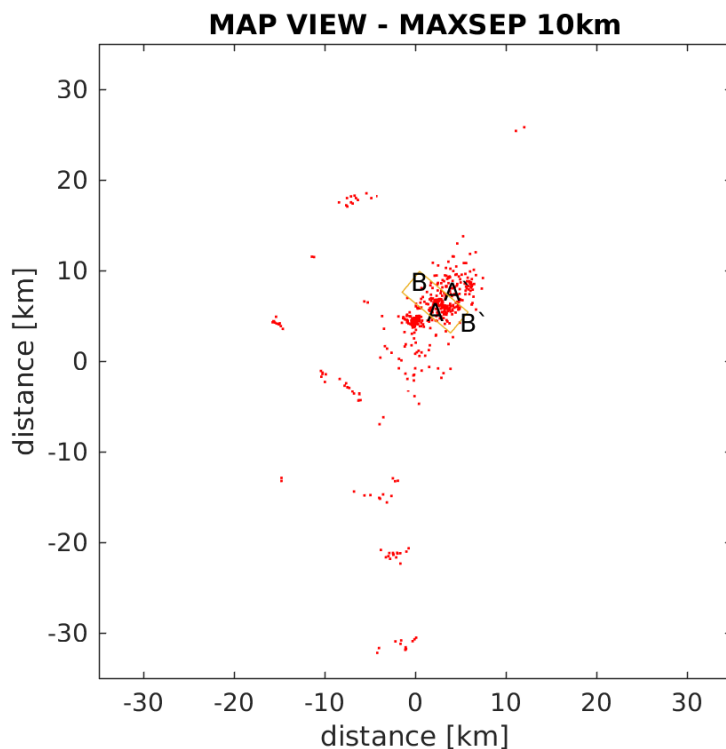
(a) Map view of the entire study area, with the 156 relocated events of main cluster 2 located within the yellow square, with A-A' and B-B' indicating the different sides of the cluster
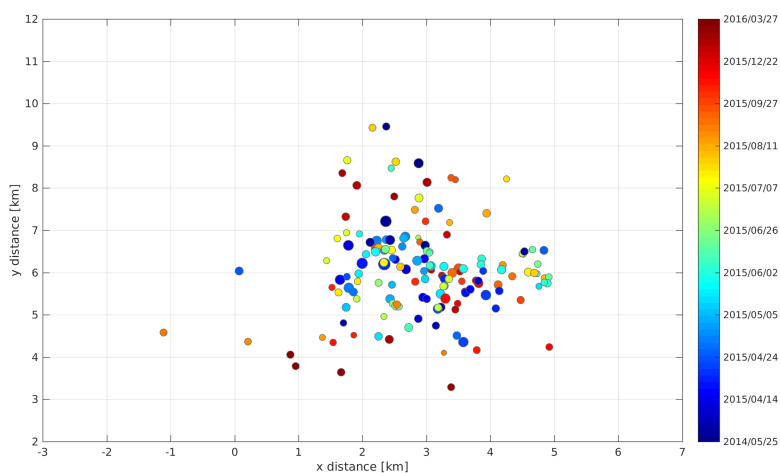
(b) Shows the earthquakes between the red square from Fig. 41a viewed from a map view. The events are plottet in different colors indicates their time of occurrence.

Figure 41: •

Fig. 42 shows (Angle in A-A' direction) the relocated hypocenters in the seismic zone. Observations within the cluster of the events time of occurrence and of and their distribution in space, gives no clear structures, and looks to be mostly randomly distributed like main cluster 1.
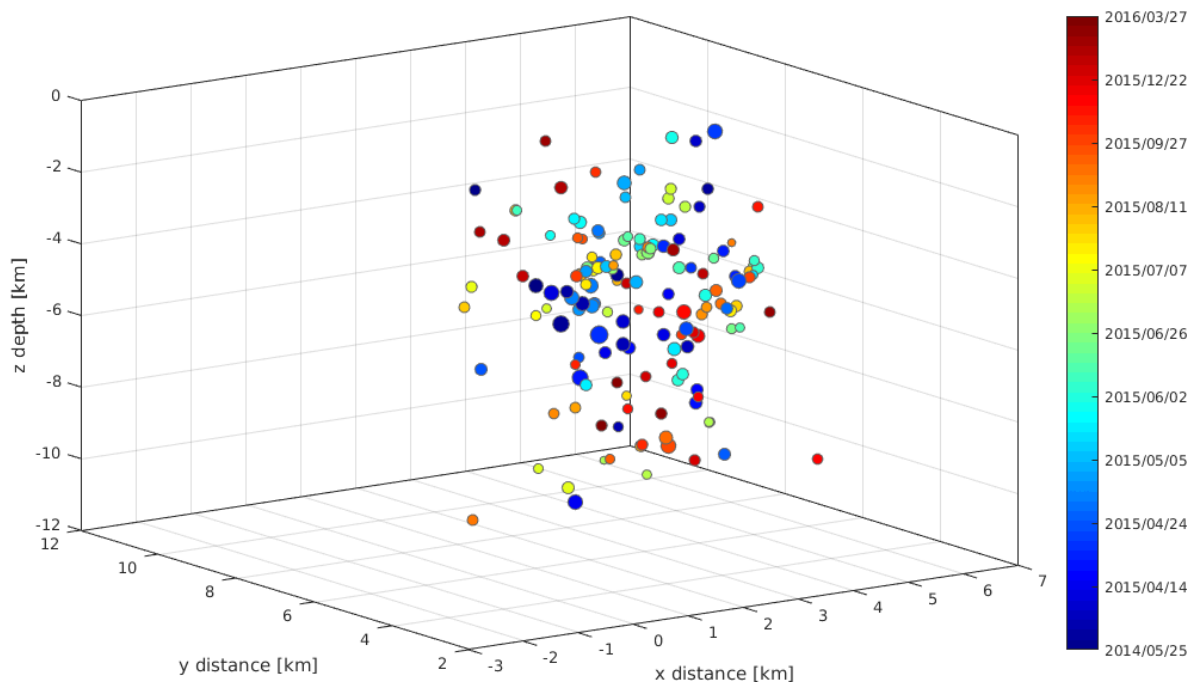
Figure 42: 3D plot of main cluster 2, in a A-A' point of view (northeast). Colors of the dots indicates time of occurrence. Event seems to be randomly distributed in time and space.
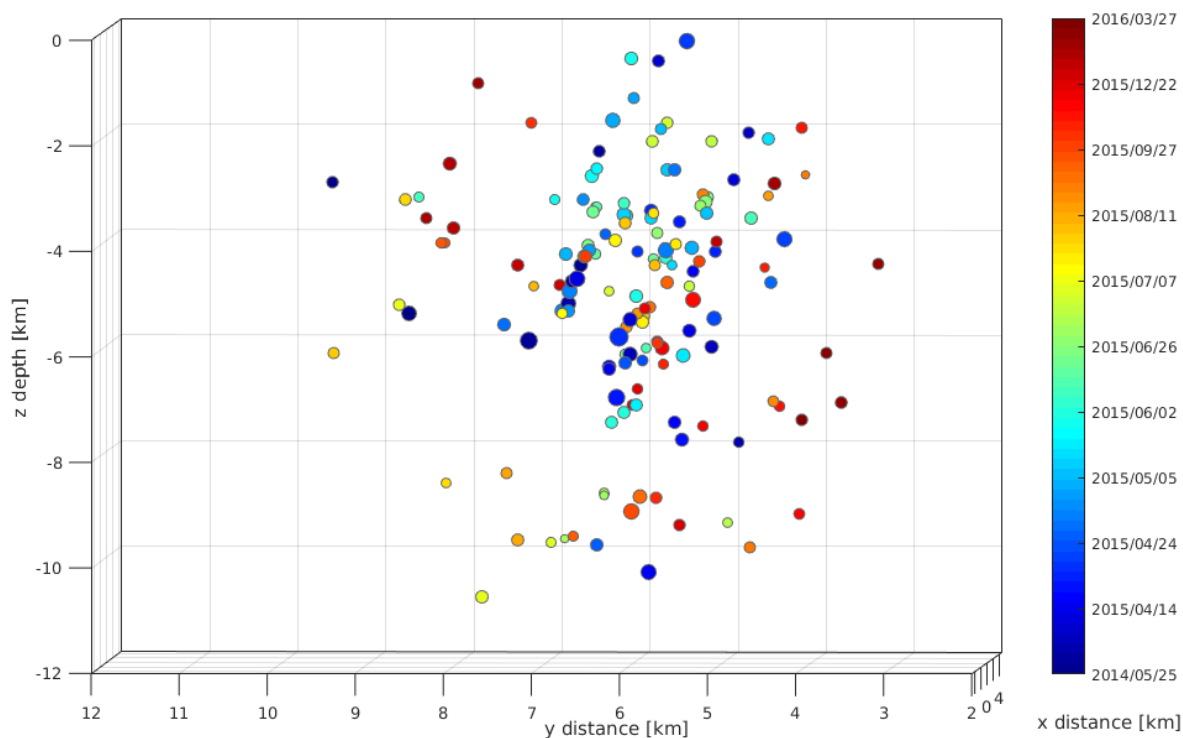

Figure 43: 3D figure of the main cluster 2. Seen from angle B-B', No vertical patterns seen. Most of the earthquakes occurs between 2 and 10 km depths.

4.3.3   Main Cluster 3

The third part of the main cluster contains 95 events with a magnitudes M_L between 0.1 - 2.0, and is relocated 4-5 km further Southwest of main cluster 2 (Fig. 37), between 66.38 - 66.37 °N close to the Jektvik. The yellow square in Fig. 44a points out where the cluster is located shown in a map view. The relocated events in main cluster 3 appear more tightly clustered compared to the previous clusters.

Zoomed in on the cluster Fig. 44b), reveals four horizontal linear features (indicated with black lines) which all seems to be in a NW-SE direction, with some being slightly more to the North. Longest line is approximately 1.5 km long and the shortest is around 0.5 km. The distribution of earthquakes over time for the linear trend is mostly between a time period of 5 months, where most of the events in this cluster are of recent time, compare to the other main clusters. Except of the linear trend furthest to the South, which seems to include events around the same time, no migration in time is observed within the cluster.

MAP VIEW - MAXSEP 10km
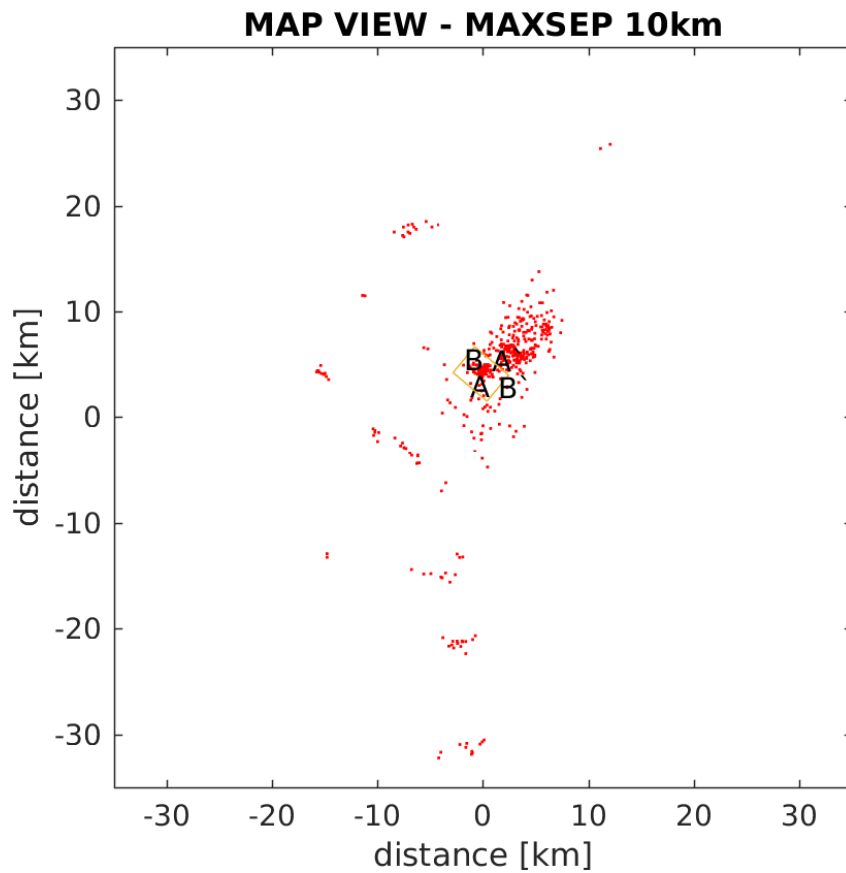
(a) Map view of the entire study area, with the 95 relocated events of main cluster 4 located within the yellow square, with A-A' and B-B' indicating the different sides of the cluster.
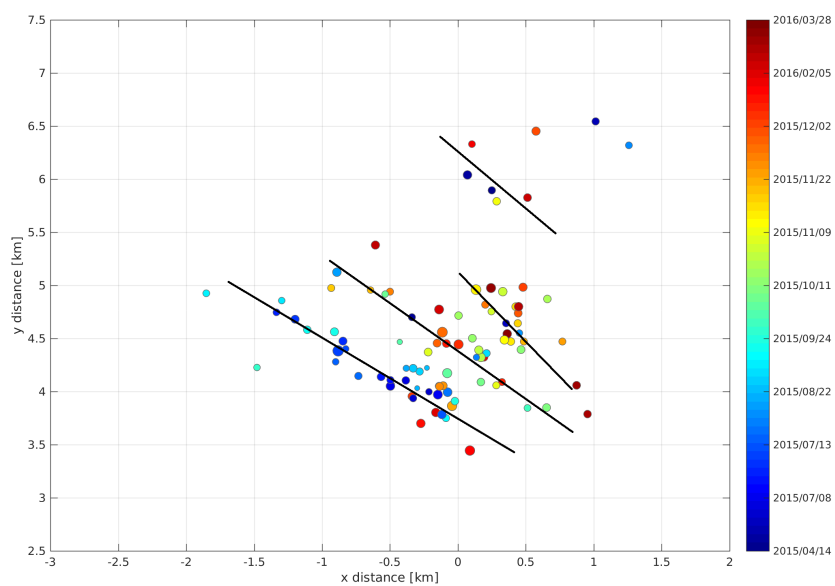
(b) Relocated events between A-A' and B-B', seen from a map view. Different colors indicate time of occurrence and the black lines suggest horizontal linear trends.

Figure 44

Fig. 45 looks into the linear trends from a SE-NE direction, trying to observe any orientation of the structures, which is seemingly difficult to identify. The longest linear trend furthest to the south, looks to be dipping to the Northeast, event gradually gets deeper from the East to the North. The linear trend furthest to the north contains the shallowest events from 3 to 5 km depths, moving towards the south the trends gets deeper with events between 5 and 10 km (Fig. 46).
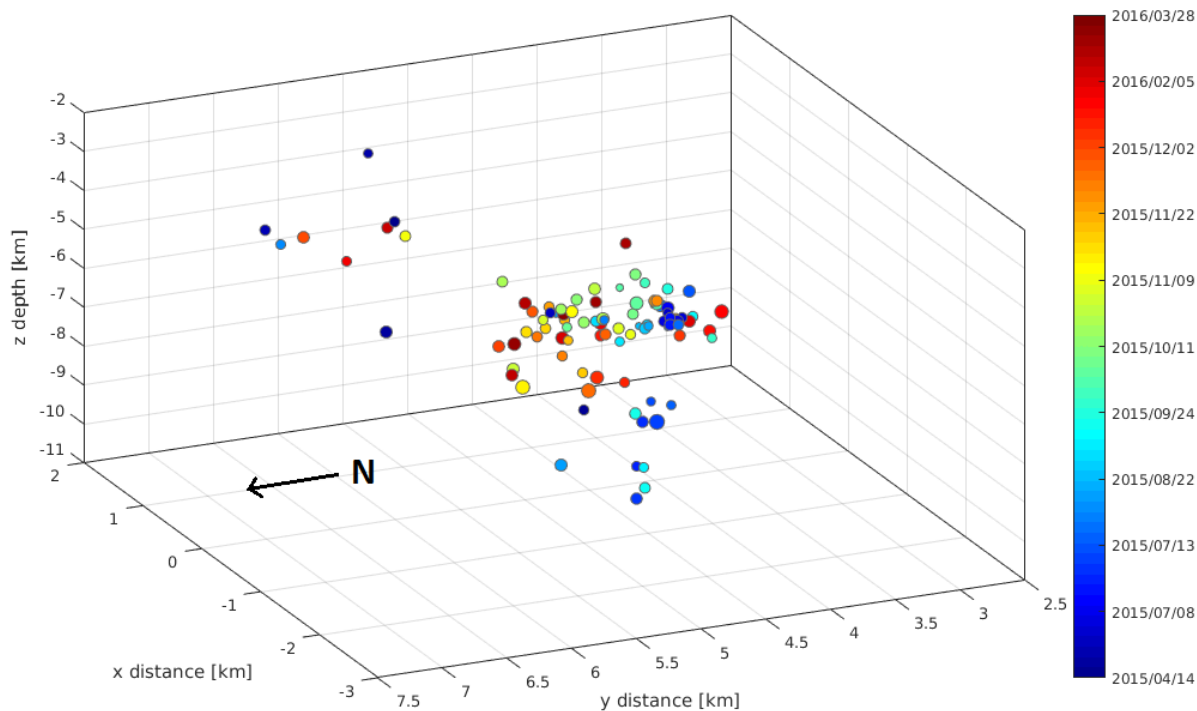

Figure 45: 3D figure of the main cluster 3, looked into SE-NE direction. Events time of occurrence is indicated with coloars. Shallowest events are located furthest North and gets deeper moving towards the South.
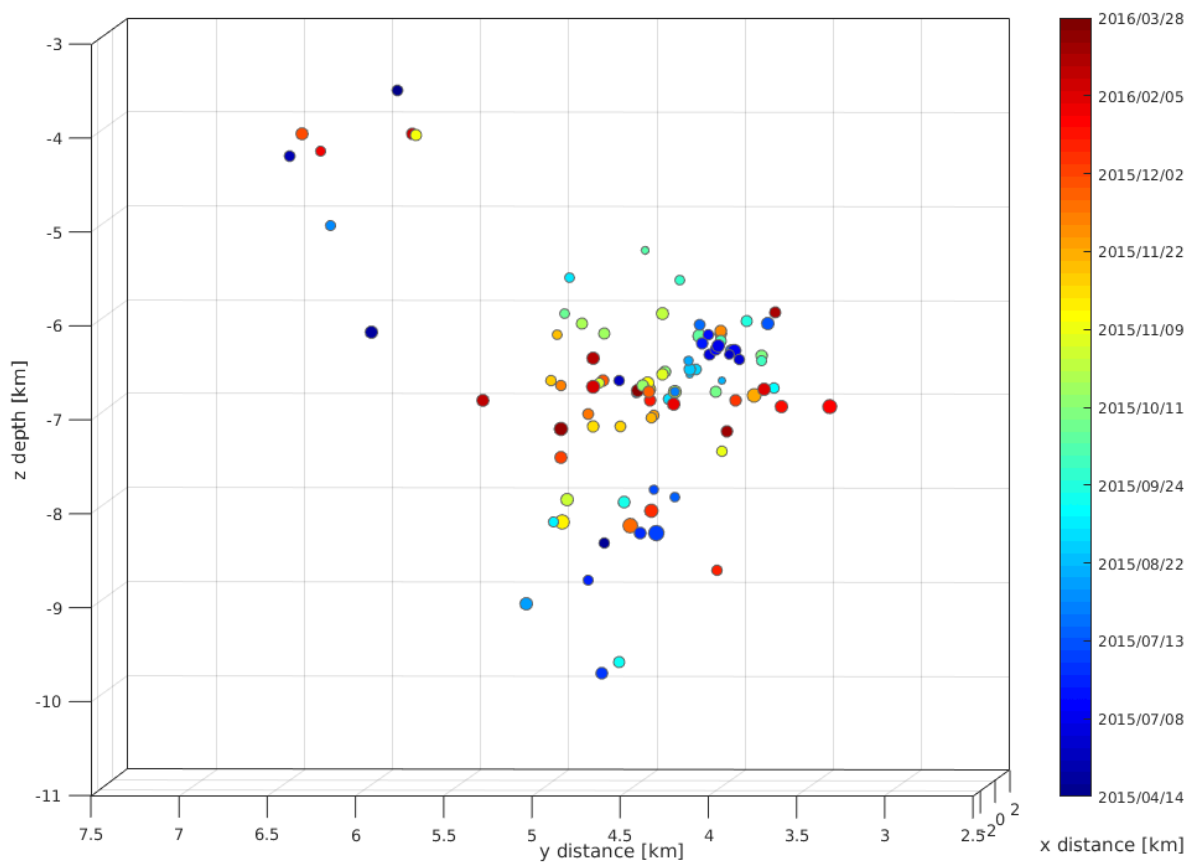
Figure 46: Shows events focal depths, viewed from angle towards B-B' of the main clust 2. Depth range is from 3.5 to 10 km, with most of the hypocenters located between 6 and 9 km. Most recently events are located at a depth of 7 km surrounded by older events.

4.3.4   Cluster 4

Cluster 4 includes 11 events with a magnitude M_L between 0.1 - 2.8, and is located West of the main clusters between 66.37 - 66.38 °N at Gjerøy (Fig. 47a). First observations suggest a clear linear alignment trending NW-SE of the relocated hypocenters. A relative small gap between each events on the line. Events are stretched over a distance of 1 km. Fig. 47b shows the events time of occurrence with different colors. Which the latest (oldest) events are located from the Northwest, and is getting younger moving further to the Southeast, could suggest they migrate in time.
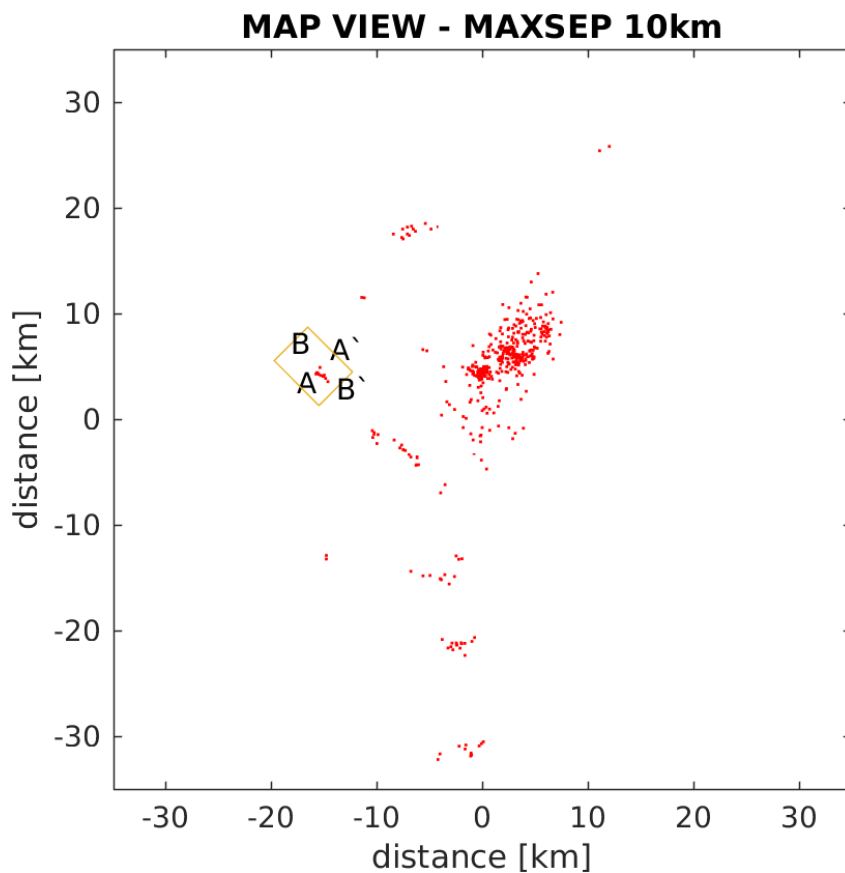
(a) Map view of the entire study area, with the 11 relocated events of cluster 4 located within the yellow square, with A-A' and B-B' indicating the different sides of the cluster.
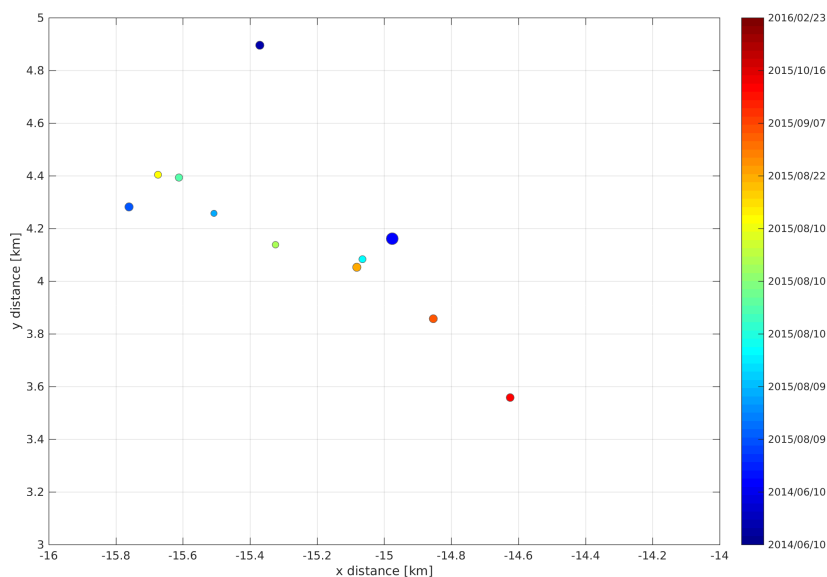
(b) The cluster 4 relocated events in a 3D plot seen from a map view, showing a linear feature.

Figure 47

Fig. 48 shows that most events belonging to the linear alignment are located within a depth range between 9.5 to 10.5 km, with three events located deeper between 11.5 and 12.5 km. Since the events seem to be migrating in time and occurring around the same depth with small distance separating them, indicates that the events in the linear alignment are connected in a structure. The attached black square is a suggestion for a fault plane.
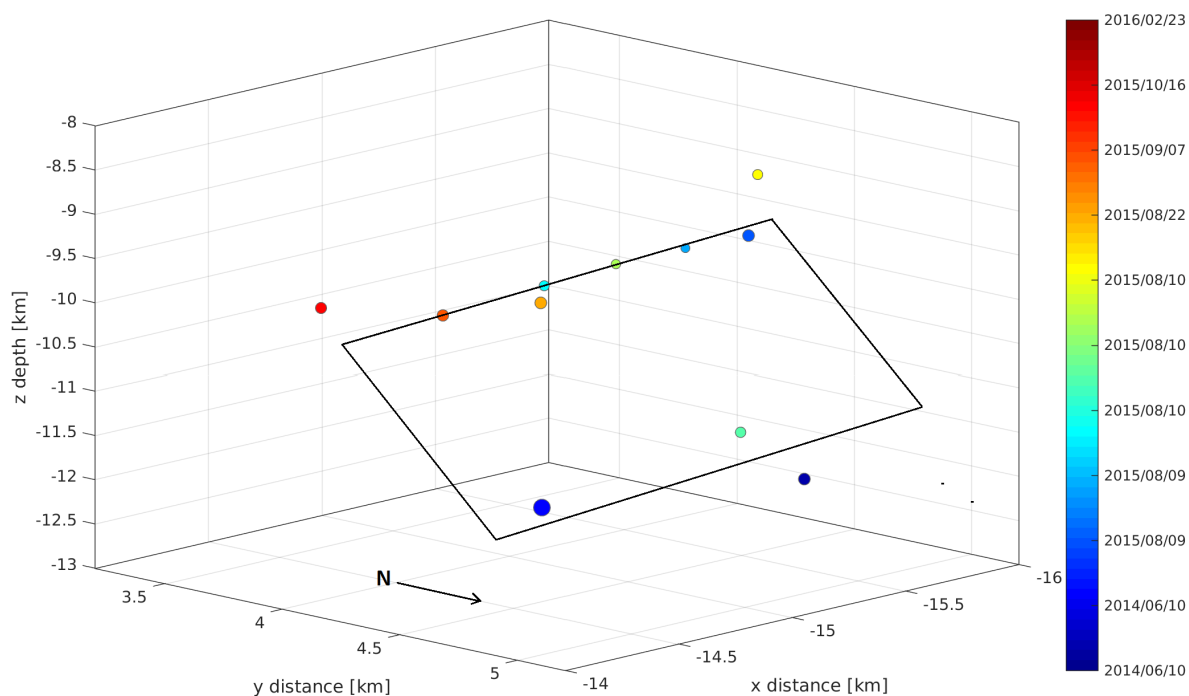

Figure 48: Geometry of cluster 4 observed from angle A-A' in a three-dimensional view, showing the hypocenters time of occurrence indicated with colors and the bar at the right side. Most events are located at equal depth around 10 km, except some of the oldest events (blue color) that are located at around 12 km. The black square indicates a suggested fault plane dipping toward the Northeast.

4.3.5 Cluster 5

Cluster 5 contains 28 events with a magnitude M_L between 0.2 - 1.3 (Fig. 49a) and is located southwest from the main clusters between 66.32 - 66.36 °N. The events are divided into two parts one further Northwest but almost parallel to the other part, with approximately a 2 km gap between them, suggest that there are two structures. Both parts are tightly clustered with one part more linear aligned in a NW-SE direction, parallel to cluster 4 (Fig. 47a) and placed in the same direction as the cluster 3 but further southeast. The events are stretched over a total distance of almost 6 km. The smallest part to the right is occurring in between a time period of two weeks, with a scattered distribution of events (Fig. 49b). The bigger linear feature to the right has a larger range in time about approximately one year, with recent events occurring furthest to the Southeast and older events occurring to the Northwest, with events appearing to

migrate from going to Northwest to Southeast in time.

MAP VIEW - MAXSEP 10km
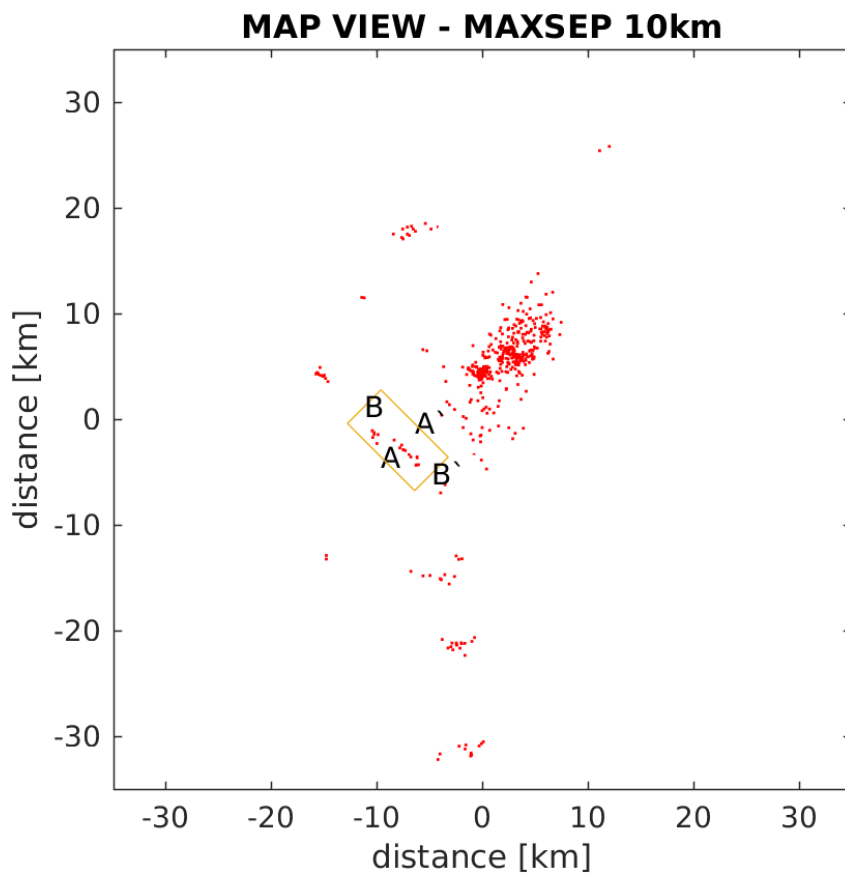
(a) Map view of the entire study area, with the 28 relocated events of cluster 5 located within the yellow square, with A-A' and B-B' indicating the different sides of the cluster.
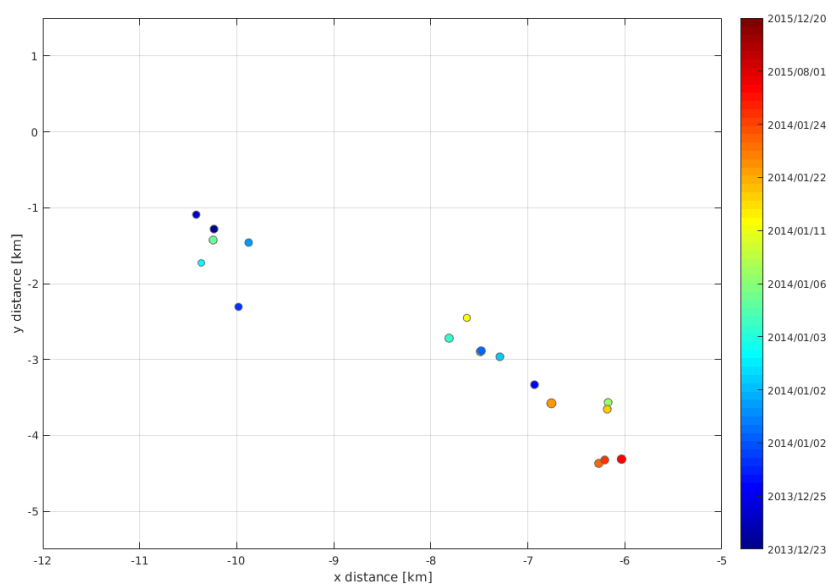
(b) Shows relocated events in cluster 5 with a 3D plot seen from a map view. The different colors indicate time of occurrence, seen from the bar at the right. Events from cluster 5 seems to be migrating in time, with the most recent events located in the southeast and the oldest events located in the northwest.

Figure 49

Fig. 50 shows that there is a gap between the two parts and are probably from different structures. Observes that events gets deeper moving to the northwest, could mean that the the linear trend furthest to the southeast is dipping to the northwest. Looking at the cluster from the B-B' point of view, shows that events are located at depths between 5.5 to 7 for the smallest part and 4 to 6.5 km for the linear part (Fig. 51).
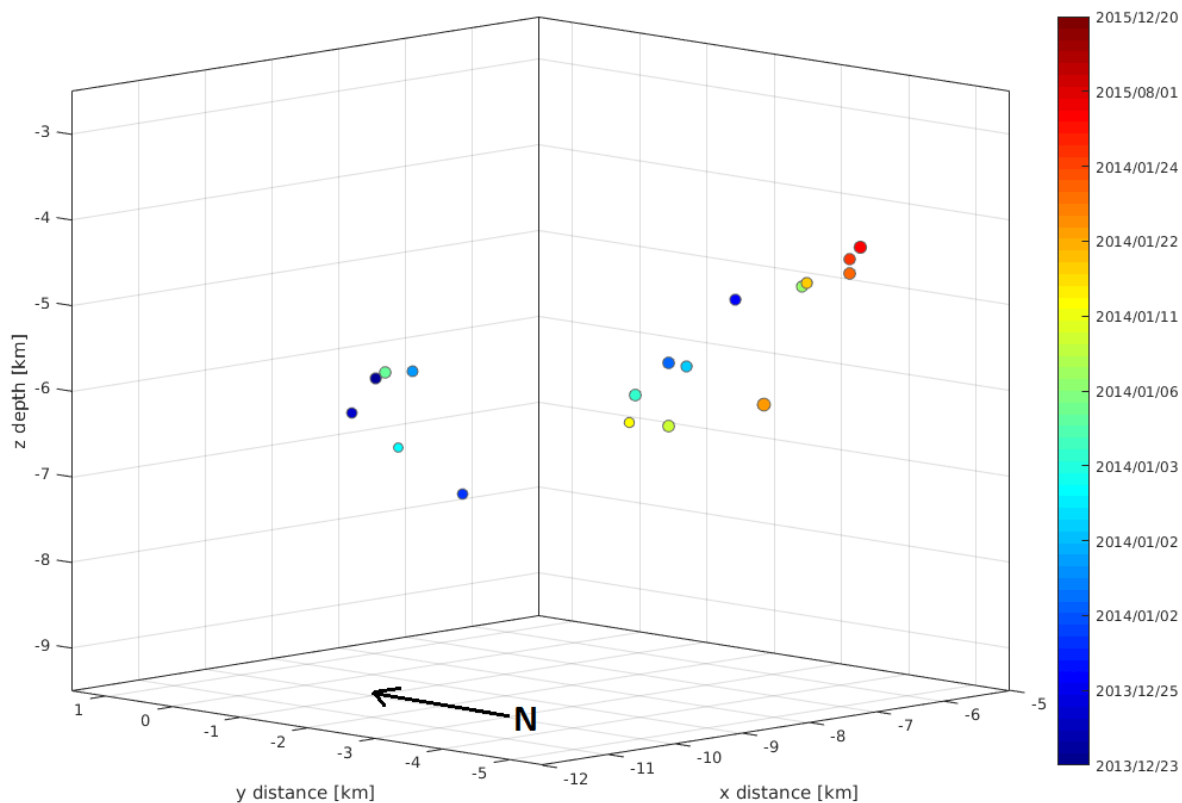
Figure 50: 3D plot of cluster 5 from the A-A' point of view, showing the hypocenters depth and time of occurrence.
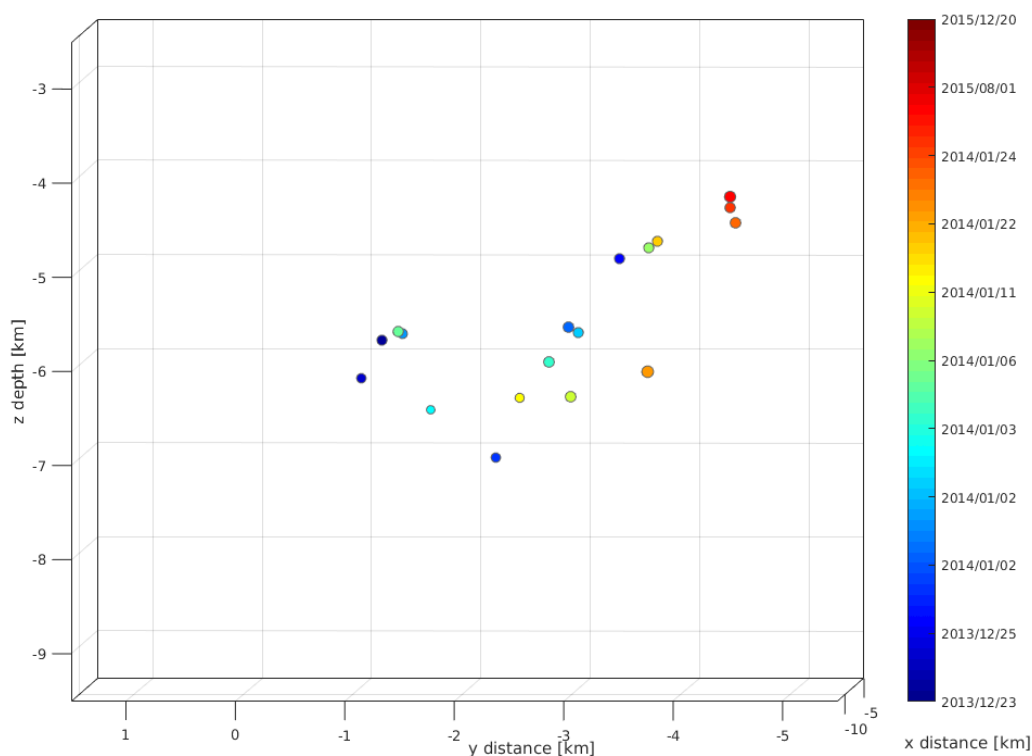
Figure 51: Cross section of cluster 5, showing the hypocenters depth and time of occurrence.

4.3.6   Cluster 6

Cluster 6 contains 10 hypocenters with a magnitude M_L between 0.1 - 1.1 (Fig. 52a), and is located North from the main clusters between Øresvik and Vassvik at 66.25 - 66.27 °N. The events are not as tightly clustered as the previous clusters, but do form a linear alignment in an almost W-S direction in a map view. The structure is stretched over a distant of 4 km with ratter large gaps up to 1 km between some events. Two events are located away from the structure which also is the most recent events in time. The time occurrence of the earthquakes are seemingly going from youngest to oldest from west to east (Fig. 52b) with a few exceptions, suggest a migration in time between a time period of almost 4 months.
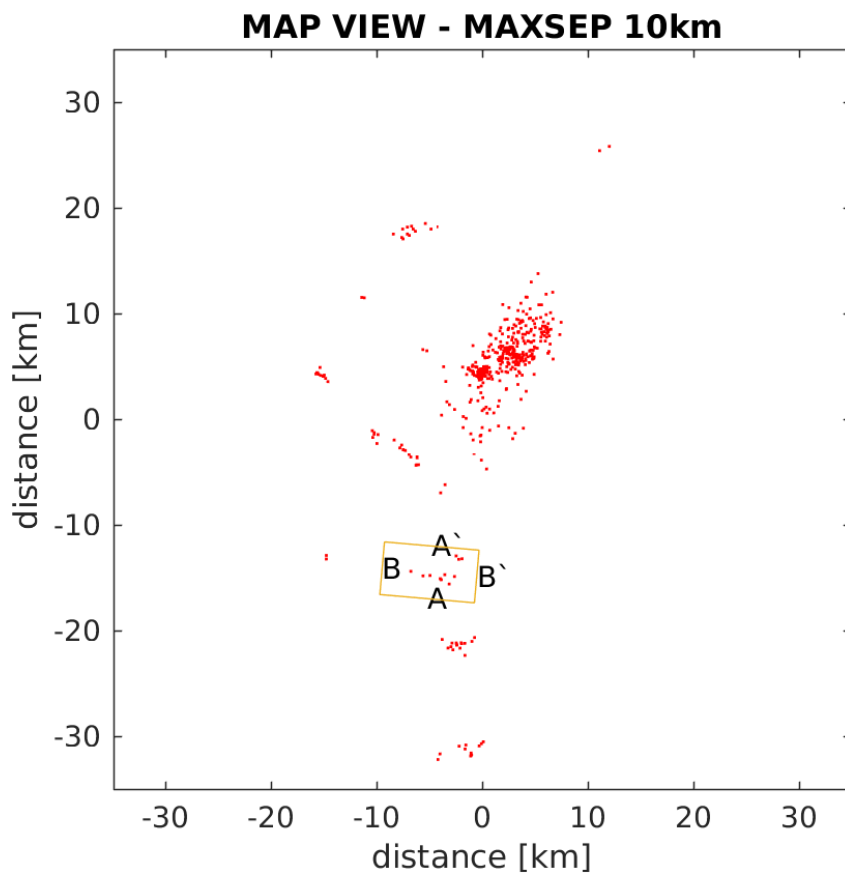
(a) Map view of the entire study area, with the relocated events of cluster 6 located within the yellow square, with A-A' and B-B' indicating the different sides of the cluster.
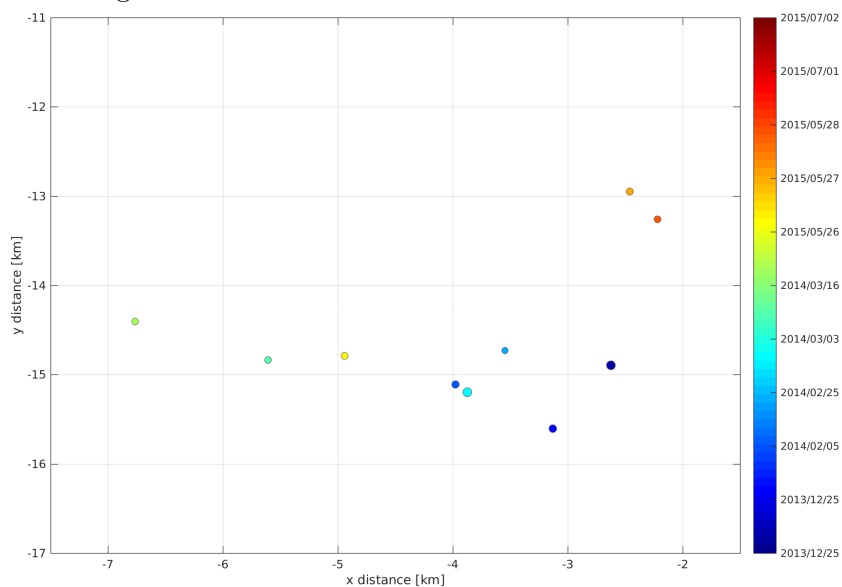
(b) Closer look on Cluster 6 in a 3D plot seen from a map view. The linear alignments horizontal direction almost E-W slightly NW-SE. Events are oldest at East and younger to the West.

Figure 52: •

Fig. 53 from a B-B' point of view divides the cluster in to three parts with different depths. The events are located at depths range from 7 to 17 km. The oldest events are located at the shallowest from 7 to 10 km, and the events occurring in the middle of the time scale are located at depths between 13 and 17 km. Most recent events are located in between at depth about 11 km.Since the linear alignements are divided into three parts, indicates that these parts are from different structures with different depths, since each part is occurring close in time. Fig. 54 shows a 3D figure of the cluster 6 almost from a W-E direction. No specific structure is seen from the three parts, and not possible to determine a fault plane. Seemingly these three parts does not belong together.
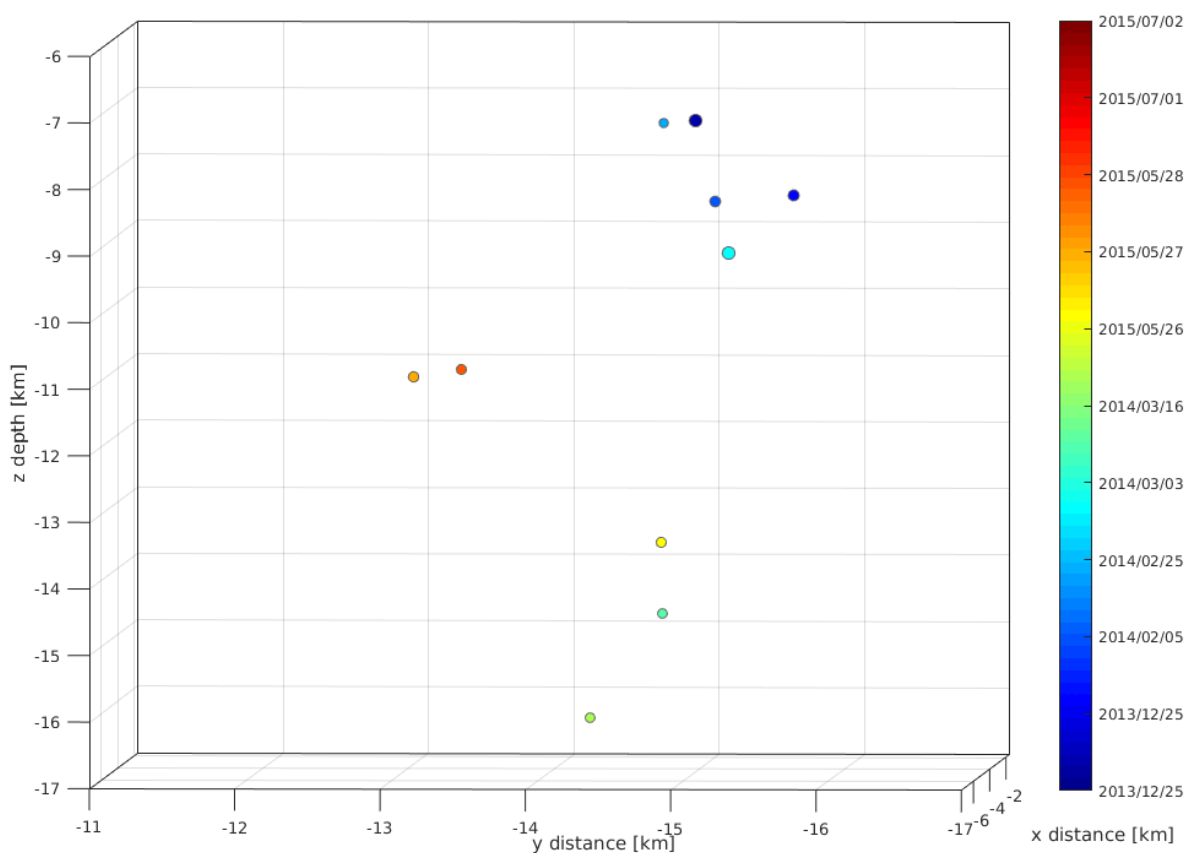
Figure 53: Shows events focal depths, viewed from angle towards B-B' of cluster 6. The events are divided into three parts with depth range from 7 to 17 km. Most recent events located in the middle at approximately 11 km, oldest events located shallowest and the events in the middle of the time scale is located deepest.
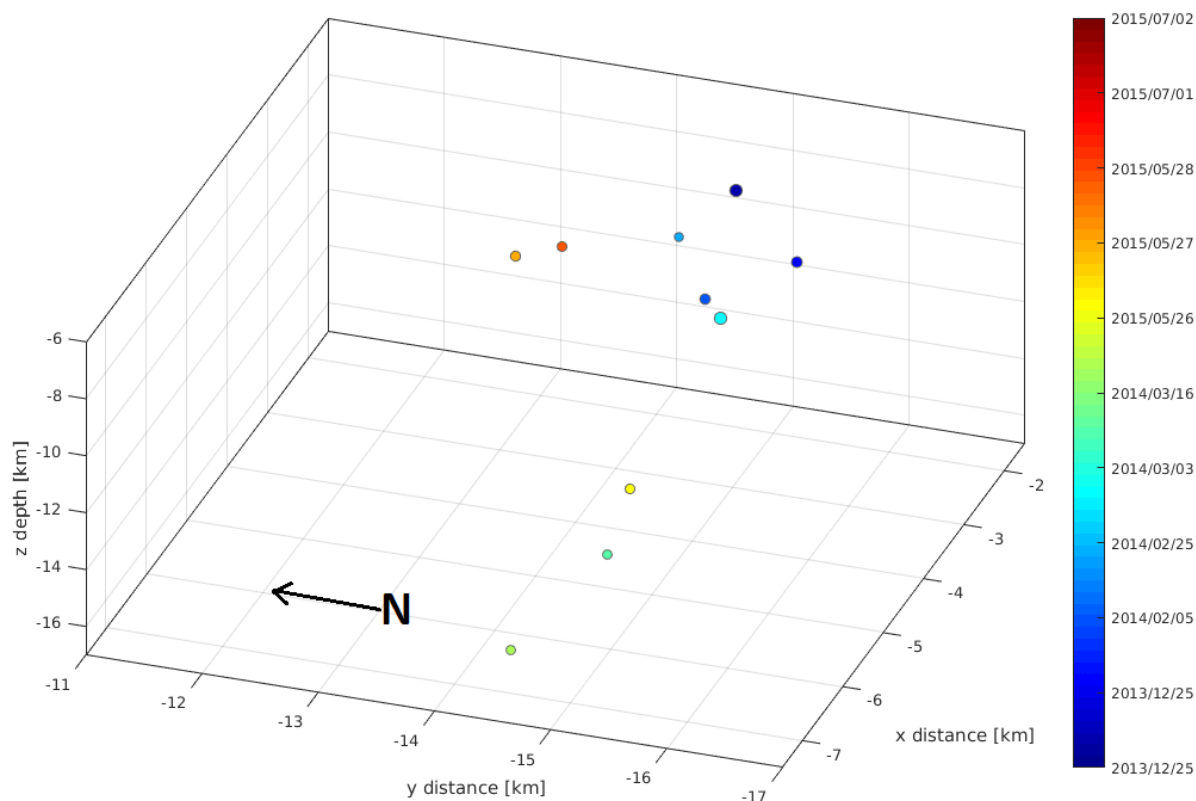
Figure 54: 3D plot of cluster 6 seen from an almost W-E direction. Seemingly from this angle no connection is observed between the parts.

4.3.7   Cluster 7

Cluster 7 contains 15 events with a magnitude M_L between 0.1 - 1.9 (Fig. 55a) is located North from the main clusters and just east of the Kvanndalsvatnet lake (Bratland) between 66.23 - 66.25 °N. The hypocenters are tightly clustered and form a lineation almost W-E direction (slightly more to the NE-SW) in a the map view. The cluster is stretched over a distant of 3-4 km with where some gaps occur, the time occurrence of the earthquakes are seemingly going from most recently to older from west to east (Fig. 55b) with a few exceptions.

MAP VIEW - MAXSEP 10km
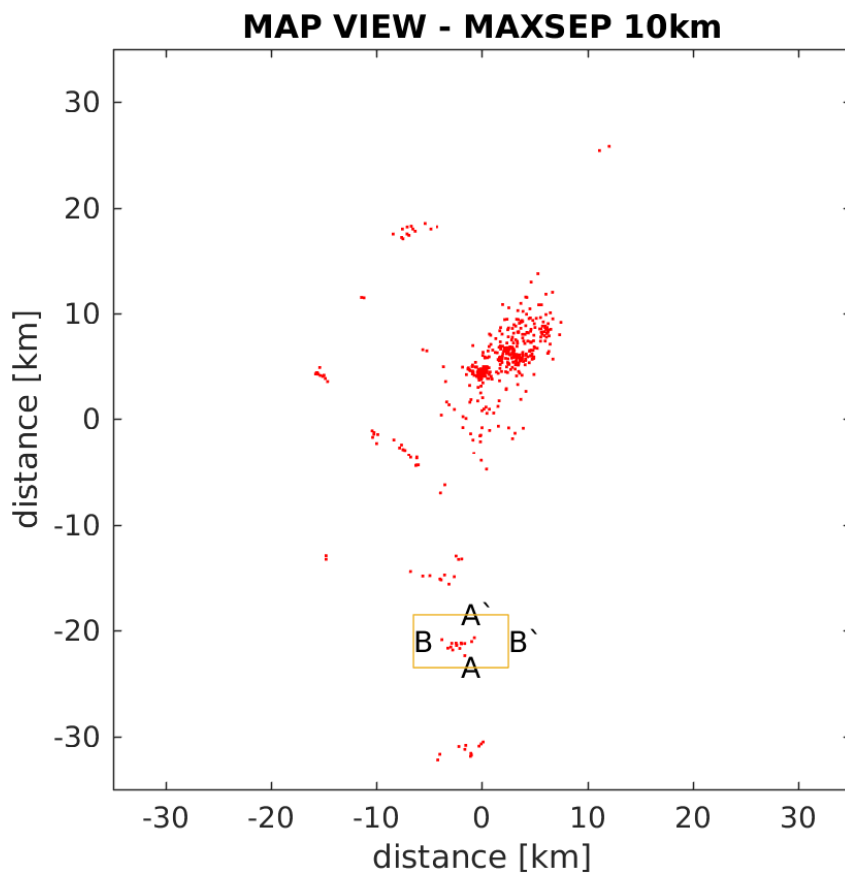
(a) Map view of the entire study area, with the 15 relocated events of cluster 7 located within the yellow square, with A-A' and B-B' indicating the different sides of the cluster.
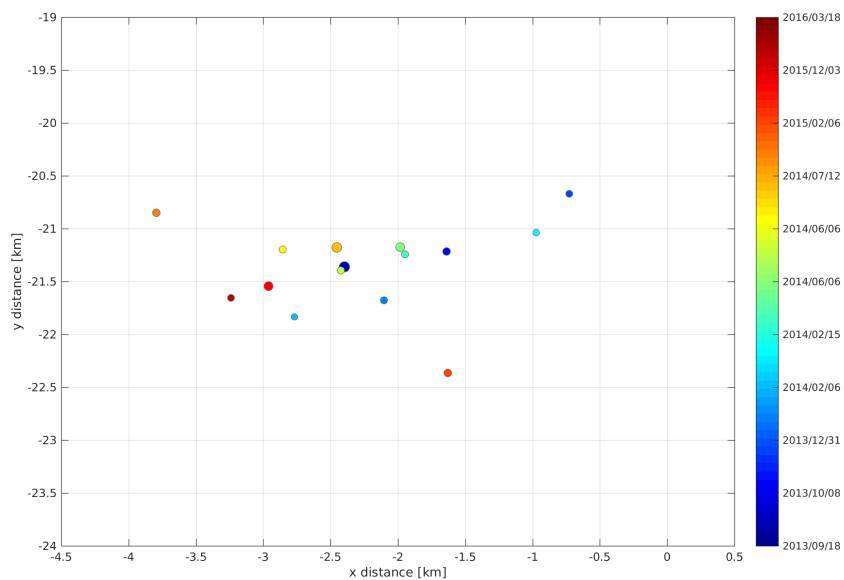
(b) The main cluster 7 relocated events in a 3D plot seen from a map view, Shows events between and °,

Figure 55

Fig. 56a show that the relocated hypocenters are located at depths range from 4 to over 13 km, with a scattered distribution. Two of the most recent events are located deepest and most recently events are located shallowest. Fig. 56b show clearer that the events in the lineation is located at different depths vertical and horizontally with a no pattern observed in time, but mostly a scattered distribution. The structure seems to be dipping slightly to the South but is almost vertical.
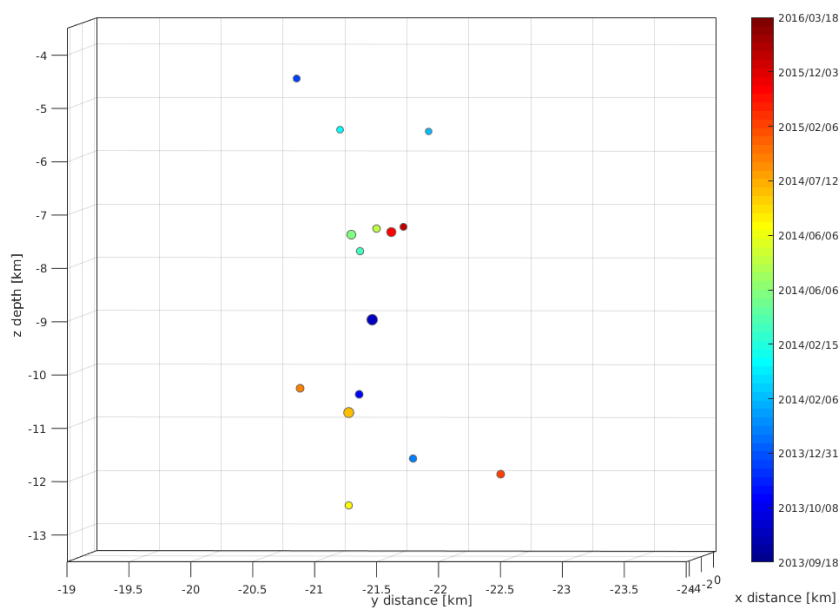
(a) view from B-B' angle, depths are from 4 to 13 km.
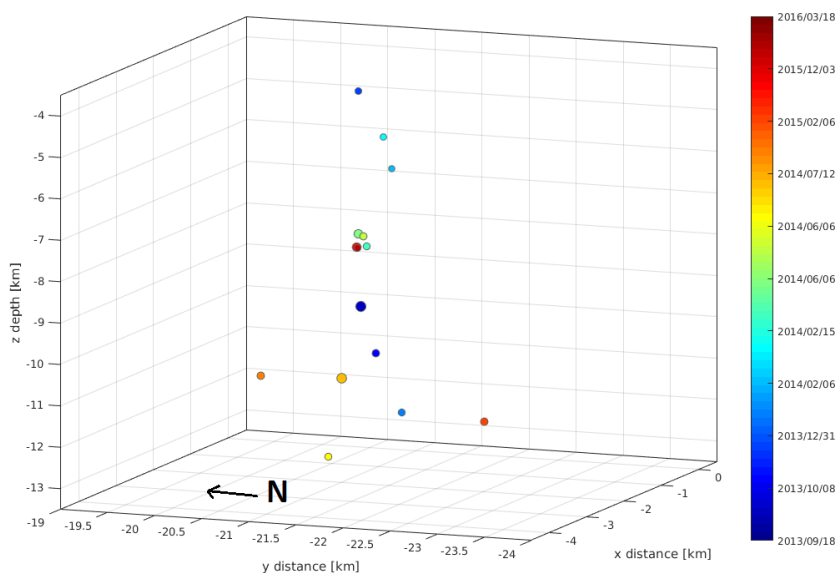
(b) Cross section viewed perpendicular to the structure.

Figure 56

4.3.8 Cluster 8

Cluster 8 shown in Fig. 57a contains 11 hypocenters with a magnitude M_L between 0.2 - 1.6 is located farthest South off all the clusters in this main research area, in the east part of the Sjona fjord between 66.18 - 66.19 °N. The hypocenters are not as tightly clustered as previous clusters and contain some larger gaps between events. The relocated hypocenters do not form as clear linear alignment as the other cluster seen above, but is migrating in time from east to west from oldest to most recently (Fig. 57b), looking to be divided into parts. The oldest events (blue color) are align in a NE-SW direction oldest to youngest from from NE to SW. Northwest from this small lineation is a part consisting of three events occurring in a time period of less than 2 months, in between the oldest and the youngest events.

MAP VIEW - MAXSEP 10km
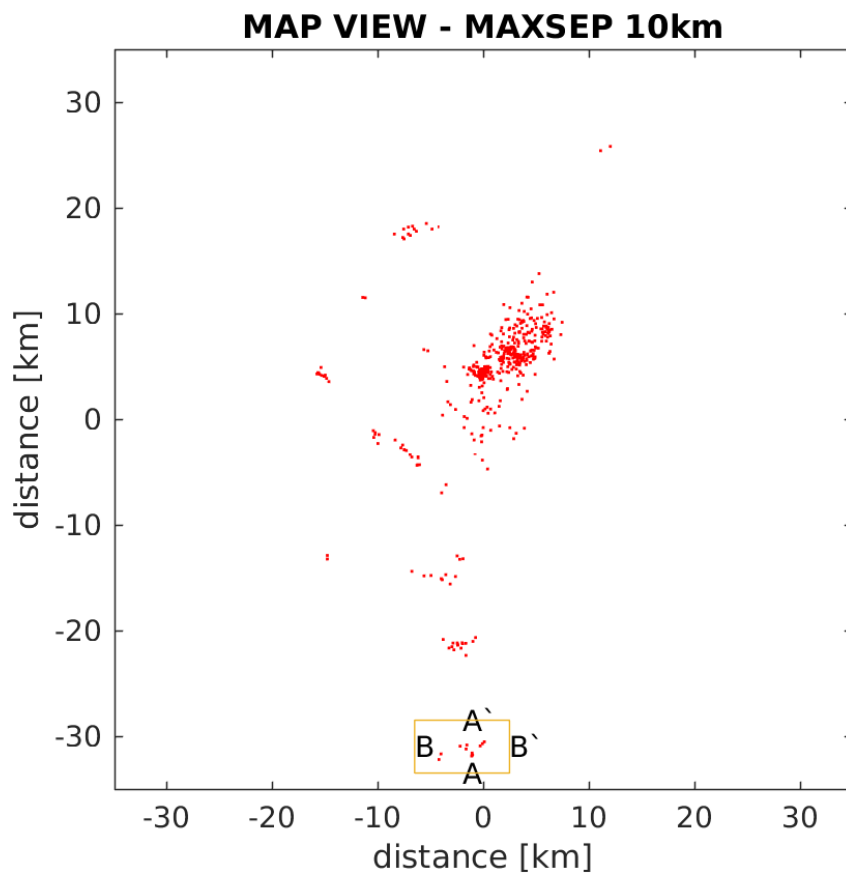
(a) Map view of the entire study area, with the 11 relocated events of cluster 8 located within the yellow square, with A-A' and B-B' indicating the different sides of the cluster.
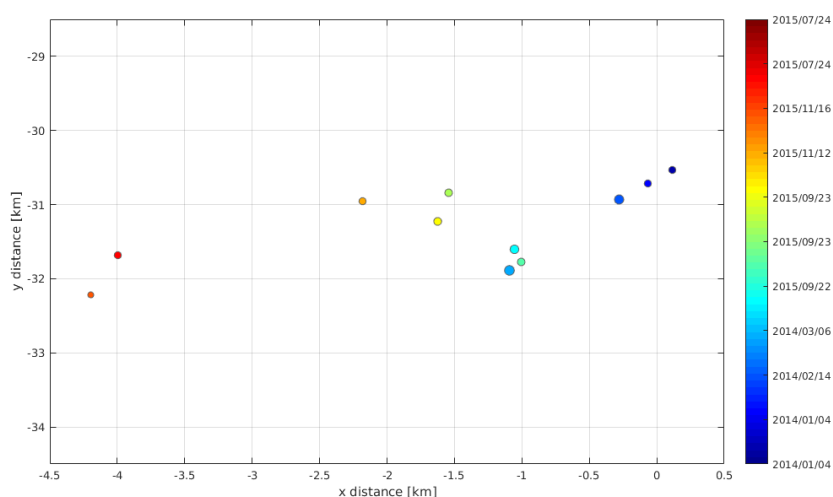

(b) The main cluster 8 relocated events in a 3D plot seen from a map view, Shows events between and °,

Figure 57: •

Fig. 58 show that the relocated hypocenter are located at depths from 4 to over 12 km, where the oldest events are located shallowest and the most recently events are located

deepest. The map view reveals no large clear lineation of hypocenters like for some clusters above, the structure include events that are within a depth of 4 to over 7 km, where the most recently events are located deepest. Fig. 59 shows a suggested fault plane attached indicated with the black plane. A little vauge, would prefer to This plot shows a clearer dipping of the structures towards the West. The two oldest events (red color) are divided from the other events at a larger depth, and further west from the other events.
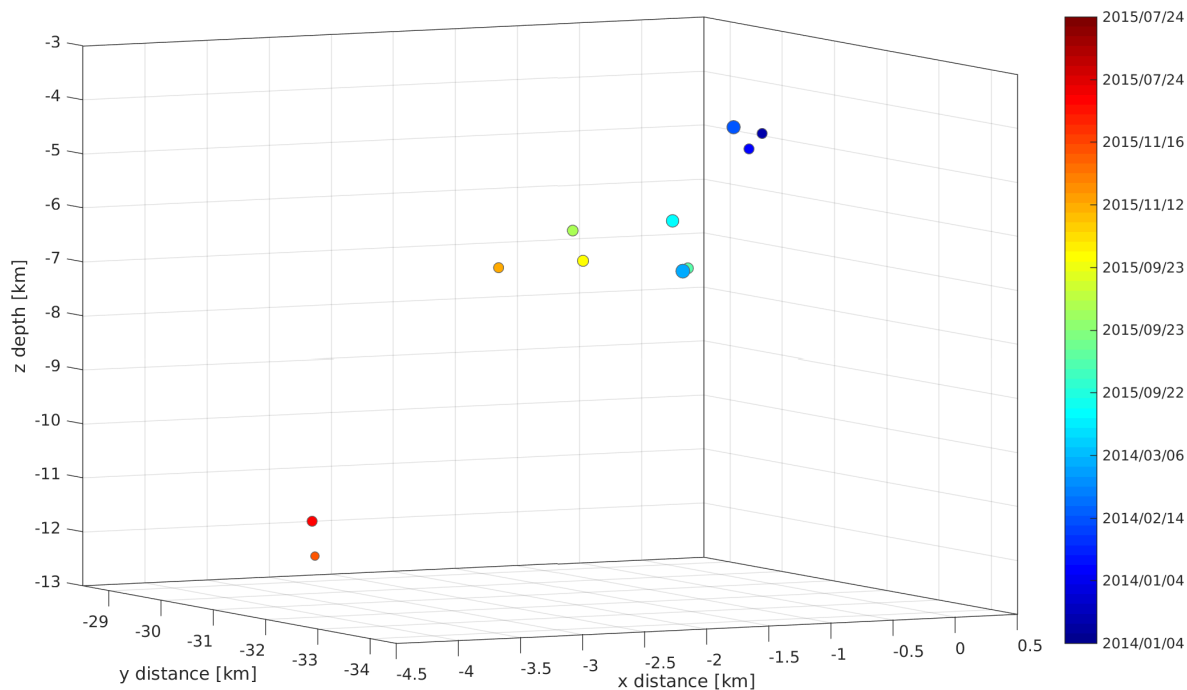
Figure 58: Point of view in the Northeast direction, show the 11 events and their depths and time of occurrence. Oldest hypocenters are located closer to the surface and recent events deeper.

Figure 59: 3D view almost perpendicular to the structure (upper events) show the dip of the structure going to the Southwest, the black square is a suggested fault plane.

5 Discussion

The purpose of this study was to investigate the earthquake swarm and other seismic features in the Nordland area, by relocating the 1208 seismic events with the use of the double difference method implemented in the hypoDD software. A large cluster of events together with five smaller clusters arranged in a linear alignment with different directions have been identif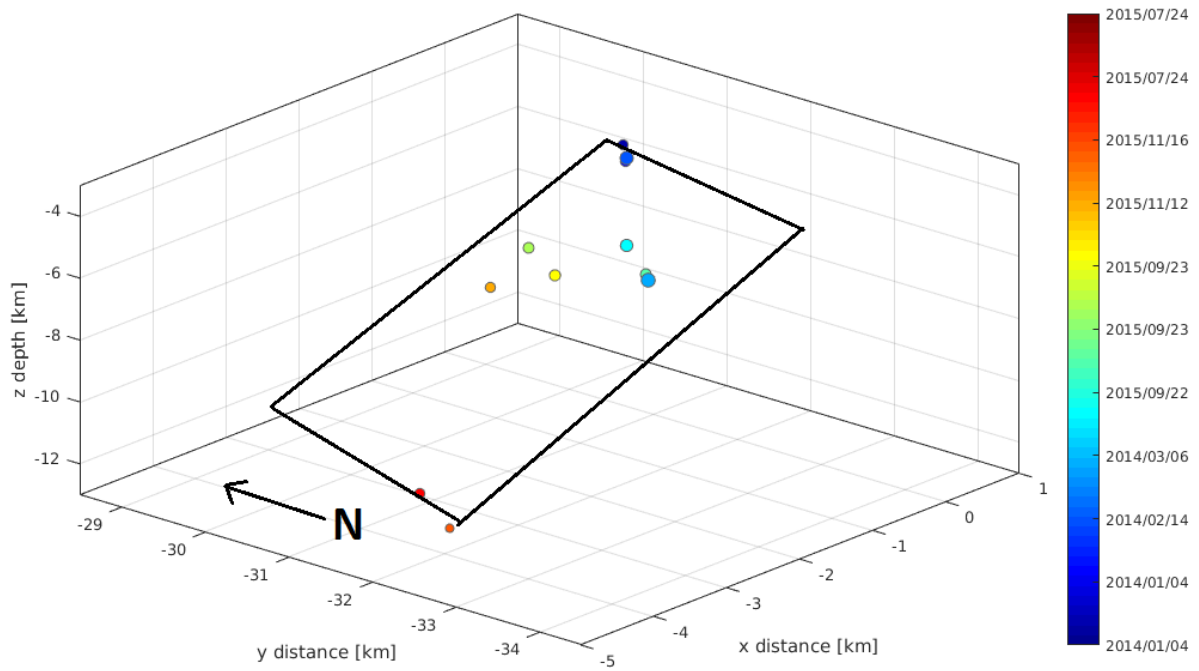ied. This chapter is divided into three sections. Key areas that will be discussed are (i) relocation process (ii) the different clusters in the Rana area (iii) comparison with other research in the same area and causes and (iiii) interpretation of the different cluster's and causes.

5.1 Relocation Process

For the Nordland area where earthquake swarms have been observed before [Bungum et al., 1979, Atakan et al., 1994, Hicks et al., 2000a]. The double difference method have shown from previous studies, improved results when earthquakes are located close to each other like in an earthquake swarm. Decreasing the uncertainties of the locations compared to when events are located individually [Waldhauser, 2001]. The seismicity image for my main study area before and after relocation, suggests an improvement in hypocenter location, showing a clear denser concentration of the seismicity. On the earthquake swarm and around. Revealing lineations trending toward NW-SE and W-E of epicenters that may be related to shallow faults, indicates that the spatial distribution of earthquakes are organized rather than random.

Evaluation of the errors with a synthetic test, demonstrate the reliability and robustness of my results. Fig. 22 shows the change in horizonal direction to be ~ 800 meter and vertical ~ 890 meters for initial locations, compared to the perfect locations in (Fig. 25). Then we compare the initial locations to the relocated events. The relocated events shows a maximum change in direction ~ 50 meter horizontal and ~ 70 meters vertical. Which implies that the relocation improves the figure by a factor of 10. These results indicates that using the double difference method improves both horizontal and vertical location accuracy.

Including both catalog data and cross correlation data, to get the most accurate travel time difference for obtaining relative hypocenter locations. In my case using cross correlation data, did not effect the locations (seen on the seismicity image) in the same degree as for other research, like the example for the Calaveras fault. Shown by comparing relocation using only catalog data Fig. 29 with relocation using both catalog and cross correlation data Fig. 33. This could mean that the events are not more correlated, suggest that they are different in location and mechanism by enough to produce different signals. In addition, it could indicate precise catalogue data and because hypoDD calculates more catalog differential travel times than cross correlation differential travel times data. The amount of cross correlation travel time differential measurements for each pair is approximately a fourth of the catalog data. Normally a better result would be to get at least half of the amount of the catalog data, for the cross correlation measurements.

Another reason, suggesting that the catalog quality is good, is the choosing of the picks (phases) of the catalog data.

With the good coverage of stations with higher quality instruments in the study area, the relocation process is not sensitive to the velocity model. Mostly because the double difference method is minimizing the effect of the velocity model errors (mentioned earlier in section 4.1) and the homogeneous geology. Compared to the study in Balfour et al. [2012] earthquakes are located beneath the San Juan Islands Washington, just above a subducting plate. Where they explore comparing velocity models based on results from tomographic studies, to standard models for the relocations. Observations show that the more detailed models result in reduced vertical relocation error and removes the effect the large velocity contrast are producing. This indicates that different geology, and much larger velocity contrast at layer boundaries. Must be the case if the velocity model should be of great concern when relocate events.

For the relocation process and the choice of parameter values for the ph2dt program. The maximum separation (MAXSEP) value especially effects the hypocenter relocation most. Trying out different values for the MAXSEP, made it possible to see how much this parameter effected the relocation process. This trial-error approach together with output from the inversion, was used to find a proper value for this study shown in Fig. 60. Comparing the smallest value MAXSEP=5 km and the highest value MAXSEP=20 km, showed a large difference in how many events included in the relocation. Where the smallest value does not cover a large enough area, so not all events that is of importance is included after the relocation process comparing Fig. 32. While using a MAXSEP of 20 km, could connect events that belongs too two different structures together. Creating one large cluster. The seismicity in this study is not covering a large area that a more optimal choice would be a value in between, and that the hypocentral separation between two events should be small compared to events station distance [Waldhauser, 2001]. The choice of a radius fell on 10 km, even though the difference between MAXSEP 10 and 15 km, were not to large. MAXSEP=10 km where chosen because it showed least scattered events after relocation. This value is also considered as a large enough search radius (MAXSEP), that all events of importance is included. Considered as also not to large for the area, in fear of connecting all events into one cluster. This formed a relocation that implies the most features in the seismicity together with a better concentration of the earthquake swarm.

The choice of damping value (DAMP) also had a seemingly large effect on the relocation. Experience from the trial and error approach, showed that if a to large or a to small value were picked, leads to events being located on top of each others or to far from each others.
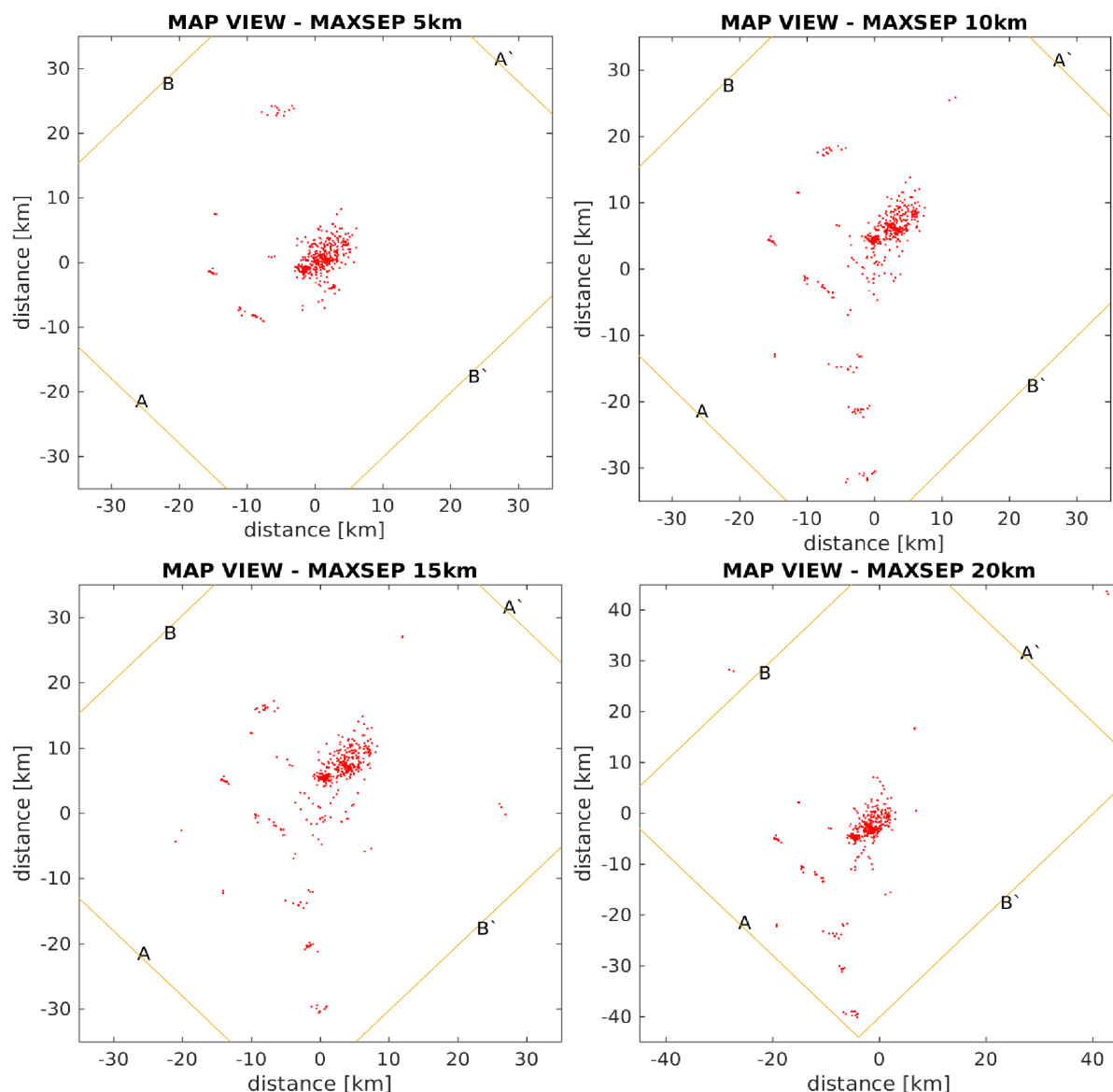
Figure 60: Comparison of all relocations using 5, 10, 15 and 20 km maximum separation values (MAXSEP). Some difference can be seen, but the linear alignments in NW-SE are mainly the same except for MAXSEP 5, which is a too small distance to include all events.

The hypocenter depths from initial locations compared to the relative location, reveals a more constrained depth distribution for the relocated events shown in Fig. 30. Excluding events at the surface and the deepest events. Showing a tighter clustering of events between 2-10 km, suggesting a similar hypocenter depth too the previous studies in Meløy, Steigen and Rana [Bungum et al., 1979, Atakan et al., 1994, Hicks et al., 2000a]. The area of northern Norway is considered to have a good station coverage giving accurate hypocentral parameters. It is fair to assume that the depths are more accurate with the relative locations. Indicated with the decrease of the RMS values for each iterations.

5.2 Comparison with previous studies and Cause

Previous studies of the seismicity in northern Norway show that earthquake swarms are frequently occurring further North of Rana in Meløy and Steigen [Bungum et al., 1979, Atakan et al., 1994, Hicks et al., 2000a]. The seismic activity in these two areas shows similarities to the Rana area in many ways, except for the amount of events recorded for the different locations, which may vary due to the improvement of the seismic network over the years. In Meløy, around 10.000 earthquakes were recorded during a 10-week period. Steigen swarm recorded 207 earthquakes during almost a year and Rana during 18 months period recorded 267 local earthquakes. These studies (described in section 4.2) show striking similarities in shallow hypocentral depths between 2-12 km, magnitude range up to $M_L 3.2$ for Meløy, over $3.0 M_c$ for Steigen and up to $M_L 2.8$ for Rana. and all areas have normal and strike slip faulting with coast-normal extension. Limitation in magnitude from M_L 0.1 to 3.5 is another indication that these are swarms. Another important factor, is that all three swarms locations share similar geological settings i.e. located along the coast of northern Norway which indicates they share similar stress-induced processes suggested in section 2.3.3. Proposed by Hicks et al. [2000a], Bungum et al. [2010] a likely explanation for the shallow and normal faulting swarms, may be related to the remaining glacial isostatic adjustment. The swarm is occurring within an area that have a high uplift gradient, which could be a stress generating mechanism able to form normal extension faults. What is considered to be the dominant force to intra-plate stress, are those related to plate tectonics like ridge push force from the North Atlantic mid-ocean ridge. Strengthening by the fact that most part of Fennoscandia show a nearly constant NW-SE directions for the horizontal stresses [Pascal et al., 2005, Gregersen and Voss, 2009, Bungum et al., 2010]. But even though suggested to be the dominant force, it is not capable by its own, to form normal faults perpendicular to the coast in a NW-SE direction in Nordland, because the direction of the ridge push compression being parallel to the faults and perpendicular to the coastline. Which means other forces must be contributing to form NW-SE oriented structures. Taking all these similarities into consideration, suggest that the stress sources forming the seismic activity along the coast of northern Norway is the same for all locations.

Upper-crustal earthquake swarms in stable continental regions are also suggested to be related to fluid intrusion in pre-existing fault zones [Assumpção, 1981, Hainzl, 2004, Uski et al., 2006, Jenatton et al., 2007, Bungum et al., 2010] , as desribed in section 4.2, my study area for the largest swarm is located near the Reppa power station (power plant), Storglomvatnet (Meløy) and Svartisen glacier, that is the main source of water reservoar for the power plant production. A source like this, that gathers a high content of water may be able to generate large enough stress, or penetrate in pre-existing structures (open faults), where water can penetrate into the crust that could lead to reactivation. Decrease of groundwater level/flow could create a water mass imbalance resulting in fluid intrusion, that may effect structures [Roeloffs et al., 2003]. A paper by King and Muir-Wood [1993] investigates what influence hydrological changes have on earthquakes, suggesting that the hydrological effect is related to the focal mechanisms, where normal faults are more effected by the hydrology (expel larger amount of water) than reverse faults. Little indications of this is still known, and the fact that the swarm is located 25 km from the

water source, and that seismicity occurred before the reservoir were filled with water. Implies that this may be a vague explanation for the area.

The relocated hypocenter locations for cluster 4 to 8 which represents linear alignment trending NW-SE direction and E-W, with shallow depths. Results obtained in the present study are in general good agreement with the results from previous work conducted in my main study area Hicks et al. [2000a] suggest similar directions, depths and magnitudes. In that study five major groups of earthquake epicenters with NNW-SSE trending distribution were located, with hypocenter depths between 4-12 km and magnitude range up to M_L 2.8. Fig. 61a from Hicks et al. [2000a] compared to Fig. 61b from my research, shows that three of the cluster (6,7 and 8) located with hypoDD are approximately located at the same locations as Hicks et al. [2000a]) with cluster 6 and 7 looking much alike in a map view, while cluster 7 shows a different direction of the linear alignment. Cluster 6 (Fig. 53) has events from 7 to 17 km depths, but are divided into what seems to be three structures. The shallowest is located between 7 and 10 km and the two next events are between 11 and 12 km depths, with magnitudes up to $M_L 1.1$, which fits the depths and magnitude of some events from Fig. 61a. Cluster 7 has events from 4 to 13 km depths and magnitudes up to $M_L 1.9$ which coincide with the results for the same location found by Hicks (2000), except two events with a slightly higher magnitude. Hypocenter depths between 4-7 km of the structure in cluster 8 correspond well to the focal depths of 4 to 6 km by Hicks (2000), and also the magnitude range up to $M_L 1.6$ agrees with the results obtained in current study showing magnitudes up to $M_L 1.6$. The earthquake group from Hicks et al. [2000a] research occurred within a time period of 3 months, the events for cluster 8 has two parts, with the shallowest events around 5 km are within a time period of over a month and the part with events from 6 to 7 km depths are within a period of 2 months except one events that is one year older.

Studies of another earthquake swarm located in Anjalankoski south-eastern Finland [Uski et al., 2006], have multiple similarities consisting of 16 earthquakes with $M_L 0.6$ to 2.1 lasting over a time period of three weeks. Located intraplate in a area with maximum uplift, with the orientation of maximum horizontal stress varying between E–W and NW–SE. Coincides with the ridge push force. Comparing results obtained in the current study with the study by Uski (2006), where available source mechanisms characterize the area as strike slip or reverse motion along vertical structures and a present uplift of 2 mm/year. Suggest that the post glacial uplift does not effect the seismicity in Anjalankoski area the same way as for the Rana area.
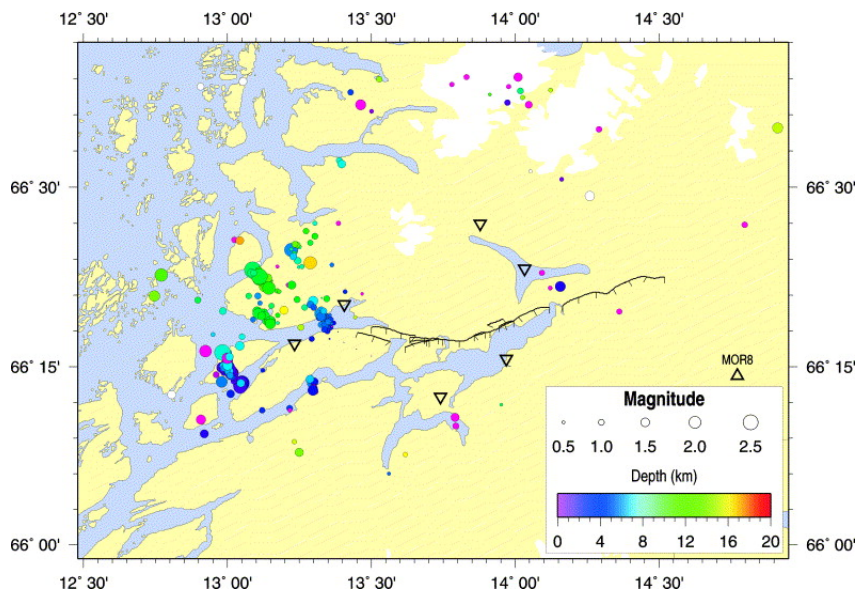
(a) Earthquakes in the Rana area, locations of five groups from Hicks et al. [2000a] paper of the seismicity activity in the Rana area.
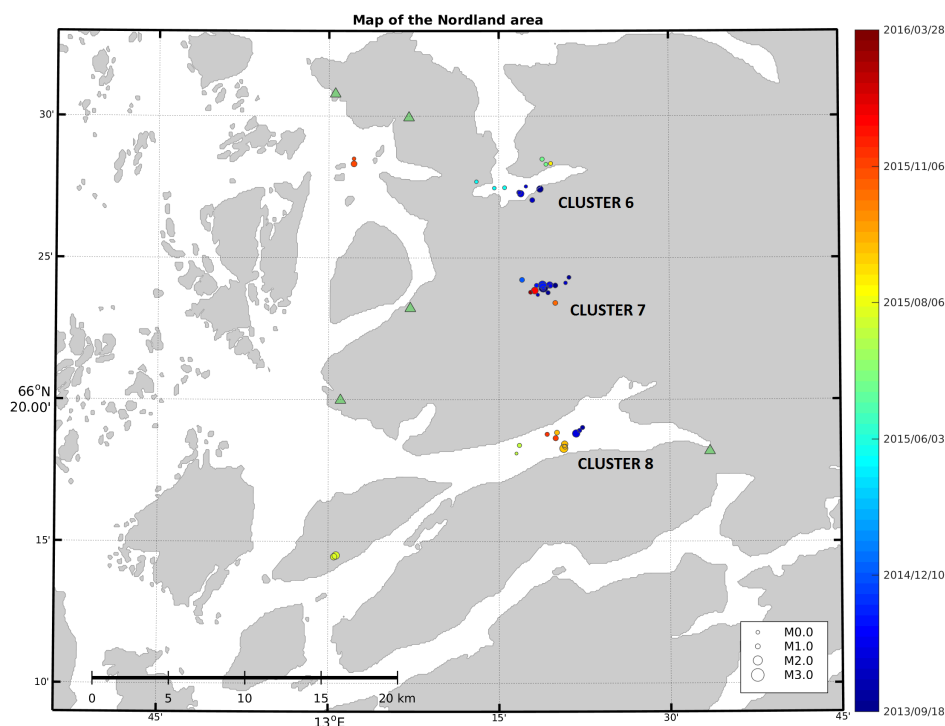
(b) Map view of cluster 6, 7 and 8 epicenter locations. These clusters are located almost at the same locations as some of the earthquake groups Hicks (2000) located. Comparison between these two shows that they are located approximately at the same focal depths and within the same magnitude range.

Figure 61: Comparison between results from the NEONOR1 project, and my results from relocating events.

Studies conducted on Iceland on intraplate earthquakes swarms[Einarsson, 1989, 1991] presents two different ways to originate intraplate earthquakes. 1) seismicity formed by internal deformation of the North American plate and 2) intraplate earthquakes formed close to the shelf edge off Eastern and Southeastern Iceland. The first is more comparable with the northern Norway seismicity, even though it is suggested to be related to the production of hot spot and intrusion of magma into the crust. The swarms comprised of a series of events along an area of 25 km, showing M_L mostly between 2-3, with hypocentral depths from 0-8 km and fault plane solution suggesting normal faulting and horizontal extension. One swarm occurred over three days recording 110 events with magnitude smaller than 2. All of this taken into consideration except the tectonics/geology difference, represents similarities in the size and depths of the events and number of events occurring within a time period.

5.3 Interpretation of structures and cause

The distribution of the earthquakes in the swarm, for main cluster 1 and main cluster 2, suggest they form a deformation volume, because of mostly randomly distribution in time and space i.e. no structure or no pattern in time of occurrence are observed. From the large scale picture, the swarm seems to be following the direction of the coast NNE-SSW and parallel to the structures along them. Zooming in on the swarms, especially on cluster 3, linear trend lines are observed in NW-SE direction. A possible suggestion may be because of local deformation due to reactivation of zones of weakness.

Described in section 4.2, Cluster 4 contains events in a 1 km linear trend in a NW-SE direction, that are migrating in time towards the Southeast. The NW-SE direction showing the same direction as previous mapped linear trends from normal faulting focal mechanism solutions. Together with the deeper events, I suggested a fault plane dipping in the Northeast. Even though I would prefer to have more events around and within the plane, making this a bit vague. It could still represent a fault plane. Reason for assuming this, is the distance between the events is at the largest approximately 400 meters and at the smallest 100 meters, and the migration in time towards the southeast, indicates that there is a connection between all events, and that this may represent a connected structure dipping to the Northwest. Extensional normal fault with 90° rotation from expected direction, can be formed as mention by both flexural forces from sediments, deglaciation and density difference. Much of the same observations counts for cluster 5. Including migration in time towards the Southeast and 11 events over a distance of 2 km. The dipping of the structure is a bit harder to determine, but from the observations, the events are deeper towards the Northwest, which may indicate the dipping direction. Both structures are parallel and almost on the same line, as to cluster 4. This may well indicate that they are formed from the same mechanism.

Present study is in generally good agreement with the previous conducted studies. Further South, cluster 6, 7 and partial 8 are shifting towards the W-E slightly WN-ES direction roughly normal to the coast. Matching the results from Hicks et al. [2000a,b], extensional horizontal stresses in WNW-ESE with normal focal mechanism solution and overcoring measurements shown in Fig. 6. Compared to the clusters in NW-SE direction,

these clusters are not showing distribution around the same depth or migration in time. This raises the question if these are from the same the stress generating processes as suggested for the structures in the NW-SE direction. Which could indicate that different forces are acting on the structures i.e. the different force creating movements that effects the area that makes up an unstable stress field causes unstable situations, and may develop complex faults or fracture zones that are not parallel to the spreading direction of the ridge push [Einarsson, 1991].

A possible explanation for the earthquake swarm, may be the location of Svartisen glacier next to the swarm. The reason for this assumption is because the distance between the swarm and the glacier is small and the glacier itself represent a large weight and possible movement related to melting. It is proposed that the glacier could produce extensive load, if the water distribution or movements are changed to one side, creating, a flexural force which may have effect on the seismicity. Preliminary results from InSAR and GPS measurments shows indication of deformation in the area [?]. On the other hand, the earthquake swarm in Steigen did not have a glacier located near it, indicating that there is more mechanism included. This is still very diffused, and not much is published about it.

Previous focal mechanism solutions found around the Rana area near the swarm and mapping of lineaments in Nordland, is dominated by normal faulting extension and lineaments in NW-SE, E-W and NNW-SSE. [Fjeldskaar et al., 2000, Hicks et al., 2000a,b, Gabrielsen et al., 2002]. Suggest that my observation of linear alignments trends in NW-SE direction near the swarm, may also be dominated by extension normal faulting. Preliminary results from the NEONOR2 project of fault plane solutions around Svartisen, shows a dominance of normal faulting in the area around the swarm, and some further South. Possible direction of the tectonic faults dominant in NW-SE. Has to be mention that these results of the type of fault plane solutions, indicates quite diffused types, but it still shows dominance of normal faulting.
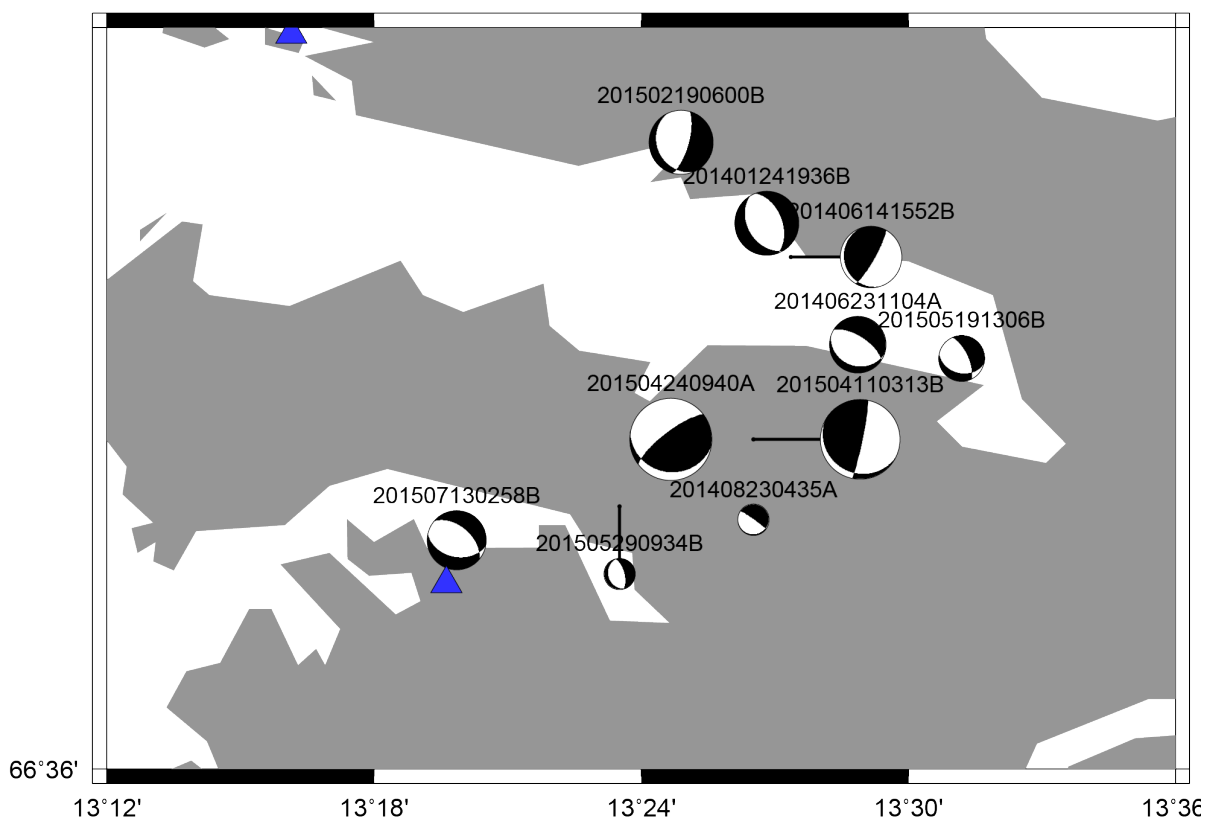
Figure 62: Fault plane solutions (FPS) from the NEONOR2 project, shows dominant normal faulting and some NW-SE directions. The quality of the FPS are A and B.

Since we in my results mostly observes linear alignments in NW-SE direction near the swarm and E-W further South, that coincides with previous studies and the new finding in the NEONOR2 project. Indicates that the direction of the extension is not far from the reality. Suggest that the most likely cause for generating stress, will still be a interaction between the dominating ridge push force, post glacial uplift (high gradient), high topography and large amount of sediments along the coast. For generating a stress direction that could explain the rotation of the faults and seismicity. Whether the high concentration of seismic activity near Svartisen occurs from the effect of the glacier, is more uncertain than these previous suggested causes.

6   Conclusions and Further Work

This thesis attempts to describe and show the relocation of earthquakes, using the double difference method, in the Nordland region. There is improvement in earthquake locations using the relative method, compared to standard absolute hypocenter locations. The relative locations are providing insight into structures, which would not be clearly visible using the absolute locations.

Based on the relocation results, combined with previously conducted studies, the following conclusions can be drawn:

- The seismicity in clusters 1, 2 and 3 altogether is found to be in the NE-SW direction. Seismicity in clusters 1 and 2 is found to be randomly distributed in time and space while cluster 3 shows significant linear alignments mostly trending NW-SE direction indicating structures that could be related to faults.

- Some linear trends shows migration in time towards SE indicating that the spatial distribution of earthquakes is organized rather than random.

- My results coincides well with previous studies conducted in Nordland area, shows many similarities in terms of locations, depths, magnitudes and linear alignments trending in the NW-SE and E-W directions.

- The most likely stress generating mechanisms in that area are ridge push, post glacial uplift and topography. The contribution of the Svartisen glacier on the stress field is still not clear but relatively high deformations observed by GPS are indicating its significant role.

- Relative locations compared to absolute location for the smallest cluster 4 to 8, shows clearly a significant denser concentration of the seismicity, which reveals lineaments in specific directions.

- The synthetic test shows that the relocated locations are reliable and robust.

- Using a MAXSEP of 10 km provided the most encouraging results, compared to lower and higher values.

- Cross correlation differential travel times for both P and S do not highly affect the seismicity image. Many events are not correlated because they are different in location and mechanism and produce different signals.

6.1   Further Work

This study contributes to the existing knowledge of the seismicity in Nordland. By determine more precise relative locations. For further study, a larger data including more cross correlation data, could illuminate a fuller extent of the structures. A weakness in this study, is the possible link between the linear alignments trending in NW-SE and E-W direction to any features on the surface (existing faults). Applying a gravitation or magnetic map under the events, may associate structures with seismicity.

A closer look into Svartisen glacier influence on the earthquake swarm, would be very interesting. Finding out how the glacier has developed in terms of movement and melting. Possibly try to relate to the shallow high concentrated seismicity and the direction of stress (strain measurements).

Other thing that would also be of interest is:

- Study the difference between the deeper and higher magnitude earthquake offshore, with the shallow lower magnitude earthquakes onshore.

- Get more reliable fault plane solutions in the area, would attribute to the relocation. May verify if the orientations that we see from the 3D view, are in agreement with the fault plane solutions.

- Explore more on the physical state of the faults (pore pressure, strength reducing mechanisms), could be more important than the seismicity. For giving more answers regarding the cause of the seismicity.

7 Appendix

7.0.1 HypoDD procedure

1) SeisanExplorer: select events from the Nordland area (xxx) for August 2013-March2016

2) hyp: relocate using hyp (HYPOCENTER)

3) Modify STATION0.HYP, make copy of stations with 5 characters and duplicate with 4 characters (e.g., NBB15 -¿ NB15)

4) hdd524 (hypodd 5 to 4):change 5 character station codes to 4 character station codes

5) nor2dd hdd524.out: converts data to phase format

6) Check for non-located events and *****, and remove, also REMOVE from hyp.out if needed, otherwise just remove lines.

7) ph2dt ph2dt.inp: convert phase to dt.ct

8) Split: create s-files to be used with corr; remove files if not producing correct data in phase.dat

9) corr: run correlation program

10) check that number of events in events.dat is same as in corr.trace

11) change 5 char station codes in dt.cc to 4 characters

7.0.2 Corr.inp

corr input file   the program can do 2 things: 1) find correlated events, in this case comment out parameter SFILE MASTER; program then correlates all events and finds groups, output in file corr.out; this should be done before 2 is attempted in addition to visual inspection   2) pick phases in events by correlating with master event, in this case define SFILE MASTER; program uses parts of master event signals and computes correlation   for the remaining events; phase output is written to corr.out   trace file corr.trace gives additional info on the program run

KEYWORD............Comments.............Par 1.....Par 2.....

SFILE MASTER file name 14-1552-08L.S201406 SFILE INDEXFILE events.lis SFILE INDEXFILE test1.lis SFILE INDEXFILE test2.lis SFILE INDEXFILE test3.lis SFILE INDEXFILE test4.lis SFILE INDEXFILE filenr.lis

minimum correlation value MIN CORR 0.8

number of stations required for event pair to be correlated MIN CORR CHAN 3

either 0. or 1. INTERACTIVE 0.

activate (1.) or deactivate (0.) filters set below FILTER 1.

time of window before phase as ratio of selected duration PRE SIGNAL 0.4

use either full trace (0.) or same criteria as for master event (1.) EVENT SELCRIT 1.

double sample rate n times N DOUBLE SRATE 0.

time window for cross-correlation matrix, 999. for max CC MATRIX WINDOW 0.

set hypocenter start latitude and longitude, 999. to not use (only affects output file, and use of location program afterwards) START LATITUDE 66.66 START LONGITUDE 13.46

set hypocenter fixed depth, 999. to not use (only affects output file, and use of location program afterwards) FIX DEPTH 999.

keep original waveform names (0.) or put corr output file names (1.) WAVENAME OUT 0.

output of correlation function, 0 for none, 1. for full data, 2 for reduced data 1 for data ¿ MIN CORRELATION, otherwise 0 WAVE CORR OUT 1.

reduce to 0 (-) and 1 (+) if set to 1, full data if set to 1. SINGLE BIT 0.

write out phases for correlation above threshold if set to 1. CONTINUOUS MODE 0.

extract event files for correlation above threshold, 0. for no extract, 1. to extract single channel used, 2. extract all channels CONTINUOUS EXTRACT 0.

flag to write corr.trace output file TRACE OUTPUT 1.

maximum distance between event pair to compute correlation MAX EVENT DISTANCE 10.

maximum distance between event and station MAX STAT DISTANCE 200.

maximum difference between average diff time and station diff time MAX DIFF TIME .2

References

Marcelo Assumpção. The nw scotland earthquake swarm of 1974. *Geophysical Journal International*, 67(3):577–586, 1981.

Kuvvet Atakan, Conrad D Lindholm, and Jens Havskov. Earthquake swarm in steigen, northern norway: an unusual example of intraplate seismicity. *Terra Nova*, 6(2): 180–194, 1994.

Natalie J Balfour, John F Cassidy, and Stan E Dosso. Identifying active structures using double-difference earthquake relocations in southwest british columbia and the san juan islands, washington. *Bulletin of the Seismological Society of America*, 102(2): 639–649, 2012.

Alvar Braathen, Øystein Nordgulen, Per-Terje Osmundsen, Torgeir B Andersen, Arne Solli, and David Roberts. Devonian, orogen-parallel, opposed extension in the central norwegian caledonides. *Geology*, 28(7):615–618, 2000.

Alvar Braathen, Per Terje Osmundsen, O Nordgulen, David Roberts, and Gurli B Meyer. Orogen-parallel extension of the caledonides in northern central norway: an overview. *Norsk Geologisk Tidsskrift*, 82(4):225–242, 2002a.

Alvar Braathen, Per Terje Osmundsen, O Nordgulen, David Roberts, and Gurli B Meyer. Orogen-parallel extension of the caledonides in northern central norway: an overview. *Norsk Geologisk Tidsskrift*, 82(4):225–242, 2002b.

Harald Brekke, Hans Ivar Sjulstad, Christian Magnus, and Robert W Williams. Sedimentary environments offshore norway—an overview. *Norwegian Petroleum Society Special Publications*, 10:7–37, 2001.

Hannes K Brueckner, Herman LM Van Roermund, and Norman J Pearson. An archean (?) to paleozoic evolution for a garnet peridotite lens with sub-baltic shield affinity within the seve nappe complex of jämtland, sweden, central scandinavian caledonides. *Journal of Petrology*, 45(2):415–437, 2004.

H Bungum, BK Hokland, Eystein Sverre Husebye, and F Ringdal. An exceptional intraplate earthquake sequence in meløy, northern norway. *Nature*, 280:32–35, 1979.

H. Bungum, A. Alsaker, L. B. Kvamme, and R. A. Hansen. Seismicity and seismotectonics of norway and nearby continental shelf areas. *Journal of Geophysical Research: Solid Earth*, 96(B2):2249–2265, 1991. ISSN 2156-2202. doi: 10.1029/90JB02010. URL `http://dx.doi.org/10.1029/90JB02010`.

H Bungum, O Olesen, C Pascal, S Gibbons, C Lindholm, and O Vestøl. To what extent is the present seismicity of norway driven by post-glacial rebound? *Journal of the Geological Society*, 167(2):373–384, 2010.

Hilmar Bungum and Odleiv Olesen. The 31st of august 1819 lurøy earthquake revisited. *Norwegian Journal of Geology*, 85:245–252, 2005.

John F Dehls, Odleiv Olesen, Lars Olsen, and Lars Harald Blikra. Neotectonic faulting in northern norway; the stuoragurra and nordmannvikdalen postglacial faults. *Quaternary science reviews*, 19(14):1447–1460, 2000.

EA Eide and J-M Lardeaux. A relict blueschist in meta-ophiolite from the central norwegian caledonides—discovery and consequences. *Lithos*, 60(1):1–19, 2002.

Páll Einarsson. Intraplate earthquakes in iceland. In *Earthquakes at North-Atlantic Passive Margins: Neotectonics and Postglacial Rebound*, pages 329–344. Springer, 1989.

Pall Einarsson. Earthquakes and present-day tectonism in iceland. *Tectonophysics*, 189 (1):261–279, 1991.

Morten Fejerskov and Conrad Lindholm. Crustal stress in and around norway: an evalu-

ation of stress-generating mechanisms. *Geological Society, London, Special Publications*, 167(1):451–467, 2000.

Willy Fjeldskaar, Conrad Lindholm, John F Dehls, and Ingrid Fjeldskaar. Postglacial uplift, neotectonics and seismicity in fennoscandia. *Quaternary Science Reviews*, 19 (14):1413–1422, 2000.

RH Gabrielsen, OF Ekern, and A Edvardsen. Structural development of hydrocarbon traps, block 2/2, norway. *Spencer, AJ, et al.(Editors-in-Chief), Habitat of Hydrocarbons of the Norwegian Continental Shelf*, pages 129–141, 1986.

Roy H Gabrielsen, Alvar Braathen, John Dehls, and David Roberts. Tectonic lineaments of norway. *Norsk Geologisk Tidsskrift*, 82(3):153–174, 2002.

DG Gee. A tectonic model for the central part of the scandinavian caledonides. *American Journal of Science*, 275:468–515, 1975.

Ludwig Geiger. Herdbestimmung bei erdbeben aus den ankunftszeiten. *Nachrichten von der Gesellschaft der Wissenschaften zu Göttingen, Mathematisch-Physikalische Klasse*, 1910:331–349, 1910.

Soren Gregersen and Peter Voss. Stress change over short geological time: the case of scandinavia over 9000 years since the ice age. *Geological Society, London, Special Publications*, 316(1):173–178, 2009.

Sebastian Hainzl. Seismicity patterns of earthquake swarms due to fluid intrusion and stress triggering. *Geophysical Journal International*, 159(3):1090–1096, 2004.

Egill Hauksson and Peter Shearer. Southern california hypocenter relocation with waveform cross-correlation, part 1: Results using the double-difference method. *Bulletin of the Seismological Society of America*, 95(3):896–903, 2005a.

Egill Hauksson and Peter Shearer. Southern california hypocenter relocation with waveform cross-correlation, part 1: Results using the double-difference method. *Bulletin of the Seismological Society of America*, 95(3):896–903, 2005b.

J Havskov, LB Kvamme, RA Hansen, H Bungum, and CD Lindholm. The northern norway seismic network: Design, operation, and results. *Bulletin of the Seismological Society of America*, 82(1):481–496, 1992.

Erik C Hicks, Hilmar Bungum, and Conrad D Lindholm. Seismic activity, inferred crustal stresses and seismotectonics in the rana region, northern norway. *Quaternary Science Reviews*, 19(14):1423–1436, 2000a.

Erik C Hicks, Hilmar Bungum, and Conrad D Lindholm. Stress inversion of earthquake focal mechanism solutions from onshore and offshore norway. *Norsk Geologisk Tidsskrift*, 80(4):235–250, 2000b.

Liliane Jenatton, Robert Guiguet, François Thouvenot, and Nicolas Daix. The 16,000-event 2003–2004 earthquake swarm in ubaye (french alps). *Journal of Geophysical Research: Solid Earth*, 112(B11), 2007.

M Keiding, C Kreemer, CD Lindholm, S Gradmann, O Olesen, and HP Kierulf. A comparison of strain rates and seismicity for fennoscandia: depth dependency of deformation from glacial isostatic adjustment. *Geophysical Journal International*, 202(2):1021–1028, 2015.

GEOFFREY CP King and R Muir-Wood. Hydrological signatures of earthquake strain. *Jour. Geoph. Res*, 98(22):035–22, 1993.

Barry R Lienert and Jens Havskov. A computer program for locating earthquakes both locally and globally. *Seismological Research Letters*, 66(5):26–36, 1995.

Henning Lorenz, David G Gee, Alexander N Larionov, and Jaroslaw Majka. The grenville–sveconorwegian orogen in the high arctic. *Geological Magazine*, 149(05): 875–891, 2012.

Joseph G Meert and Trond H Torsvik. The making and unmaking of a supercontinent: Rodinia revisited. *Tectonophysics*, 375(1):261–288, 2003.

Kiyoo Mogi. Some discussions on aftershocks, foreshocks and earthquake swarms: the fracture of a semi-infinite body caused by an inner stress origin and its relation to the earthquake phenomena (third paper). 1963.

RM Nadeau, W Foxall, and TV McEvilly. Clustering and periodic recurrence of microearthquakes on the san andreas fault at parkfield, california. *Science*, 267(5197): 503–507, 1995.

O Nordgulen, Alvar Braathen, Fernando Corfu, Per Terje Osmundsen, and Tore Husmo. Polyphase kinematics and geochronology of the late-caledonian kollstraumen detachment, north-central norway. *NORSK GEOLOGISK TIDSSKRIFT*, 82(4):299–316, 2002.

ODLEIV Olesen, SVEIN Gjelle, HERBERT Henkel, TA Karlsen, LARS Olsen, and TERJE Skogseth. Neotectonics in the ranafjorden area, northern norway. *Norges geologiske undersøkelse Bulletin*, 427:5–8, 1995.

Odleiv Olesen, John Dehls, Hilmar Bungum, Fridtjof Riis, Erik Hicks, Conrad Lindholm, Lars H Blikra, Willy Fjeldskaar, Lars Olsen, Oddvar Longva, et al. Neotectonics in norway, final report. *Geological Survey of Norway, Report*, 2000.

Odleiv Olesen, Erik Lundin, O Nordgulen, Per Terje Osmundsen, Jan Reidar Skilbrei, Mark A Smethurst, Arne Solli, Tom Bugge, and Christine Fichler. Bridging the gap between the onshore and offshore geology in nordland, northern norway. *Norsk Geologisk Tidsskrift*, 82(4):243–262, 2002.

Odleiv Olesen, Lars Harald Blikra, Alvar Braathen, John F Dehls, Lars Olsen, Leif Rise, David Roberts, Fridtjof Riis, Jan Inge Faleide, and Einar Anda. Neotectonic deformation in norway and its implications: a review. *NORSK GEOLOGISK TIDSSKRIFT*, 84(1):3–34, 2004.

Odleiv Olesen, Hilmar Bungum, John Dehls, Conrad Lindholm, Christophe Pascal, and David Roberts. Neotectonics, seismicity and contemporary stress field in norway– mechanisms and implications. *NGU Special Publication*, 13:145–174, 2013a.

Odleiv Olesen, Hilmar Bungum, John Dehls, Conrad Lindholm, Christophe Pascal, and David Roberts. Neotectonics, seismicity and contemporary stress field in norway– mechanisms and implications. *NGU Special Publication*, 13:145–174, 2013b.

PT Osmunden, A Braathen, Ø Nordgulen, D Roberts, and E Eide. The devonian nesna shear zone, north-central norwegian caledonides, and its regional implications. *Journal of the Geological Society of London*, 160:137–150, 2003.

PT Osmundsen, A Braathen, Ø Nordgulen, D Roberts, GB Meyer, and E Eide. The devonian nesna shear zone and adjacent gneiss-cored culminations, north–central norwegian caledonides. *Journal of the Geological Society*, 160(1):137–150, 2003.

Voss Ottemöller and Havskov. *SEISAN EARTHQUAKE ANALYSIS SOFTWARE FOR WINDOWS, SOLARIS, LINUX and MACOSX , 2014.*, 2014.

L Ottemöller and CW Thomas. Highland boundary fault zone: Tectonic implications of the aberfoyle earthquake sequence of 2003. *Tectonophysics*, 430(1):83–95, 2007.

Christopher C Paige and Michael A Saunders. Lsqr: An algorithm for sparse linear equations and sparse least squares. *ACM Transactions on Mathematical Software (TOMS)*, 8(1):43–71, 1982.

Christophe Pascal, David Roberts, and Roy H Gabrielsen. Quantification of neotectonic stress orientations and magnitudes from field observations in finnmark, northern norway. *Journal of Structural Geology*, 27(5):859–870, 2005.

David Roberts. The scandinavian caledonides: event chronology, palaeogeographic settings and likely modern analogues. *Tectonophysics*, 365(1):283–299, 2003.

David Roberts and David G Gee. An introduction to the structure of the scandinavian caledonides. *The Caledonide orogen–Scandinavia and related areas*, 1:55–68, 1985.

Evelyn Roeloffs, Michelle Sneed, Devin L Galloway, Michael L Sorey, Christopher D Farrar, James F Howle, and Jennifer Hughes. Water-level changes induced by local and distant earthquakes at long valley caldera, california. *Journal of Volcanology and Geothermal Research*, 127(3):269–303, 2003.

Erling Rykkelid and Arild Andresen. Late caledonian extension in the ofoten area, northern norway. *Tectonophysics*, 231(1):157–169, 1994a.

Erling Rykkelid and Arild Andresen. Late caledonian extension in the ofoten area, northern norway. *Tectonophysics*, 231(1):157–169, 1994b.

Robert W Simpson, Russell W Graymer, Robert C Jachens, David A Ponce, and Carl M Wentworth. Cross-sections and maps showing double-difference relocated earthquakes from 1984-2000 along the hayward and calaveras faults, california. Technical report, 2004.

Seth Stein and Michael Wysession. *An introduction to seismology, earthquakes, and earth structure*, chapter 7, pages 416–422. John Wiley & Sons, 2003.

Lynn R Sykes. Earthquake swarms and sea-floor spreading. *Journal of Geophysical Research*, 75(32):6598–6611, 1970.

TH Torsvik, MA Smethurst, JOSEPH G Meert, R Van der Voo, WS McKerrow, MD Brasier, BA Sturt, and HJ Walderhaug. Continental break-up and collision in the neoproterozoic and palaeozoic—a tale of baltica and laurentia. *Earth-Science Reviews*, 40(3):229–258, 1996.

Trond H Torsvik and L Robin M Cocks. Earth geography from 400 to 250 ma: a palaeomagnetic, faunal and facies review. *Journal of the Geological Society*, 161(4):555–572, 2004.

Trond H Torsvik and L Robin M Cocks. Norway in space and time: a centennial cavalcade. *Norwegian Journal of Geology*, 85(1-2):73–86, 2005.

Trond H Torsvik and Rob Van der Voo. Refining gondwana and pangea palaeogeography: estimates of phanerozoic non-dipole (octupole) fields. *Geophysical Journal International*, 151(3):771–794, 2002.

Marja Uski, Timo Tiira, Annakaisa Korja, and Seppo Elo. The 2003 earthquake swarm in anjalankoski, south-eastern finland. *Tectonophysics*, 422(1):55–69, 2006.

Rob Van der Voo and Trond H Torsvik. Evidence for late paleozoic and mesozoic non-dipole fields provides an explanation for the pangea reconstruction problems. *Earth and Planetary Science Letters*, 187(1):71–81, 2001.

Felix Waldhauser. hypodd–a program to compute double-difference hypocenter locations. 2001.

Felix Waldhauser and William L Ellsworth. A double-difference earthquake location algorithm: Method and application to the northern hayward fault, california. *Bulletin of the Seismological Society of America*, 90(6):1353–1368, 2000.

Felix Waldhauser and William L Ellsworth. Fault structure and mechanics of the hayward fault, california, from double-difference earthquake locations. *Journal of Geophysical Research: Solid Earth*, 107(B3), 2002.

R Muir Wood. The scandinavian earthquakes of 22 december 1759 and 31 august 1819. *Disasters*, 12(3):223–236, 1988.

Robert Muir Wood. Extraordinary deglaciation reverse faulting in northern fennoscandia. In *Earthquakes at North-Atlantic passive margins: neotectonics and postglacial rebound*, pages 141–173. Springer, 1989.